KTH Computer Science
and Communication

Robotic manipulation under uncertainty and limited dexterity

FRANCISCO ELI VIÑA BARRIENTOS

Doctoral Thesis
Stockholm, Sweden 2016

TRITA-CSC-A-2016:15
ISSN-1653-5723
ISRN-KTH/CSC/A–16/15
ISBN 978-91-7729-022-3

Computer Vision and Active Perception
School of Computer Science and Communication
KTH Royal Institute of Technology
SE-100 44 Stockholm, Sweden

Copyright © 2016 by Francisco Eli Viña Barrientos except where otherwise stated.

Tryck: Universitetsservice US-AB 2016

Abstract

Robotic manipulators today are mostly constrained to perform fixed, repetitive tasks. Engineers design the robot's workcell specifically tailored to the task, minimizing all possible *uncertainties* such as the location of tools and parts that the robot manipulates. However, autonomous robots must be capable of manipulating novel objects with unknown physical properties such as their inertial parameters, friction and shape. In this thesis we address the problem of *uncertainty* connected to kinematic constraints and friction forces in several robotic manipulation tasks. We design adaptive controllers for opening one degree of freedom mechanisms, such as doors and drawers, under the presence of uncertainty in the kinematic parameters of the system. Furthermore, we formulate adaptive estimators for determining the location of the contact point between a tool grasped by the robot and the environment in manipulation tasks where the robot needs to exert forces with the tool on another object, as in the case of screwing or drilling. We also propose a learning framework based on Gaussian Process regression and dual arm manipulation to estimate the static friction properties of objects. The second problem we address in this thesis is related to the mechanical simplicity of most robotic grippers available in the market. Their lower cost and higher robustness compared to more mechanically advanced hands make them attractive for industrial and research robots. However, the simple mechanical design restricts them from performing *in-hand manipulation*, i.e. repositioning of objects in the robot's hand, by using the fingers to push, slide and roll the object. Researchers have proposed thus to use *extrinsic dexterity* instead, i.e. to exploit resources and features of the environment, such as gravity or inertial forces, that can help the robot to perform regrasps. Given that the robot must then interact with the environment, the problem of uncertainty becomes highly relevant. We propose controllers for performing *pivoting*, i.e. reorienting the grasped object in the robot's hand, using gravity and controlling the friction exerted by the fingertips by varying the grasping force.

Sammanfattning

De flesta robotarmar är idag begränsade till att göra repetitiva (uppgifter). Ingenjörer designar robotens arbetsmiljö för att passa uppgiften och minska osäkerheter i robotens perception, t.ex. lokalisering av verktyg som roboten manipulerar. Framtidens autonoma robotar måste kunna manipulera nya föremål med okända fysiska egenskaper såsom tröghet, friktion och form. Denna avhandling behandlar problemet med osäkerheter som uppstår från kinematiska begränsningar och friktionskrafter i olika robotuppgifter. Vi konstruerar adaptiva regulatorer för att öppna t.ex. dörrar och lådar, i närvaro av osäkerhet kring systemets kinematiska parameter. Vi formulerar också adaptiva filter för att beräkna kontaktpunkters plats mellan verktyg som roboten använder och robotens omgivning, t.ex. när roboten skruvar eller borrar. Vi föreslår ocksåen maskininlärningsmetod baserad påGaussiska Processer och två-armsmanipulation för att beräkna objektens statiska friktionsegenskaper. Det andra problem som vi behandlar är relaterat till de mekaniskt simpla robothänder som typiskt förekommer i industrin. Deras lägre kostnader och högre robusthet gör dem, jämfört med mer mekaniskt avancerade händer, mer attraktiva för industriella- och forskningsändamål. Deras enkla mekaniska konstruktion begränsar dock deras förmåga att genomföra *in-hand manipulation*, vilket betyder att roboten ompositionerar föremål i robotens hand, genom att trycka föremålet med fingrarna och låta det glida och rulla runt. Forskare har föreslagit *extrinsic dexterity* (extrinsisk fingerfärdighet) istället, d.v.s. att utnyttja resurer i robotens omgivning. Dessa kan vara exempelvis gravitation och tröghetskrafter, vilka kan underlätta in-hand manipulation. Roboten måste dåinteragera med sin omgiving, vilket gör osäkerhetsproblemet mycket relevant. Vi föreslår regulatorer för att låta roboten svänga objekt, d.v.s. att omorientera föremål i handen genom utnyttjande av gravitation och kontroll av fingrarnas friktionskrafter.

Acknowledgments

This thesis is the product of a four year journey, where I believe my own work accounts only for a small portion of the accomplishments. It was you: my dear friends, supervisors and family that really made this happen. There were plenty of ups and downs along the way as in any PhD (and, believe me, many times I felt there were more downs than ups), but your advice, support and friendship gave me the strength and inspiration I really needed to keep going. In the end, it has worked out better than I expected and I can say it was definitely worth the effort. I will have many fond memories to share when people ask me about my PhD. I truly hope that, when you think back to these four years, you cherish them as much as I do.

I would like to thank Dani, my main supervisor, who first took me in as a master thesis student back in 2010. I still remember the first time we met, where you showed me the brand new Dumbo robot arms in a box and asked me to get them up and running and 'do something' with them. Never in my mind did I expect that 'doing something' plus four years down the road would lead to a PhD. I know I've been a pain at times, so I thank you very much for your patience and for helping me mature and grow. You helped me to look beyond the immediate problems and struggles in my PhD and showed me how to correct my mistakes but at the same time also identify my own skills and potential. I have come to appreciate very much your 'straight-to-the-point' style of supervision combined with the right dose of open-mindedness and flexibility.

I would also like to thank my cosupervisors: Yiannis and Christian. Your technical input and feedback got me on the right track when I was totally lost, and greatly improved the quality and relevance of my work in the rare occasions when I wasn't so lost. I hope that this thesis makes justice to the dedication and help I received from you. Thanks also to Yasemin who supervised me in the beginning of my PhD. I admire the patience and confidence you had in me despite my frequent lack of optimism regarding research results. A big thanks to Patric as well, who, although was not my own supervisor, I consider as a mentor who I've enjoyed talking to and sharing opinions with during lunch conversations and the robotics course.

My gratitude also goes to the wonderful people of CVAP, both old-timers and newcomers. We've been together in many places around the globe: Atlanta, India, Hong Kong, Seattle, Vancouver, Hamburg, Kiruna... We've shared many unforgettable experiences and I have learned much from you. Sharing a workplace with such intelligent, ambitious and talented people who are so social and friendly is something I will miss very much when my time at CVAP is over. This genuine sense of companionship is a rare gem that you should be very proud of. I feel very fortunate that throughout these years we have become such great friends rather than just 'colleagues'.

There is also a very special group of old friends that I would like to thank, team-Venezuela: Rafael, Veluska, Monika, Gilfredo, Francisco, Yasmin, Elias, Gabriela, Javier, Juan, David, Luis, Carlos and Carlos. We've been great friends back at home since a decade ago (yes, it has actually been that long), and I am glad to have shared with you what is now our second home, Stockholm. Your trustworthiness and cheerfulness have made my PhD all the more memorable. Your good venezuelan humor has cheered me up at times when I felt pessimistic at work. Every time I talk to someone about my venezuelan friends, I cannot help but smile and rejoice at the thought of such loyal friends, of knowing that we hold the kind of friendship that lasts for a lifetime.

A special thanks also to my good friends, Sara and Karl. I have enjoyed very much our regular weekend dinners where you have kindly taught me much about Sweden and its culture and told me many inspiring tales about your adventures around the world.

A quien más agradezco, a mi querida familia: mamá, papá, Carlos Enrique, Estefanía, Kari, Diego y Sebastián. Este trabajo lo dedico a ustedes, agradeciendo el gran cariño y apoyo incondicional que me han brindado. Gracias por guiarme y darme confianza y aliento. Mis logros se los debo a ustedes. A pesar de la distancia, ustedes han sido y siempre serán mi mayor fuente de inspiración. Los quiero mucho.

Contents

Contents **vii**

I Introduction **1**

1 Introduction **3**
1 Thesis Contributions 8
2 Thesis Outline 10

2 Uncertainty and Extrinsic Dexterity in Robotic Manipulation **15**
1 Problem Statement 15
2 Challenges 18

3 Summary of Papers **25**
A An Adaptive Control Approach for Opening Doors and Drawers under Uncertainties 25
B Online Contact Point Estimation for Uncalibrated Tool Use 27
C Predicting Slippage and Learning Manipulation Affordances through Gaussian Process Regression 29
D In-hand Manipulation Using Gravity and Controlled Slip 31
E Adaptive Control for Pivoting with Visual and Tactile Feedback . 33

4 Conclusions **35**
1 Future Work 36

Bibliography **39**

II Included Publications **45**

A An Adaptive Control Approach for Opening Doors and Drawers under Uncertainties **A1**
1 Introduction A3

2 Related Work and our Contributions A5
3 System and Problem Description A8
4 Control Design A13
5 Scenarios and Evaluation A21
6 Experiments A22
7 Conclusions A27
References A34

B Online Contact Point Estimation for Uncalibrated Tool Use B1
1 Introduction B3
2 Related Work B4
3 Kineto-Statics Formulation B6
4 Methodology B9
5 Experiments B12
6 Conclusions B14
7 Appendix B15
References B16

C Predicting Slippage and Learning Manipulation Affordances through Gaussian Process Regression C1
1 Introduction C3
2 Related Work C5
3 Physics and Learning Model C7
4 Towards Learning Manipulation Affordances C11
5 Experimental evaluation C12
6 Conclusions and Future Work C15
References C16

D In-hand Manipulation Using Gravity and Controlled Slip D1
1 Introduction D3
2 Related Work D5
3 Modeling D7
4 Sliding mode control design D8
5 Experimental evaluation D10
6 Conclusions and Future Work D13
References D14

E Adaptive Control for Pivoting with Visual and Tactile Feedback E1
1 Introduction E3
2 Related Work E5
3 Modeling E7
4 Control Design E9
5 Experimental Evaluation E12
6 Conclusions and Future Work E18

References E19

Part I

Introduction

Chapter 1

Introduction

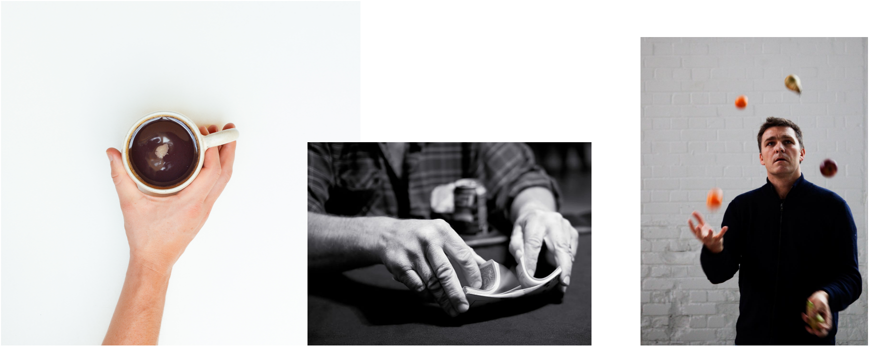

(a) Grasping a cup. Source: [19].

(b) Shuffling cards. Source: [28].

(c) Juggling balls. Source: [48].

Figure 1: Examples of manipulation tasks.

Manipulation is the process of physically interacting with objects using our hands [35]. The most fundamental tasks that we perform on a daily basis, such as drinking a cup of coffee or opening a door, require employing our hands to manipulate different kinds of objects and tools. The ease and precision with which we execute these manipulation tasks is the consequence of a long process which has brought the human species to the forefront of the evolutionary chain. No other animal species can rival humans' manipulation capabilities, and this is not only due to the more advanced mechanical design and dexterity of our hands and body, but also due to e.g. the complex tactile sensing in our skin which allows us to quickly detect when objects are slipping from our hands [27], our vision system which easily detects and recognizes objects in our surroundings, and, above all, our superior brain which swiftly processes all of these sensory signals to control with great precision the required motion of our arms and hands to perform these tasks. Figure 1 shows examples of manipulation tasks, which can be quite diverse in terms of dynamics, ranging from "static" tasks such as grasping and holding a cup, to more dynamic tasks such as shuffling a deck of cards or juggling.

Despite billion dollar investments from the largest tech companies around the world [9], and significant breakthroughs in the development of computer hardware and sensing technologies in recent years, *robotic manipulation* is still far behind what humans can accomplish and it remains largely an unsolved scientific problem. The most trivial manipulation tasks for humans, such as grasping objects and opening doors, are still active research topics even after decades of research efforts.

The only well established robotic manipulation systems are industrial manipulators such as the ones shown in Figure 2 which operate in car manufacturing assembly lines. These industrial manipulators can, however, cannot be classified as intelligent robots since they execute repetitive tasks such as assembly of parts, welding or painting with little to no tolerance for failure or error handling in the task. If part of the manufacturing process fails, e.g. when there is a broken or defective part or a misassembled piece, then the robot usually either lacks sensing capabilities to detect it or intelligent built-in functionality to safely recover from such errors. An experienced human operator must then intervene in the process, and reset the robot to its default operating conditions so that the assembly line can resume normal operation.

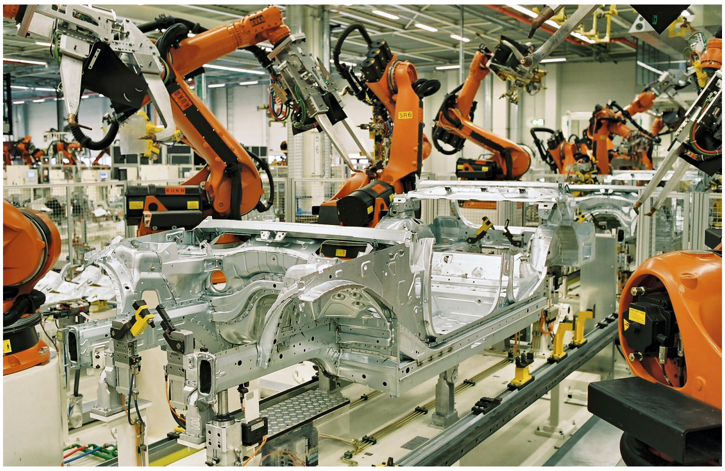

Figure 2: Kuka manipulators welding in a car manufacturing assembly line. Source: [31].

In order to reduce the risk of these errors which stall the manufacturing process, robotics engineers spend considerable effort in designing and tuning the robot workcells so that all of the tools and parts that the manipulator uses are placed at carefully selected locations that the robot knows beforehand with millimetric accuracy. Furthermore, the grippers and tools that are mounted on these manipulators are designed and calibrated specifically for the task that the robot performs, which means that a tremendous engineering effort is required in order to readapt the system to even slight changes in the specifications of the task.

All of these engineering efforts essentially attempt to minimize as much as possible all sources of *uncertainty* in the system. If autonomous robots are to operate in unstructured environments such as households, then they must be capable of coping with imperfect knowledge of the physical properties of objects they intend to manipulate. These may be for instance inertial parameters, friction, stiffness, shape and pose. We can illustrate the problem of uncertainty taking robotic grasping as an example. If the robot underestimates an object's friction coefficient, then it may apply excessive grasping forces to prevent slippage that can potentially damage the object. On the other hand, if the robot overestimates the friction coefficient, then it may apply grasping forces which are insufficient to prevent slippage of the object.

Humans are naturally capable of coping with uncertainty when manipulating objects: we seamlessly grasp and manipulate new objects that we have not encountered before even though we do not know a priori some of its physical properties, such as the weight or friction. Our advanced sensing capabilities allow us to quickly estimate these properties when manipulating the object, while our brain learns and stores this knowledge so that it can be used as a prior next time we encounter the object.

One interesting aspect about many *parametric* uncertainties in manipulation is that they can only be measured once the object has actually been manipulated. Examples include an object's weight, which the robot can only measure once it lifts the object, and friction, which the robot can only estimate if there is relative motion between the hand of the robot and the object. The robot has three possible possibilities to disambiguate these uncertainties:

- *Assume a priori known* physical parameters.
- *Premanipulate* the object prior to execution of the task in order to estimate the parameters.
- *Estimate online* the parameters while executing the manipulation task.

These approaches are not necessarily mutually exclusive, as evidenced by the way humans perform manipulation. Our cognitive system generates *priors* for manipulation which are collected from previous experiences of manipulating similar objects. *Premanipulation* can serve as an initialization step for manipulation, such as when we slightly shake a container to guess the volume of its contents and hence roughly anticipate its weight. *Online estimation* can then be used to compensate for any potential disturbances and/or refine the estimates provided by the priors and premanipulation steps.

Although there has been formidable progress in robotic hardware capabilities in the last decade, they still have significant limitations which hinder robotic manipulation. For instance, 3D cameras have difficulties in detecting transparent objects while most tactile sensors lack the robustness necessary to be used reliably in manipulation tasks.

Robotic hands are no exception to this problem. Most commercially available hands have relatively simple mechanical designs with *limited dexterity*, i.e. they have few degrees of actuation. These kinds of robotic hands are significantly more widespread both in industrial and research robots when compared to dexterous hands with a large number of degrees of freedom. Figure 3 confirms this observation: it shows a picture survey of the grippers available at the *Computer Vision and Active Perception Laboratory* (CVAP) where this thesis was developed.

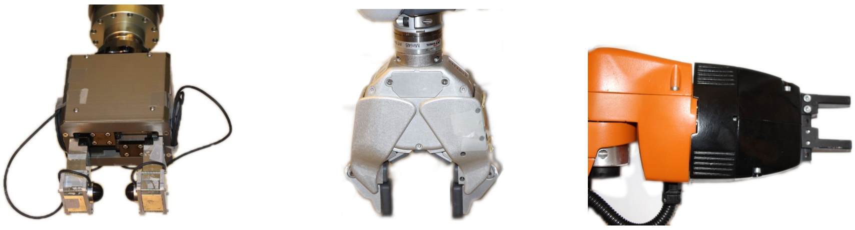

(a) Schunk parallel gripper.

(b) PR2 gripper.

(c) Youbot gripper.

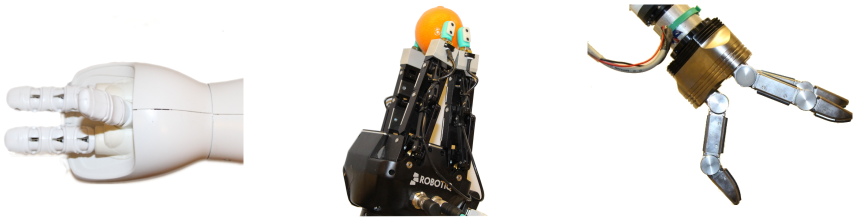

(d) NAO robot gripper.

(e) Robotiq 3-finger gripper.

(f) Schunk Dexterous Hand.

Figure 3: Robotic grippers available at the Computer Vision and Active Perception Laboratory (CVAP), KTH Royal Institute of Technology.

The most striking similarity between the majority of these robotic hands is their simple mechanical design: many of them have only two fingers and/or one degree of actuation as is the case of the Schunk parallel gripper (Figure 3a), the PR2's gripper (Figure 3b), the Youbot's gripper (Figure 3c) and the NAO robot's gripper (Figure 3d). Even more sophisticated hands such as the Robotiq 3-Finger gripper shown in Figure 3e only have one degree of actuation per finger which can be commanded to open/close but there is no encoder feedback which reports back the position of the fingers. The most dexterous hand at CVAP is the Schunk hand shown in Figure 3f with seven degrees of freedom, however this is still far below the number of articulations of the human hand (27) and the bulkiness of the fingers hinders the hand from performing precise manipulation of small objects.

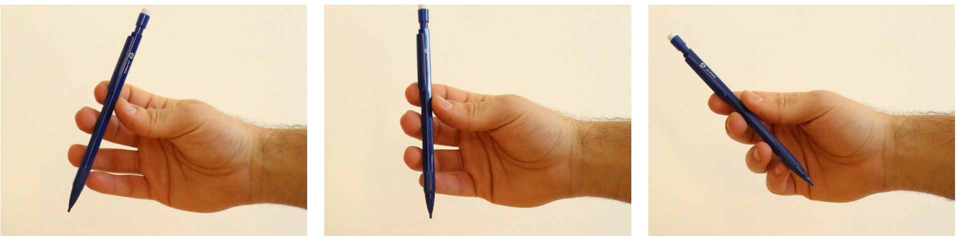

Figure 4: Example of in-hand manipulation by using the fingertips to push a grasped pencil to a new position in the hand.

Robotic hands with just one or two degrees of freedom are far more popular than highly articulated ones mainly due to their reduced cost and complexity as well as their robustness. However, the mechanical simplicity of these hands can represent a challenge when performing *in-hand manipulation* (also referred to in the literature as *regrasping*) which consists of adjusting the relative position between a grasped object and the hand as shown in Figure 4.

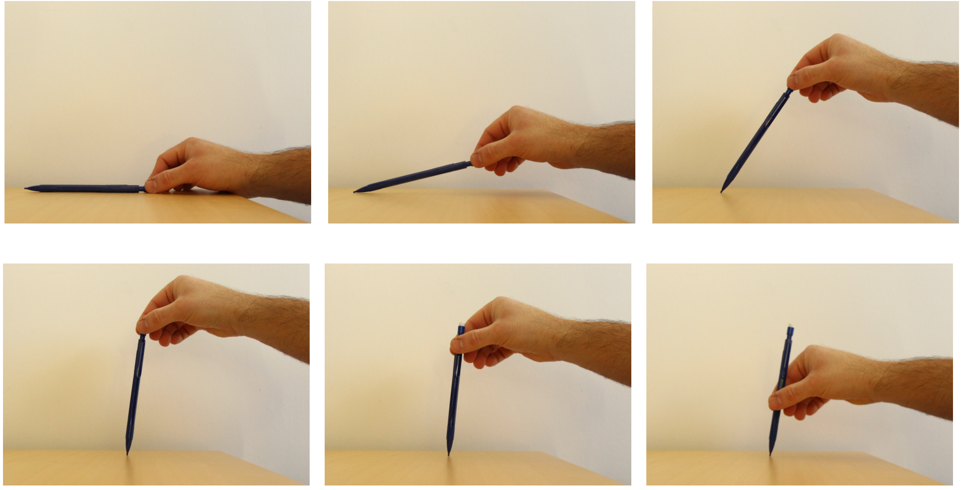

Figure 5: Example of in-hand manipulation by exploiting gravity and contact with the environment.

Humans typically perform in-hand manipulation in order to regrasp an object or tool in a position which is more comfortable or appropriate for performing a given task. We can accomplish this by coordinating the motion of the fingers in order to push, slide and/or roll the grasped object into a new grasp configuration as shown in Figure 4. This is however not possible to replicate in robots with simple hands such as the ones shown in Figure 3, due to their lack of dexterity.

Therefore, manipulation research has recently directed its efforts instead to finding novel ways to exploit resources available in the robot's environment to facilitate in-hand manipulation. Figure 5 illustrates another example of in-hand manipulation of a pencil, but instead of relying on multiple fingers to push the pencil, the person moves its arm and exploits gravity and the stable contact with the table in order to first lift the pencil while allowing it to rotate, and then sliding the fingers down into a position which allows the person to write with the pencil.

This kind of dexterity has been coined in the literature as *extrinsic dexterity* [13]. It represents a fundamental change in the traditional philosophy of improving in-hand manipulation by endowing the robot's hand with multiple fingers, by instead keeping simple hardware and focusing on motion planning and control algorithms that can make clever use of resources external to the robot, such as gravity, inertial forces and external support objects.

1 Thesis Contributions

This thesis focuses on two problems related to robotic manipulation, the first being the uncertainty over physical properties of the objects that the robot manipulates. Many of these properties are unknown a priori to the robot, and they can only be measured either online while performing the task or with some premanipulation procedures prior to the execution of the task.

In our work we focus on kinematic and friction uncertainties in door opening, tool-tip calibration and slippage prediction.

The second problem addressed in this thesis is how to perform in-hand manipulation when the embodiment (hand) of the robot has limited dexterity. We follow the idea of extrinsic dexterity, i.e. to take advantage of resources external to the robot's embodiment, such as gravity in our case.

The specific contributions of the thesis are detailed bellow and Table 1 contains a summary as well as a publication timeline for the topics discussed in this thesis.

Door opening under kinematic uncertainties. We propose online adaptive controllers for manipulating one degree of freedom mechanisms, i.e. doors and drawers. We assume that the robot has already grasped the door's handle and that there is uncertainty regarding the kinematic parameters of the mechanism, such as the direction of motion of the door. The proposed adaptive controllers estimate these parameters while simultaneously moving the mechanism in the desired direction and regulating the forces exerted by the robot. The approach can be used to open different kinds of one degree of freedom mechanisms such as sliding and revolute doors and drawers with velocity controlled manipulators equipped with force/torque sensing.

Contact point estimation. We present an adaptive estimator based on force/torque sensor measurements that determines the location of the contact point between the

Topic	**Conferences and/or journal publications**	**Contributions**
Door opening	IROS[1] 2012 , ICRA[2] 2013, TRO[3] 2016	Implementation and experimental evaluation. Wrote the experimental results section of the paper.
Contact point estimation	ICRA 2014	Implementation and experimental evaluation. Wrote the experimental results section of the paper.
Slippage prediction	Humanoids[4] 2013	Design, implementation and experimental evaluation. Wrote the majority of the paper.
Pivoting using extrinsic dexterity	IROS 2015, ICRA 2016	Design, implementation and experimental evaluation. Wrote the majority of the papers.

[1] IEEE/RSJ International Conference on Intelligent Robots and Systems.
[2] IEEE International Conference on Robotics and Automation.
[3] IEEE Transactions on Robotics.
[4] IEEE-RAS International Conference on Humanoid Robots

Table 1: Summary of contributions of the four topics discussed in this thesis work, along with the conference and/or journal venues in which they have been published.

tip of a tool grasped by a robot and the surface of contact. Contrary to vision-based approaches, this approach does not rely on a priori known visual models of the tool nor is it affected by visual occlusions. The fundamental assumption in this work is that the grasp is rigid, i.e. there is no relative motion between the grasped tool and the robot's hand. In the work we prove theoretically the stability and convergence of the estimator given that the applied forces on the tool tip provide persistent excitation and evaluate the approach experimentally.

Slippage prediction. We introduce a learning method based on Gaussian Processes to estimate the maximum static friction force and torque that a grasp can withstand before slippage of the grasped object occurs. We use a dual arm robot equipped with force/torque sensors and collect training data by holding the object in one hand while sliding or pushing with the other hand to observe the maximum static friction for a set of grasp configurations. Our approach thus combines the robustness of learning methods [3] to modeling errors while providing physical bounds on the stability of the grasp.

Pivoting using extrinsic dexterity. We propose sliding mode and adaptive controllers for pivoting, a type of in-hand manipulation in which an object rotates within the robot's hand. We perform pivoting by allowing gravity to rotate the object towards a desired goal position in the robot's hand while regulation the motion by adjusting the grasping force of a one degree of freedom parallel gripper. Differently from most recent approaches to in-hand manipulation with extrinsic dexterity which use open-loop motion planning approaches [11, 23, 42], we use closed loop feedback control taking into consideration friction and inertial uncertainties. We track the object's orientation through a vision tracking system and use tactile sensing to compensate for errors in the friction parameters.

2 Thesis Outline

The rest of the thesis is structured as follows:

2.1 Chapter 2: Uncertainty and Extrinsic Dexterity in Robotic Manipulation

We discuss the two aforementioned problems pertaining to robotic manipulation which are studied in this thesis: uncertainty about the physical properties of manipulated objects and the lack of (intrinsic) dexterity of robot hands. We motivate the need for online feedback control and estimation as well as learning methods in order to cope with parametric uncertainties inherent to many manipulation tasks. Furthermore, we argue in favor of closed loop controllers that can exploit resources in the robot's environment, i.e. extrinsic dexterity, to perform a wide variety of in-hand manipulation tasks even though the robot hand may be quite limited in terms of dexterity.

2.2 Chapter 3: Summary of Papers

We summarize the conference and journal publications included in Part II of this thesis and their contributions with respect to the state of the art.

2.3 Chapter 4: Conclusion

We conclude with a discussion on the results achieved by this work and the potential work for continuing this in the future.

2.4 Part II: Included Papers

We include one journal and four conference publications in Part II of this thesis. These publications are listed in this section along with their abstract and contributions.

Paper A: An Adaptive Control Approach for Opening Doors and Drawers under Uncertainties

> Yiannis Karayiannidis, Christian Smith, **Francisco E. Viña B.**, Petter Ögren, and Danica Kragic. In *IEEE Transactions on Robotics*, February 2016.

Abstract:
We study the problem of robot interaction with mechanisms that afford one degree of freedom motion, e.g. doors and drawers. We propose a methodology for simultaneous compliant interaction and estimation of constraints imposed by the joint. Our method requires no prior knowledge of the mechanisms' kinematics, including the type of joint — prismatic or revolute. The method consists of a velocity controller which relies on force/torque measurements and estimation of the motion direction, the distance and the orientation of the rotational axis. It is suitable for velocity controlled manipulators with force/torque sensor capabilities at the end-effector. Forces and torques are regulated within given constraints, while the velocity controller ensures that the end-effector of the robot moves with a task-related desired tangential velocity. We give proof that the estimates converge to the true values under valid assumptions on the grasp, and error bounds for setups with inaccuracies in control, measurements, or modelling. The method is evaluated in different scenarios opening a representative set of door and drawer mechanisms found in household environments.
Contribution by the author:
Implemented and evaluated experimentally the adaptive controllers proposed in this paper. Wrote the experimental results section of this paper.

Paper B: Online Contact Point Estimation for Uncalibrated Tool Use

> Yiannis Karayiannidis, Christian Smith, **Francisco E. Viña B.**, and Danica Kragic. In *Proceedings of the 2014 IEEE International Conference on Robotics and Automation (ICRA'14)*, Hong Kong, China, May 2014.

Abstract:
One of the big challenges for robots working outside of traditional industrial settings is the ability to robustly and flexibly grasp and manipulate tools for various tasks. When a tool is interacting with another object during task execution, several problems arise: a tool can be partially or completely occluded from the robot's view, it can slip or shift in the robot's hand - thus, the robot may lose the information about the exact position of the tool in the hand. Thus, there is a need for online calibration and/or recalibration of the tool. In this paper, we present a model-free online tool-tip calibration method that uses force/torque measurements and an adaptive estimation scheme to estimate the point of contact between a tool

and the environment. An adaptive force control component guarantees that interaction forces are limited even before the contact point estimate has converged. We also show how to simultaneously estimate the location and normal direction of the surface being touched by the tool-tip as the contact point is estimated. The stability of the the overall scheme and the convergence of the estimated parameters are theoretically proven and the performance is evaluated in experiments on a real robot.

Contribution by the author:
Implemented and evaluated experimentally the adaptive contact point estimator proposed in this paper. Wrote the experimental results section of the paper.

Paper C: Predicting Slippage and Learning Manipulation Affordances through Gaussian Process Regression

> **Francisco E. Viña B.**, Yasemin Bekiroglu, Christian Smith, Yiannis Karayiannidis and Danica Kragic. In *Proceedings of the 2013 IEEE-RAS International Conference on Humanoid Robots (Humanoids'13)*, Atlanta, USA, October 2013.

Abstract:
Object grasping is commonly followed by some form of object manipulation – either when using the grasped object as a tool or actively changing its position in the hand through in-hand manipulation to afford further interaction. In this process, slippage may occur due to inappropriate contact forces, various types of noise and/or due to the unexpected interaction or collision with the environment.

In this paper, we study the problem of identifying continuous bounds on the forces and torques that can be applied on a grasped object before slippage occurs. We model the problem as kinesthetic rather than cutaneous learning given that the measurements originate from a wrist mounted force-torque sensor. Given the continuous output, this regression problem is solved using a Gaussian Process approach.

We demonstrate a dual armed humanoid robot that can autonomously learn force and torque bounds and use these to execute actions on objects such as sliding and pushing. We show that the model can be used not only for the detection of maximum allowable forces and torques but also for potentially identifying what types of tasks, denoted as *manipulation affordances*, a specific grasp configuration allows. The latter can then be used to either avoid specific motions or as a simple step of achieving in-hand manipulation of objects through interaction with the environment.

Contribution by the author:
Designed the learning framework of maximum static friction forces and torques based on Gaussian Process regression. Implemented the dual arm premanipulation procedures for collecting the required training data. Verified the learned GP model experimentally. Wrote the majority of the paper.

Paper D: In-hand Manipulation Using Gravity and Controlled Slip

> **Francisco E. Viña B.**, Yiannis Karayiannidis, Karl Pauwels, Christian Smith and Danica Kragic. In *Proceedings of the 2015 IEEE/RSJ International Conference on Intelligent Robots and Systems (IROS'15)*, Hamburg, Germany, October 2015.

Abstract:
In this work we propose a sliding mode controller for in-hand manipulation that repositions a tool in the robot's hand by using gravity and controlling the slippage of the tool. In our approach, the robot holds the tool with a pinch grasp and we model the system as a link attached to the gripper via a passive revolute joint with friction, i.e., the grasp only affords rotational motions of the tool around a given axis of rotation. The robot controls the slippage by varying the opening between the fingers in order to allow the tool to move to the desired angular position following a reference trajectory. We show experimentally how the proposed controller achieves convergence to the desired tool orientation under variations of the tool's inertial parameters.

Contribution by the author:
Designed and evaluated experimentally the proposed sliding mode controller for pivoting with gravity and controlled slip. Wrote the majority of the paper.

Paper E: Adaptive Control for Pivoting with Visual and Tactile Feedback

> **Francisco E. Viña B.**, Yiannis Karayiannidis, Christian Smith and Danica Kragic. In *Proceedings of the 2016 IEEE International Conference on Robotics and Automation (ICRA'16)*, Stockholm, Sweden, May 2016.

Abstract:
In this work we present an adaptive control approach for pivoting, which is an in-hand manipulation maneuver that consists of rotating a grasped object to a desired orientation relative to the robot's hand. We perform pivoting by means of gravity, allowing the object to rotate between the fingers of a one degree of freedom gripper and controlling the gripping force to ensure that the object follows a reference trajectory and arrives at the desired angular position. We use a visual pose estimation system to track the pose of the object and force measurements from tactile sensors to control the gripping force. The adaptive controller employs an update law that accommodates for errors in the friction coefficient, which is one of the most common sources of uncertainty in manipulation. Our experiments confirm that the proposed adaptive controller successfully pivots a grasped object in the presence of uncertainty in the object's friction parameters.

Contribution by the author:
Designed and evaluated experimentally the adaptive controller for pivoting an object under uncertainty in the friction coefficient. Wrote the majority of the paper.

Other Publications. I have also contributed to the following publications during my PhD studies, which have not been included in this thesis.

Yuquan Wang, **Francisco E. Viña B.**, Yiannis Karayiannidis, Christian Smith and Petter Ögren. Dual Arm Manipulation using Constraint Based Programming. In *the 19th IFAC World Congress (IFAC'14)*, Cape Town, South Africa, August 2014.

Francisco E. Viña B., Christian Smith, Danica Kragic and Yiannis Karayiannidis. Adaptive Contact Point Estimation for Autonomous Tool Manipulation. In *Autonomous Grasping and Manipulation Workshop. 2014 IEEE International Conference on Robotics and Automation (ICRA'14)*, Hong Kong, China, May 2014.

Yiannis Karayiannidis, Christian Smith, **Francisco E. Viña B.**, and Danica Kragic. Online Kinematics Estimation for Active Human-Robot Manipulation of Jointly Held Objects. In *Proceedings of the 2013 IEEE/RSJ International Conference on Intelligent Robots and Systems (IROS'13)*, Tokyo, Japan, November 2013.

Yiannis Karayiannidis, Christian Smith, **Francisco E. Viña B.**, Petter Ögren, and Danica Kragic. Interactive perception and manipulation of unknown constrained mechanisms using adaptive control. In *Mobile Manipulation Workshop on Interactive Perception. 2013 IEEE International Conference on Robotics and Automation (ICRA'13)*, Karlsruhe, Germany, May 2013.

Yiannis Karayiannidis, Christian Smith, **Francisco E. Viña B.**, Petter Ögren, and Danica Kragic. Model-free robot manipulation of doors and drawers by means of fixed-grasps. In *Proceedings of the 2013 IEEE International Conference on Robotics and Automation (ICRA'13)*, Karlsruhe, Germany, May 2013.

Yiannis Karayiannidis, Christian Smith, **Francisco E. Viña B.**, Petter Ögren, and Danica Kragic. Design of force-driven online motion plans for door opening under uncertainties. In *Workshop on Real-time Motion Planning: Online, Reactive and in Real-time. 2012 IEEE/RSJ International Conference on Intelligent Robots and Systems (IROS'12)*, Vilamoura, Portugal, October 2012.

Yiannis Karayiannidis, Christian Smith, **Francisco E. Viña B.**, Petter Ögren, and Danica Kragic. “Open Sesame!” - Adaptive Force/Velocity Control for Opening Unknown Doors. In *Proceedings of the 2012 IEEE/RSJ International Conference on Intelligent Robots and Systems (IROS'12)*, Vilamoura, Portugal, October 2012.

Chapter 2

Uncertainty and Extrinsic Dexterity in Robotic Manipulation

1 Problem Statement

Robots operating in unstructured environments encounter novel objects in the environment whose physical properties are unknown. Furthermore, even if the robot is manipulating a previously encountered object, its physical properties may change according to how the robot manipulates it, e.g. applying a sufficiently high grasping force can deform the shape of an object. Thus, an important research question is how to formulate control or learning methods for robotic manipulation that can cope with these physical uncertainties and still accomplish the objectives of the manipulation task. Some examples of some of these physical properties (or parameters) and their impact on some manipulation tasks include:

- **Inertial parameters**, i.e. weight, center of mass and moments of inertia. When throwing an object, the amount of throwing force that we need to exert on the object depends on its inertial characteristics.

- **Visual features**, which are necessary in order to visually detect and track the object as it is being manipulated. Humans excel at segmenting and recognizing objects in cluttered scenes as well as estimating their pose. Furthermore, they can perform accurate visual control of the motion of the arm and hand in order to grasp the objects. On the other hand, visual pose estimation and tracking has been a long standing research question in the vision community, and to a large extent remains an unsolved problem today. The most common approach to simplify the problem is to use either fiducial markers or objects with distinctive visual features such as color, shape or texture [40].

- **Kinematic constraints**, which restrict the motion of certain kinds of objects along specific directions. There is a wide spectrum of objects and tools both in household environments and industrial settings which are mechanically designed with kinematic constraints, such as scissors, doors, drawers and cranks as shown in Figure 1. Manipulating these mechanisms along the constraint direction(s) generates undesired forces which need to be regulated by the robot in order to avoid damaging the mechanism and/or robot itself. Furthermore, in order to manipulate (open or close) the mechanism correctly the robot either needs to know a priori which are the directions in which the mechanism affords motion, or it must be able to estimate them online while performing the task.

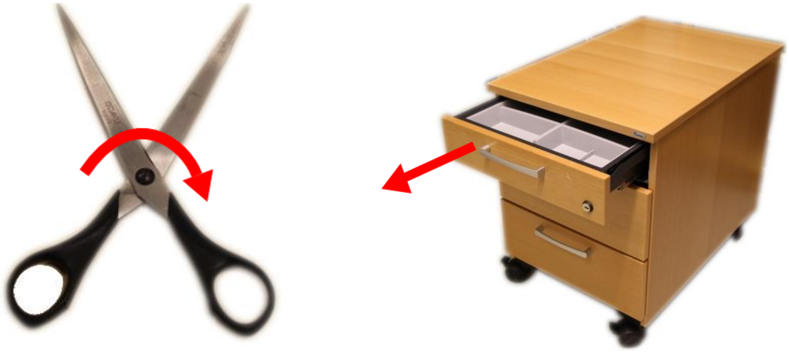

(a) A pair of scissors which affords rotational motion around its hinge.

(b) A drawer which affords linear motion along the indicated direction.

Figure 1: Examples of objects with different kinematic constraints. These objects afford motion along one direction, hence they are commonly referred to as *one degree of freedom mechanisms*.

- **Friction**, which emerges when two surfaces come into contact. It plays a key role in robotic manipulation since some form of contact is required between the robot's embodiment (arms or hands) and manipulated objects. Wrongly estimated friction coefficients can lead to either undesired slippage of the object or excessive grasping forces that can damage te object. It can also generate positioning errors when performing in-hand manipulation tasks where sliding friction is relevant.

In this thesis we focus on parametric uncertainties related to *kinematic constraints* and *friction* properties of objects grasped by the robot. We study the problem of compliant manipulation of different one degree of freedom mechanisms such as revolute and sliding doors and drawers whose kinematic model and parameters are unknown a priori. Furthermore, we study manipulation tasks were the robot exerts forces on a surface with a tool as shown in Figure 2. In these tasks the motion of the tool is constrained by the surface of contact and the kinematic variable of interest is the location of the *contact point* between the tool-tip and the surface. Estimating the location of this contact point is essential for many applications such as drilling or screwing, where the robot must carefully position the tool-tip on a specific location of an object's surface. In our work we also address the research question of how a robot can autonomously learn the maximum *friction* force and torque that a grasp can withstand before the grasped object slips in the robot's hand.

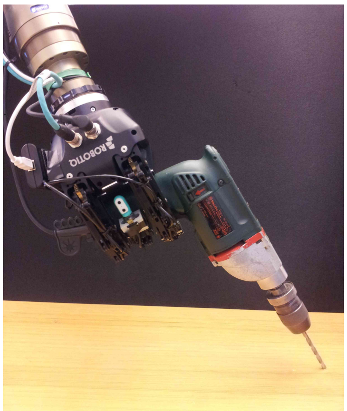

Figure 2: Robot manipulating a tool in contact with a surface.

In-hand manipulation is a fundamental skill required by robots that perform tasks with tools. Many tools, for instance screwdrivers, hammers and drills, need to be grasped in a specific location and orientation in order to afford the execution of the task. However, when the robot initially grasps a tool errors in modeling, grasp execution or at the manipulator control level may cause the resulting grasp to differ from the robot's initially planned grasp. It is then necessary to perform a readjustment of the grasp configuration, which can be done by replacing the tool on its original location (typically a table or some kind of fixture), releasing it and attempting to regrasp it. A more efficient method is to perform *in-hand manipulation*, i.e. to reposition the object without releasing it from the grasp.

The classic approach to in-hand manipulation is to use highly dexterous hands with multiple fingers and joints to push, slide and/or roll the grasped object to a new configuration [12, 15, 20, 38, 46]. However, simple robotic hands with few degrees of freedom lack the dexterity to perform in-hand manipulation in this manner. An alternative is to use *extrinsic dexterity*, i.e. to take advantage of resources external to the robot such as [13]:

- **Inertial forces**. The robot can displace a grasped object by accelerating the manipulator, causing the generated inertial forces on the object to drag it to a new configuration [42].

- **External support objects**. If there are fixed objects in the robot's environment, such as tables, the robot can use them as support for pushing the grasped object into a new relative pose in the hand as shown in Figure 3.

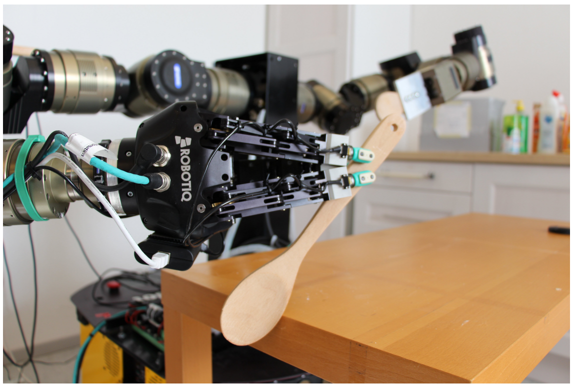

Figure 3: In-hand manipulation by pushing.

- **Gravity**. The robot can momentarily release a grasped object, allowing gravity to pull the object down while closing the grasp once the object reaches the desired location.

From these examples it is evident that there is a broad range of regrasps that can be achieved even with relatively simple robotic hands. These methods can also be combined sequentially in case one of them is insufficient to achieve the desired regrasp [13]. Extrinsic dexterity introduces new research questions regarding perception, control and motion planning for in-hand manipulation, given the uncertainties that take place when interacting with the environment.

In our work we study *pivoting*, which is an in-hand manipulation skill that consists of rotating the manipulated object around a fixed axis. We consider uncertainties in the inertial parameters of the grasped object and the torsional friction coefficient. We formulate the problem from a control perspective, using gravity to rotate the object towards the desired orientation while varying the grasping force of a one degree of freedom parallel gripper in order to control the object's trajectory.

2 Challenges

In this section we describe the scientific challenges related to kinematic and friction uncertainties as well as extrinsic dexterity in manipulation and how they are correlated in certain manipulation tasks. We present previous works related to these research topics and specify which of their shortcomings we address in this thesis work.

2.1 Kinematic uncertainties

When manipulating one degree of freedom mechanisms, the robot may not have a priori knowledge of the kinematic model of the mechanism, i.e. it may not be able to detect if it is a sliding mechanism, such as a sliding door or a drawer, which affords translational motion in a specific direction or if the mechanism rotates around a hinge, as in the case of a revolute door. Furthermore, the robot may be uncertain about kinematic parameters of the mechanism such as the location of the hinge, which determines the radius of the trajectory of revolute doors, and/or the direction of motion in which the mechanism affords motion. It is necessary to have appropriate estimates of these parameters as well as the correct model of the mechanism, since any deviation from the mechanism's nominal trajectory will give rise to interaction forces that need to be regulated, otherwise they can damage the robot and/or mechanism itself.

Velocity filtering solutions have been proposed in the literature to tackle the door kinematics estimation problem. Lutscher et al. propose an admittance controller whose velocity reference is provided by an averaging filter [32]. Ma et al. proposed a velocity and impedance controller for manipulating revolute doors, where the kinematics of the door were estimated based on the measured velocity of the end effector [34]. Position-based estimation of door kinematics has also been considered in several works. For instance, Peterson et al. use the manipulator's end-effector trajectory to estimate the location of the rotation axis and radius of the trajectory of a revolute mechanism [41].

Some works employ probabilistic methods to learn and identify kinematically constrained mechanisms. Sturm et al. use visual measurements to learn the kinematic parameters of doors [43]. Barragan et al. propose a Bayesian identification method where the robot manipulates the mechanism in different directions and classifies the kinematic model among a set of models such as revolute and sliding mechanisms and latches [2]. However, these works do not consider regulation of interaction forces between the robot and the mechanism.

The main limitation with these previous works is that they do not consider simultaneous online kinematics estimation and force regulation. In Paper A we present adaptive controllers which simultaneously estimate the kinematic parameters of the mechanism while manipulating it in a compliant manner such that it regulates the interaction forces. The approach does not require prior information of the kinematic model (revolute door or sliding door/drawer) nor parameters of the door and the adaptive estimates are theoretically proven to achieve correct identification.

Manipulation tasks such as drilling require accurate estimation of the location of the contact point between the tip of a tool held by the robot and a surface of contact. Operators of industrial manipulators typically calibrate the location of the robot's tool-tip manually through a procedure commonly referred to as TCP (Tool Center Point) calibration. The operator carefully places the robot tool-tip in contact with a fixture and reorients the tool in several configurations until the robot obtains enough measurements to estimate the location of the tool-tip. High accuracy can be achieved through this method, but it requires time-consuming, manual calibration from an experienced operator.

Some previous works focus on in-hand localization of objects grasped by the robot. Kubus et al. estimate the pose of grasped objects by using previously identified inertial parameters of the objects [30]. However, this method requires unconstrained motion of the manipulator and object. Hebert et al. fuse vision, force/torque and proprioception data to localize an object held by the robot [22]. This approach requires, however, an a priori known visual model of the object.

Contact point estimation can also be determined by visual tracking of the tool. Krainin et al. propose a framework for building 3D models of objects grasped by the robot, and then using the learned model to track the pose of the object in the robot's hand [29]. The main limitation of vision based approaches is that their performance is sensitive to visual occlusions of the tool or object.

In Paper B we propose an adaptive estimator based on force/torque sensor measurements for contact point estimation. The proposed method does not rely on any model of the tool and is thus not affected by visual occlusions. Furthermore, the adaptive estimator is theoretically proven to converge to the contact point if the forces at the tool-tip provide persistent excitation.

2.2 Friction uncertainties

Friction phenomena arise when two surfaces come into contact. They are a natural component of many grasping and manipulation tasks, for instance:

- Static friction forces are crucial to attain stable grasps on objects. If the applied friction forces are below a certain threshold then the object may begin to slip in the robot's hand [5, 36].
- In-hand manipulation is commonly achieved through some form of sliding of the grasped object in the robot's hand [8, 12]. In this case the kinetic (sliding) friction takes a prominent role as compared to stable grasping.
- Nonprehensile manipulation tasks, i.e. manipulation without form or force closure grasps, are also affected by sliding friction phenomena. Examples of this kind of manipulation include pushing objects in order to slide them on a surface or sliding them in the robot's hand [33].
- Friction forces may not only be present at the task level during manipulation, but also internally in the manipulator itself. The motors of the joints that compose robotic manipulators can exhibit significant static and dynamic friction effects, which need to be compensated appropriately in order to achieve accurate control of the manipulator [14, 16, 39, 50].

Even though friction has been extensively studied by the grasping, manipulation and control community, it remains a formidable challenge in manipulation mainly due to the fact that it is difficult for the robot to know a priori (before manipulating or grasping the object) exactly what are the friction properties of the object. Paradoxically, these properties can actually only be measured once the robot actually manipulates the object, by e.g. pushing it against a table [45].

Another challenging aspect of friction is related to modeling. Several kinds of friction models have been proposed in the literature, which range from classic static models such as the Coulomb friction model to dynamic models such as the *LuGre* friction model, which accounts for friction phenomena such as hysteresis and the rate of change of applied forces [14]. Furthermore, experimental evidence has shown that friction is affected by environmental factors such as humidity, temperature and lubrication of the contacting surfaces.

Nonetheless, the most common approach taken by roboticists for developing manipulation tasks is to assume a friction model which is suitable for the particular task at hand in order to make the problem tractable. The chosen model should be complex enough to model the most relevant dynamics of the system, yet simple enough so that it is feasible to formulate controllers or motion planning algorithms and so that the friction forces expected from the model are measurable by the robot's tactile and/or force sensors.

Given a choice of friction model, what remains unknown are the parameters that define that model. Once again, there are three alternatives to cope with these *parametric uncertainties* of the friction model

- Assume *a priori known* friction parameters.
- *Premanipulate* the object prior to the task in order to estimate its friction properties, i.e. test the object before manipulating it. This can be achieved by e.g. sliding the robot's fingers over the object while it is standing on a table.
- *Estimate online* the friction parameters while performing the manipulation task.

In the case of grasp planning it is commonly assumed that the friction forces follow a classic static Coulomb model [4]

$$f_t \leq \mu_s f_n \tag{2.1}$$

where f_t, f_n are the tangential and normal forces respectively and μ_s is the *static friction coefficient*. The Coulomb model states that slippage of the object occurs when the tangential forces f_t surpass a limit $\mu_s f_n$ proportional to the normal forces and the friction coefficient.

In grasping applications it is usually possible to measure normal forces via tactile or force/torque sensors, therefore one of the main sources of uncertainty is the friction coefficient μ_s. Some works on grasp planning assume the friction coefficient to be known a priori by the robot [6, 17], while other works provide robustness to modeling errors by synthesizing grasps whose stability is less sensitive to changes in the friction coefficient [21].

Research from neuroscience suggests that tactile sensing plays a crucial role even in the most simple manipulation tasks such as picking and placing of objects [27]. The human hand is endowed with advanced tactile afferents that detect both low and high frequency deformations of the skin which can be used for detecting slippage and contact events. These in turn trigger appropriate motor responses for increasing the grasping force to stabilize the grasp or for releasing an object once it has made contact with a surface.

These observations have inspired the development of tactile sensors for the purpose of robotic grasping, specially for slippage detection and control. Tremblay et al. developed tactile sensors which provide measurements of the high frequency vibrations generated on the sensor's surface just before slippage occurs [47]. These signals are then used to estimate the friction coefficient. Holweg et al. perform frequency analysis of tactile signals to detect slippage [24]. Other approaches reported in the literature complement tactile sensing with machine learning techniques [3, 10, 26]. Machine learning is useful for robotic grasping in order to cope with the high degree of modeling uncertainty of the friction phenomena involved. Bekiroglu et al. also merge different sensory modalities such as vision and tactile to classify grasps as stable or unstable before lifting the object [3]

The are a number of issues that make most tactile sensors today unsuitable for robotics applications. On one hand it is not yet a mature technology and lacks standardization. Furthermore, tactile sensors tend to be costly, fragile and noisy, hence they are not as widely used in industrial and research robots as other kinds of sensors. For this reason we propose in Paper C a framework for learning the maximum static friction force and torque by means of dual arm manipulation and force/torque sensors, which are in general more reliable and widespread than tactile sensors. We design dual arm premanipulation procedures in which we grasp an object in one hand and push it with the other hand of the robot in order to observe the maximum static friction forces and torques for a set of parametrized grasps. We then use these measurements to train a Gaussian Process, which in turn can be used to predict the friction of new grasp configurations as well as provide confidence bounds on those estimates.

With in-hand manipulation, it is no longer sufficient to consider solely static friction effects as in grasping since it commonly requires some form of sliding of the grasped object in the robot's hand, therefore sliding friction forces start having a larger influence in manipulation dynamics than their static counterparts. This opens a new range of challenges given the variety of existing sliding friction models and the difficulties involved in estimating their parameters in practice. Since sliding friction is strongly connected to our work on pivoting with extrinsic dexterity, we defer details of this discussion to the next section.

2.3 Extrinsic dexterity

Dafle et al. originally proposed the concept of *extrinsic dexterity*, showing how even simple robotic hands are capable of performing different kinds of regrasps (in-hand manipulation) by exploiting gravity, inertial forces and external support objects [13]. Furthermore, they showed that it is possible to structure these individual in-hand manipulation skills in a graph so that by combining two or more of these skills in sequence the robot can accomplish more sophisticated regrasps. This proof of concept paper clearly illustrated that it is *mechanically* possible for a robot with simple hands to perform in-hand manipulation, without taking into consideration the problem of uncertainty in perception or control that emerge when interacting with the environment which we have discussed in previous sections.

This has been a common trend among the most recent works on in-hand manipulation with extrinsic dexterity. Holladay et al. proposed a motion planning framework for extrinsic *pivoting*, where the robot initially plans a grasping location on an object in order to lift it and exert inertial forces on it so that it rotates to a desired configuration [23]. The authors show that this approach is more efficient than repeatedly repicking and replacing the object on a surface until achieving the desired orientation since it reduces execution time and the required manipulator motion. The proposed approach however assumes knowledge of the torsional friction between the robot's fingertips and the manipulated object and the regrasp is operated in an open loop fashion, hence it cannot compensate for modeling errors or disturbances.

Dafle et al. study the problem of prehensile pushing, i.e. in-hand manipulation by pushing objects in the robot's hand against the environment [11]. In this case in-hand manipulation is enabled by the motion of the manipulator and the availability of fixed contacts ("external pushers") in the environment. The authors study the effects of different contact geometries – point, line and planar contacts – on the motion of the object. The authors assume perfect knowledge of the friction characteristics of the grasped object, its pose relative to the robot's hand and the location of the external pushers. Additionally, the proposed framework operates in an open loop without feedback control.

On the other hand, Shi et al. propose a motion planning framework for sliding objects in the robot's hand by exerting inertial forces on the object generated by the manipulator's trajectory [42]. The approach takes into consideration potential errors of the friction coefficient by repeatedly sliding the object until it reaches the desired configuration. The proposed method is however executed in an open loop, which leads in some cases to errors in the final pose of the manipulated object.

These examples highlight the importance of including feedback control for in-hand manipulation in order to compensate for modeling errors and disturbances in the system. Furthermore, there are two common sources of uncertainty that one can identify in many of the previously mentioned works:

- **Visual tracking** of the manipulated object and/or external objects. Tracking is necessary in order to control the motion of the object and to detect when it has reached the desired pose. In the case of prehensile pushing it is necessary to estimate the location of potential contact surfaces where the robot can push the object.

- **Friction forces**, primarily between the grasped object and the robot's hand. Almost all of the in-hand manipulation skills studied so far in the literature rely on some form of sliding of the grasped object in the robot's hand, therefore the resulting motion of the object is heavily influenced by sliding friction forces. However, these works often assume known friction coefficients

The problem of *visual tracking* is still an open research question in the vision community, and the most common solution employed in manipulation tasks, including our own works on pivoting (Papers D and E) is to use a vision tracking system tuned specifically for the set of objects that the robot manipulates. This is often accomplished by using objects with a priori known visual models with distinctive features such as color, shape or texture.

Friction modeling and control, particularly *sliding* friction, has been extensively studied by the control community. A number of dynamic models have been suggested in the literature such as the *Dahl* model, the *Bristle* model [37] and the *LuGre* model [14]. However, these studies on have been geared towards friction *compensation*, as is typically the case in motors. The main assumption in these works is that the friction forces can be modeled as additive disturbances which need to be estimated and compensated by the controller. In the case of in-hand manipulation, this is a valid assumption if the grasping force is kept fixed.

The previously mentioned works on extrinsic regrasps [11, 23, 42] have considered *fixed pinch grasps*, i.e. grasping with two fingertips, where the distance between the fingers is kept constant, which, in turn, keeps the grasping force and friction at the contact constant as well. However, this friction can be controlled by varying the distance between the fingertips of the robot hand. This represents an additional control input that the robot could exploit to better control the motion of the object during in-hand manipulation. Controlling it appropriately can also help to reduce the required effort of the manipulator, since the robot could decrease the friction at the contact when it needs to slide the object and increase it again once the object is close to its desired position in order to secure the grasp.

In our works on *extrinsic pivoting* (Papers D and E) we show how a a robot can use gravity and friction control to reorient an object in the hand. We use static models based on limit surfaces [18, 25, 51], which are the preferred choice in the literature for in-hand manipulation problems. Furthermore, in Paper E we design adaptive controllers to cope with the problem of uncertainty on the friction coefficients of the limit surface model.

Chapter 3

Summary of Papers

A An Adaptive Control Approach for Opening Doors and Drawers under Uncertainties

In this work we address the problem of manipulation of one degree of freedom mechanisms, such as revolute doors, sliding doors and drawers as shown in Fig. 1. We assume that the kinematic parameters of the mechanism are not known exactly beforehand by the robot, which is a common situation in practice given robot calibration errors or estimation errors from the perception system. These kinematics parameters include the motion axis which is the direction along which the mechanism affords motion (axis $\mathbf{x}_h$ in Fig. 1), the axis of rotation (axis $\mathbf{y}_h$ in Fig. 1a and 1c) and the radius from the door hinge to the handle which is useful for classifying revolute and sliding mechanisms. A door opening controller should be able to estimate these parameters online while manipulating the mechanism as well as regulate the forces applied on the mechanism. Errors in the estimation of these parameters will lead to deviations from the nominal trajectory of the mechanism which in turn will generate undesired forces on the door/manipulator.

A number of solutions to the door opening problem have been proposed in the literature, including velocity averaging solutions [32], position-based estimation [1, 41] and probabilistic approaches [43, 44]. The main limitation with these approaches is that they do not tackle all of the aforementioned problems, i.e. simultaneous estimation of kinematic constraints and control and force regulation while being capable of manipulating different kinds of revolute or sliding mechanisms. In our work we propose adaptive controllers that are able to manipulate the different mechanisms shown in Fig. 1 while simultaneously estimating the kinematic constraints and regulating the forces and torques exerted by the manipulator. The method requires a velocity controlled manipulator equipped with a force/torque sensor. We evaluate the proposed method with different doors and drawers both in simulation and experiments with a robot setup.

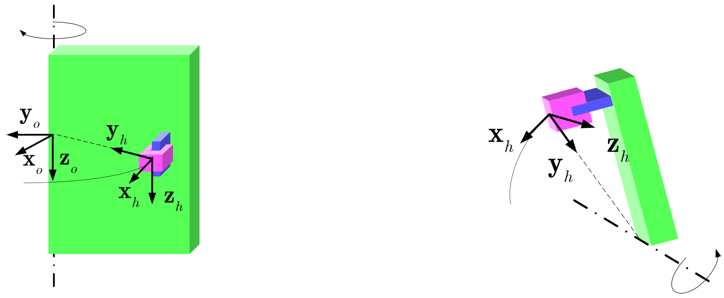
$\mathbf{y}_o$
$\mathbf{x}_o$
$\mathbf{z}_o$
$\mathbf{y}_h$
$\mathbf{x}_h$
$\mathbf{z}_h$
$\mathbf{x}_h$
$\mathbf{y}_h$
$\mathbf{z}_h$

(a) Rotating mechanisms in regular doors and cupboards.

(b) Rotating mechanisms in ovens or washing machines.

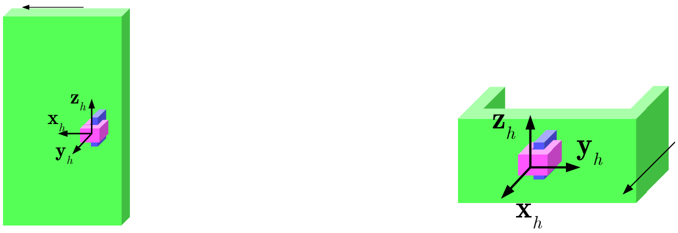
$\mathbf{z}_h$
$\mathbf{x}_h$
$\mathbf{y}_h$
$\mathbf{z}_h$
$\mathbf{y}_h$
$\mathbf{x}_h$

(c) Sliding mechanisms in closets.

(d) Mechanism in drawers.

Figure 1: Examples of rotating/sliding doors and drawers with revolute and prismatic joints.

B Online Contact Point Estimation for Uncalibrated Tool Use

Many robotic applications, such as drilling, require manipulating a tool and making contact with the tool-tip on a surface as shown in Fig. 2. To perform this kind of task it is essential to obtain accurate estimates of the contact point between the tool-tip and the surface of contact.

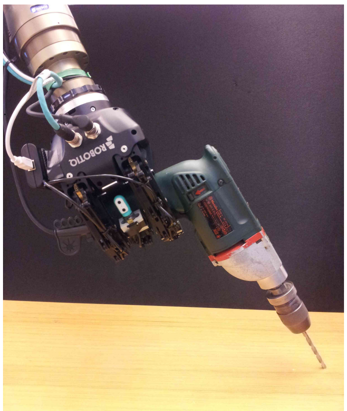

Figure 2: Robot manipulating a tool in contact with a surface.

This problem can be tackled by tracking the tool with a vision system, however the main limitation of vision based approaches is that they normally require an a priori known visual model of the tool and that they have difficulties coping with visual occlusions. A common approach, typically used in industrial settings, is to assume prior knowledge of the tool's geometry and perform an offline calibration procedure to measure the location of the tool-tip.

In this paper we propose an adaptive estimator that uses force-torque sensor measurements to determine the contact location between a tool grasped by the robot and the surface of contact. Thus, the proposed method does not require an a priori known model of the tool. Furthermore, our main assumption is that the tool is held rigidly by the robot. We provide proof that the estimator converges to the actual location of the contact point if certain persistent excitation criteria are fulfilled. Additionally, the estimator operates online while the robot is performing the manipulation task, and we show experimentally that it provides accurate estimates of about 5 mm given for a 30 cm tool length.

C Predicting Slippage and Learning Manipulation Affordances through Gaussian Process Regression

In this work we study the problem of estimating the maximum friction force and torque that an object grasped by the robot can withstand before the object slips. Previous works approach this problem by assuming known geometry and friction coefficient of the grasped objects, which is then used to define a Grasp Wrench Space (GWS) as well as other grasp quality measures which provide an indication of the stability of a grasp [7, 17]. However, the performance of these methods is limited in practice by modeling errors of the object's geometry and its friction characteristics. Other approaches use learning methods to provide some robustness to these modeling errors. Bekiroglu et. al. study the grasp stability assessment problem, where the robot uses visual and tactile feedback to decide if a grasp is stable or not before lifting a grasped object [3]. The proposed learning framework requires human supervision for labeling stable and unstable grasps. The main limitation of this approach is that it does not provide information about physical bounds on the wrenches that the grasp can withstand, but rather a measure of certainty of how stable the grasp is.

In our work we propose learning continuous bounds on the wrenches that can be applied on an object grasped by a robot under different grasp configurations. We thus formulate grasp stability as a regression problem and the robot collects training data via dual arm manipulation actions as shown in Fig. 3. These actions allow the robot to observe the maximum static friction force and torque which we then use to train a Gaussian Process. Our approach thus leverages the robustness of machine learning methods to modeling errors while yielding physical measures of the stability of the grasp.

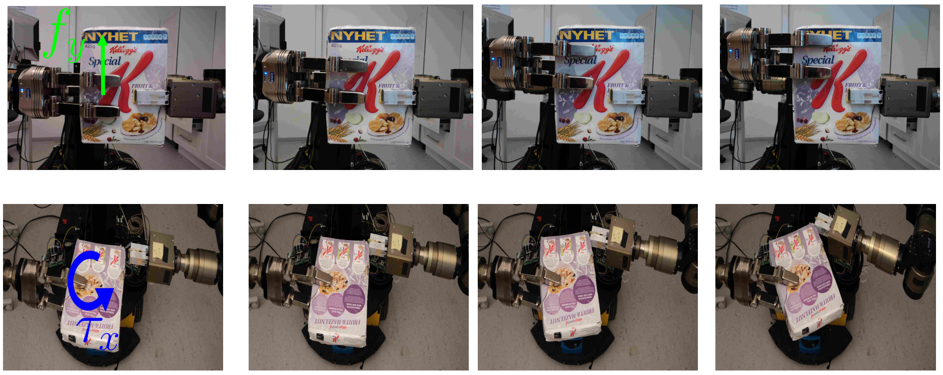

Figure 3: Dual arm manipulation actions for learning static friction. Top row: sliding action for training on the maximum static linear friction f_{slip}. Bottom row: pushing action for training on the maximum static rotational friction τ_{slip}.

D In-hand Manipulation Using Gravity and Controlled Slip

Most commercially available robotic grippers are relatively simple from a mechanical point of view with few degrees of freedom. This is largely due to their lower cost and higher robustness when compared to other more complex robotic grippers. In order to compensate for this lack of dexterity from the hardware, researchers have proposed to use *extrinsic dexterity*, i.e. to take advantage of resources external to the robot in order to perform in-hand manipulation [13]. The robot can use e.g. a table to push an object against it and reposition the object in the grasp or accelerate the manipulator so that the manipulated object slides in the grasp towards a desired configuration. In our work we study the specific in-hand manipulation skill of *pivoting*, which consists of rotating an object in the robot's hand as shown in Fig. 4. The object rotates due to the gravitational pull on its center of mass, while the robot controls the trajectory of the object by modulating the gripper's grasping force. In our work we assume that the robot is equipped with a 1 DOF gripper, that a visual model of the object is available so that its pose can be tracked via a vision system, and that the object rotates around a known rotation axis.

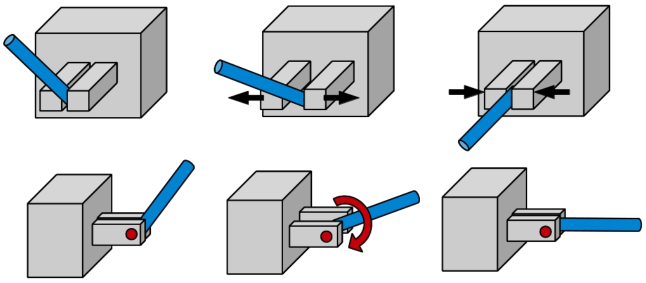

Figure 4: Pivoting with gravity by controlling the gripping force exerted by a two finger pinch grasp. The top row shows how the robot opens and closes the gripper to control the object's rotational motion induced by gravity. The object rotates around a fixed axis of rotation connecting the two fingers as shown in the bottom row.

This approach to pivoting has similarities with previous work on friction modeling and control [14, 37]. However, the majority of these works model friction as a control disturbance to the system, which is estimated and then compensated through a feedforward term in the control signal. In our case, friction is actually a control input to the system, hence we cannot directly apply these previous methods to our work. Other works on use of nonlinear control techniques for Antilock Braking Systems (ABS) do use friction as a control input, but the control objective is to maximize the friction between the road and the vehicle's tires [49].

On the other hand, most recent approaches to in-hand manipulation with extrinsic dexterity use open-loop motion planning strategies [13, 23, 42]. These approaches are not always feasible in practice given the presence of uncertainty on the physical properties of manipulated objects and the environment and since open loop approaches cannot account for disturbances that may arise during execution of the task. In contrast, we propose in our work a sliding mode feedback controller for pivoting which can handle variations of the inertial parameters of the grasped object. The controller uses as input the tracked pose of the object via a vision system and controls the grasping force so that the object reaches the desired orientation. Our experiments show that the proposed controller pivots a grasped object successfully to the desired orientation, despite changes in its inertial parameters.

E Adaptive Control for Pivoting with Visual and Tactile Feedback

In this paper we revisit the in-hand manipulation problem with extrinsic dexterity. We build on the same idea of the previous paper from Section 3.D of pivoting with gravity and controlling the grasped object's slippage via the grasping force. The main addition in this work is to use adaptive control and tactile sensing in the control loop as shown in Fig. 5.

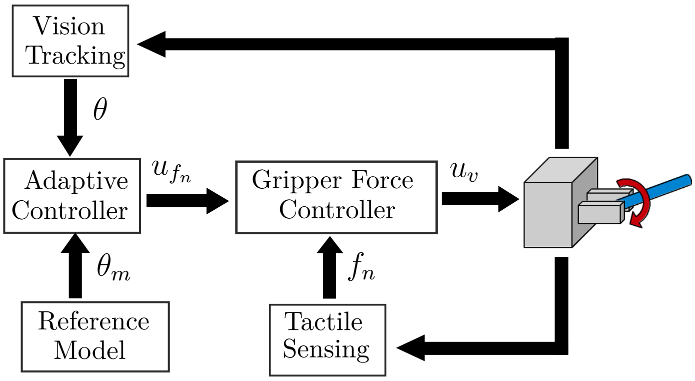

Figure 5: Overview of our proposed adaptive control scheme for pivoting with visual and tactile sensing.

The tactile sensing allows us to control more accurately the grasping force exerted by the gripper on the object and the adaptive controller can adapt to errors in the friction parameters of the object. Previous works on in-hand manipulation often consider the friction coefficient known a priori [11, 23]. In our experiments we illustrate how errors in the friction coefficients can have a negative impact on the tracking performance of a feedback linearization pivoting controller, and how our adaptive controller corrects these errors. Furthermore, we show that the adaptive controller still pivots the object correctly when changing the friction properties of the object.

Chapter 4

Conclusions

This thesis addressed two challenging problems in robotic manipulation, namely kinematic and friction uncertainties of objects manipulated by the robot and how to perform in-hand manipulation with low dexterity robotic hands using the concept of intrinsic dexterity. We studied these problems in several manipulation scenarios such as door opening, tool-tip calibration, slippage prediction and pivoting, and we have shown how different learning and feedback control methods are suitable for coping with uncertainties.

We developed an adaptive control scheme for manipulating one degree of freedom mechanisms. Our method is based on a kineto-static formulation and it is capable of manipulating mechanisms with different types of joints, i.e. revolute or sliding mechanisms, as well as with different grasping constraints of the door handle, such as fixed grasps and passive grasps that afford rotational motion around the door handle. Contrary to previous works, our adaptive control scheme simultaneously estimates the kinematic parameters of the mechanism while regulating the forces exerted on it.

Furthermore, we proposed an adaptive estimator based on force/torque sensing for estimating the location of the contact point between a tool grasped by the robot and a surface of contact. Our approach does not require an a priori model of the tool nor is it sensitive to visual occlusions in contrast to most vision based approaches. Furthermore, the contact point can be estimated autonomously by the robot, while in industrial robots it is commonly performed through a procedure commonly referred to as TCP (Tool Center Point) calibration, where an experienced operator places the robot in at least 4 different orientations with respect to a fixture in the environment.

We have also shown that learning methods are suitable for estimating friction parameters of objects grasped by the robot. We proposed a learning framework with Gaussian Process regression together with dual arm manipulation where the robot can autonomously learn the object's maximum static friction force and torque. The robot grasps the object with one hand and slides or pushes the object with the other hand while monitoring the friction forces through a wrist-mounted force-torque sensor. The maximum force/torque bounds learned by the Gaussian Process can then be used by the robot in order to avoid slippage of the object while manipulating it. On the other hand, it can also serve as an initial step for in-hand manipulation, given that typically in-hand manipulation requires sliding of the object in the robot's hand. With our learned friction model the robot knows the minimum required force and/or torque to break the equilibrium of a given grasp configuration.

Finally, in our work on extrinsic pivoting we have highlighted the importance of feedback control to achieve reliable pivoting in the presence of uncertainties in the friction and inertial parameters. We perform pivoting by using a simple one degree of freedom gripper, where we modulate the applied grasping force in order to allow gravity to reorient the object to the desired configuration. Most recent works have studied in-hand manipulation with extrinsic dexterity from a mechanical and motion planning perspective, disregarding the essential problem of uncertainty, which becomes a highly relevant problem for extrinsic regrasps given that the robot must interact with the environment in order to achieve the manipulation objectives. We designed a sliding mode controller for pivoting an object with uncertain inertial parameters. We also showed how incorrect estimates of the friction coefficient can significantly degrade control performance, and how adding tactile sensing and adaptive control alleviates this issue. Our adaptive controller is also capable of pivoting the object if the material at the surface of contact changes, i.e. if the friction properties of the object change.

1 Future Work

There are a number of directions of research one can explore to follow up on the results and observations formulated in this thesis work. We can expand our adaptive control framework for manipulation of one degree of freedom mechanisms to mechanisms with a larger number of degrees of freedom. Two degree of freedom mechanisms with combined sliding and revolute joints are common e.g. in manufacturing and assembly tasks where the robot has to slide a part of a device such as a cell phone battery into the phone. Due to modeling, perception or control errors there may be some uncertainty regarding the location of the grasped pieces in the robot's hands. This uncertainty can generate undesired forces that need to be compensated at the control level. Furthermore, in order to formulate a controller for this assembly task the robot requires knowledge of the contact point between the pieces, which we can obtain through the adaptive estimators proposed in this thesis.

Furthermore, we can complement our control formulation for pivoting with other forms of in-hand manipulation where friction uncertainties are relevant, such as in extrinsic pushing or by exerting inertial forces by accelerating the robot manipulator. In the case of extrinsic pivoting by pushing the grasped object against another fixed object in the environment, the generated kinematic constraints resemble our work on door opening. By combining these different methods we can achieve a more diverse set of regrasps.

Another interesting venue of future work connected to extrinsic regrasps is related to grasp planning. Both our work and most recent works assume a given grasp configuration before the robot performs in-hand manipulation. However, the way that the robot grasps the object determines a set of kinematic constraints that may or may not afford the execution of the desired regrasp. In the case of our work on pivoting we assume that the robot initially grasps the object at one of its edges so that the gravitational torque generated on the object's center of mass is sufficient to reorient it to the desired position. Furthermore, the initial grasp also contains the axis of rotation along the direction of actuation of the fingertips. The robot should thus be capable of autonomously planning grasp configurations that afford the required regrasps.

Another interesting avenue of research would be an integration of the approaches proposed here. We can for instance use our learning framework of static friction forces as an initialization step for in-hand manipulation, where we refine the friction estimates through adaptive control.

Bibliography

[1] Saleh Ahmad, Hongwei Zhang, and Guangjun Liu. Multiple working mode control of door opening with a mobile modular and reconfigurable robot. *IEEE/ASME Trans. on Mechatronics*, 18(3):833–844, 2013.

[2] P. R. Barragan, L. P. Kaelbling, and T. Lozano-Perez. Interactive bayesian identification of kinematic mechanisms. In *IEEE International Conference on Robotics and Automation*, pages 2013–2020, May 2014.

[3] Y. Bekiroglu, J. Laaksonen, J.A. Jorgensen, V. Kyrki, and D. Kragic. Assessing grasp stability based on learning and haptic data. *IEEE Transactions on Robotics*, 27(3):616–629, june 2011.

[4] A. Bicchi. On the closure properties of robotic grasping. *The International Journal of Robotics Research*, 14(4):319–334, 1995.

[5] A. Bicchi and V. Kumar. Robotic grasping and contact: a review. In *IEEE International Conference on Robotics and Automation*, volume 1, pages 348 –353 vol.1, 2000.

[6] C. Borst, M. Fischer, and G. Hirzinger. Grasping the dice by dicing the grasp. In *Proc. IEEE International Conference on Intelligent Robots and Systems*, volume 4, pages 3692 – 3697 vol.3, oct. 2003.

[7] Ch. Borst, M. Fischer, and G. Hirzinger. Grasp planning: how to choose a suitable task wrench space. In *Proc. IEEE International Conference on Robotics and Automation*, volume 1, pages 319 – 325 Vol.1, april-1 may 2004.

[8] D. L. Brock. Enhancing the dexterity of a robot hand using controlled slip. 1987.

[9] K. Buchan. Google's robot army in action. `http://www.theguardian.com/technology/2014/feb/10/robots-artificialintelligenceai`, February 2014. Accessed: February 17th, 2016.

[10] G. Canepa, R. Petrigliano, M. Campanella, and D. De Rossi. Detection of incipient object slippage by skin-like sensing and neural network processing.

IEEE Transactions on Systems, Man, and Cybernetics, 28(3):348 –356, jun 1998.

[11] N. Chavan-Dafle and A. Rodriguez. Prehensile pushing: In-hand manipulation with push-primitives. In *IEEE/RSJ International Conference on Intelligent Robots and System*, pages 6215–6222, 2015.

[12] A.A. Cole, Ping Hsu, and S.S. Sastry. Dynamic control of sliding by robot hands for regrasping. *IEEE Transactions on Robotics and Automation*, 8(1): 42–52, Feb 1992.

[13] N.C. Dafle, A. Rodriguez, R. Paolini, Bowei Tang, S.S. Srinivasa, M. Erdmann, M.T. Mason, I. Lundberg, H. Staab, and T. Fuhlbrigge. Extrinsic dexterity: In-hand manipulation with external forces. In *IEEE International Conference on Robotics and Automation*, pages 1578–1585, May 2014.

[14] C.C. De Wit, H. Olsson, K.J. Åström, and P. Lischinsky. A new model for control of systems with friction. *IEEE Transactions on Automatic Control*, 40 (3):419–425, Mar 1995.

[15] L. Droukas, Y. Karayiannidis, and Z. Doulgeri. Force/position/rolling control for spherical tip robotic fingers. In *IEEE/RSJ International Conference on Intelligent Robots and Systems*, pages 858–863, Sept 2015.

[16] M. Feemster, P. Vedagarbha, D.M. Dawson, and D. Haste. Adaptive control techniques for friction compensation. In *American Control Conference*, volume 3, pages 1488–1492 vol.3, Jun 1998.

[17] C. Ferrari and John Canny. Planning optimal grasps. In *Proc. IEEE International Conference on Robotics and Automation*, pages 2290–2295 vol.3, 1992.

[18] S. Goyal. *Planar sliding of a rigid body with dry friction: limit surfaces and dynamics of motion.* PhD thesis, Cornell University, 1989.

[19] E. Gregory. Mans hand holding coffee cup on white background, September 2014. URL `https://www.pexels.com/photo/coffee-cup-hand-mug-5172/`. Accessed: February 17th, 2016.

[20] L. Han and J. C. Trinkle. Dextrous manipulation by rolling and finger gaiting. In *IEEE International Conference on Robotics and Automation*, volume 1, pages 730–735 vol.1, May 1998.

[21] K. Hang, F. T Pokorny, and D. Kragic. Friction coefficients and grasp synthesis. In *IEEE/RSJ International Conference on Intelligent Robots and Systems*, pages 3520–3526, 2013.

[22] P. Hebert, N. Hudson, J. Ma, and J. Burdick. Fusion of stereo vision, force-torque, and joint sensors for estimation of in-hand object location. In *IEEE International Conference on Robotics and Automation*, pages 5935–5941, 2011.

[23] A. Holladay, R. Paolini, and M.T. Mason. A general framework for open-loop pivoting. In *IEEE International Conference on Robotics and Automation*, pages 3675–3681, May 2015.

[24] EGM Holweg, H Hoeve, W Jongkind, L Marconi, C Melchiorri, and C Bonivento. Slip detection by tactile sensors: algorithms and experimental results. In *IEEE International Conference on Robotics and Automation*, volume 4, pages 3234–3239, 1996.

[25] R. D. Howe and M. R. Cutkosky. Practical force-motion models for sliding manipulation. *The International Journal of Robotics Research*, 15(6):557–572, 1996.

[26] N. Jamali and C. Sammut. Slip prediction using hidden markov models: Multidimensional sensor data to symbolic temporal pattern learning. In *IEEE International Conference on Robotics and Automation*, pages 215–222, 2012.

[27] R. S. Johansson and J. R. Flanagan. Coding and use of tactile signals from the fingertips in object manipulation tasks. *Nature Reviews Neuroscience*, 10 (5):345–359, 2009.

[28] T. Klassy. Man's hand holding coffee cup on white background, November 2005. URL `https://en.wikipedia.org/wiki/File:Riffle_shuffle.jpg`. Accessed: February 17th, 2016.

[29] Michael Krainin, Peter Henry, Xiaofeng Ren, and Dieter Fox. Manipulator and object tracking for in-hand 3d object modeling. *The International Journal of Robotics Research*, 30(11):1311–1327, 2011.

[30] D. Kubus, T. Krüger, and F. M. Wahl. On-line rigid object recognition and pose estimation based on inertial parameters. In *EEE/RSJ International Conference on Intelligent Robots and Systems*, pages 1402–1408, San Diego, CA, 2007.

[31] BMW Werk Leipzig. Spot welding in the automotive industry. `https://en.wikipedia.org/wiki/KUKA#/media/File:BMW_Leipzig_MEDIA_050719_Download_Karosseriebau_max.jpg`, July 2005. Accessed: March 24th, 2016.

[32] E. Lutscher, M. Lawitzky, G. Cheng, and S. Hirche. A control strategy for operating unknown constrained mechanisms. In *IEEE International Conference on Robotics and Automation*, pages 819–824, may 2010.

[33] K.M. Lynch and M.T. Mason. Stable pushing: Mechanics, controllability, and planning. *The International Journal of Robotics Research*, 15(6):533–556, 1996.

[34] D. Ma, H. Wang, and W. Chen. Unknown constrained mechanisms operation based on dynamic hybrid compliance control. In *IEEE International Conference on Robotics and Biomimetics*, pages 2366–2371, dec. 2011.

[35] M.T. Mason. *Mechanics of Robotic Manipulation*. MIT Press, 2001. ISBN 9780262133968.

[36] C. Melchiorri. Slip detection and control using tactile and force sensors. *IEEE/ASME Transactions on Mechatronics*, 5(3):235 –243, sep 2000.

[37] H. Olsson, K. J. Åström, C. C. De Wit, M. Gäfvert, and P. Lischinsky. Friction models and friction compensation. *European journal of control*, 4(3):176–195, 1998.

[38] E. Paljug, X. Yun, and V. Kumar. Control of rolling contacts in multi-arm manipulation. *IEEE Transactions on Robotics and Automation*, 10(4):441–452, Aug 1994.

[39] G. Palli, G. Borghesan, and C. Melchiorri. Modeling, identification, and control tendon-based actuation systems. *IEEE Transactions on Robotics*, 28(2):277–290, April 2012.

[40] K. Pauwels and D. Kragic. Simtrack: A simulation-based framework for scalable real-time object pose detection and tracking. In *IEEE/RSJ International Conference on Intelligent Robots and Systems*, 2015.

[41] L. Peterson, D. Austin, and D. Kragic. High-level control of a mobile manipulator for door opening. In *IEEE/RSJ International Conference on Intelligent Robots and Systems*, volume 3, pages 2333–2338, 2000.

[42] J. Shi, J.Z. Woodruff, and K.M. Lynch. Dynamic in-hand sliding manipulation. In *IEEE/RSJ International Conference on Intelligent Robots and Systems*, pages 870–877, 2015.

[43] J. Sturm, A. Jain, C. Stachniss, C.C. Kemp, and W. Burgard. Operating articulated objects based on experience. In *IEEE/RSJ International Conference on Intelligent Robots and Systems*, pages 2739–2744, 2010.

[44] J. Sturm, C. Stachniss, and W. Burgard. A probabilistic framework for learning kinematic models of articulated objects. *Journal of Artificial Intelligence Research*, 41:477–526, 2011.

[45] T. Sugaiwa, G. Fujii, H. Iwata, and S. Sugano. A methodology for setting grasping force for picking up an object with unknown weight, friction, and stiffness. In *IEEE-RAS International Conference on Humanoid Robots*, pages 288 –293, dec. 2010.

[46] K. Tahara, S. Arimoto, and M. Yoshida. Dynamic object manipulation using a virtual frame by a triple soft-fingered robotic hand. In *IEEE International Conference on Robotics and Automation*, pages 4322–4327, May 2010.

[47] M.R. Tremblay and M.R. Cutkosky. Estimating friction using incipient slip sensing during a manipulation task. In *Proc. IEEE International Conference on Robotics and Automation*, pages 429 –434 vol.1, may 1993.

[48] A. Tyler. Ewen 'the juggler' sturgeon, February 2009. URL `https://www.flickr.com/photos/andy_tyler/3308288463`. Accessed: February 22nd, 2016.

[49] C. Ünsal and P. Kachroo. Sliding mode measurement feedback control for antilock braking systems. *IEEE Transactions on Control Systems Technology*, 7(2):271–281, March 1999.

[50] W. F. Xie. Sliding-mode-observer-based adaptive control for servo actuator with friction. *IEEE Transactions on Industrial Electronics*, 54(3):1517–1527, June 2007.

[51] N. Xydas and I. Kao. Modeling of contact mechanics and friction limit surfaces for soft fingers in robotics, with experimental results. *The International Journal of Robotics Research*, 18(9):941–950, 1999.

Part II

Included Publications

Paper A

An Adaptive Control Approach for Opening Doors and Drawers under Uncertainties

Published in
IEEE Transactions on Robotics, February 2016

An Adaptive Control Approach for Opening Doors and Drawers under Uncertainties

Yiannis Karayiannidis, Christian Smith, Francisco E. Viña B.,
Petter Ögren, and Danica Kragic

Abstract

We study the problem of robot interaction with mechanisms that afford one degree of freedom motion, e.g. doors and drawers. We propose a methodology for simultaneous compliant interaction and estimation of constraints imposed by the joint. Our method requires no prior knowledge of the mechanisms' kinematics, including the type of joint — prismatic or revolute. The method consists of a velocity controller which relies on force/torque measurements and estimation of the motion direction, the distance and the orientation of the rotational axis. It is suitable for velocity controlled manipulators with force/torque sensor capabilities at the end-effector. Forces and torques are regulated within given constraints, while the velocity controller ensures that the end-effector of the robot moves with a task-related desired tangential velocity. We give proof that the estimates converge to the true values under valid assumptions on the grasp, and error bounds for setups with inaccuracies in control, measurements, or modelling. The method is evaluated in different scenarios opening a representative set of door and drawer mechanisms found in household environments.

1 Introduction

Robots operating in domestic environments need the ability to interact with doors, drawers, and cupboards, all of which exhibit various kinematic constraints due to the joints attaching them to the environment. The variation in size, orientation and type of joints makes it intractable to provide a robot with predefined kinematic models of all the mechanisms it may encounter. Prior knowledge of mechanisms could conceptually be combined with observations from cameras, laser-range finders or other distal sensors to infer a prior model of a mechanism. However, in domestic and other human-centric environments, occlusions, poor lighting, and the presence of previously un-encountered mechanism types make it very difficult to produce reliable systems based on these approaches. One could also imagine a situation where the constraints change dynamically during the manipulation, for example if the constraints are imposed on the mechanism by another agent — e.g. a human doing collaborative work with robot — whose intended actions cannot be inferred from prior observation alone [15]. Therefore, the performance, robustness, and generality of constrained manipulation tasks can be significantly improved if the need to have prior knowledge of the constraints is removed. In the general case, the uncertainties in the manipulation of such constrained kinematic mechanisms, e.g. doors and drawers, can be divided into two main categories:

Dynamic uncertainties which are related to the dynamic model of the door or the drawer: door's inertia, dynamics of the hinge mechanism etc.

Kinematic or Geometric uncertainties which are related to the kinematic model of the door or the drawer: type of the joint that models the kinematic mechanism, which may be prismatic or revolute, size of the door, location and orientation of the hinge, etc.

This categorization has been applied to several problems in robot control, like motion control [6] and force/motion control [5]. From a control perspective, the door opening problem can be regarded as a force/motion control problem in which the robot workspace can be divided into motion and force controlled subspaces according to the concept of hybrid force/motion control [30, 37]. In robot interaction tasks, the identification of geometric or kinematic uncertainties is crucial for defining a kinetostatically consistent Task Frame [4] to correspond to a real compliant motion. Several different methods have been proposed for directly calculating or estimating kinematic parameters, that can be twist-based or wrench-based, by exploiting the concept of reciprocity under ideal conditions [8]. For manipulation of kinematically constrained objects like doors and drawers, twist-based estimation has been used (Section 2) since it is more robust when forces e.g. friction or rotational spring forces arise along the motion directions. A common characteristic shared by the majority of the works proposed in the literature is that the combined dynamics of estimation, tracking, and force control are not considered. This can been considered as a source of disturbance to the identification (which may result in inaccurate and unsafe task execution), as have been pointed out in e.g. [3].

In this work, we consider a general robotic setup with a manipulator equipped with a wrist force/torque sensor, and we propose an adaptive controller which can be easily implemented for dealing with the kinematic uncertainties of doors and drawers. The proposed control scheme which is inspired by the adaptive surface slope learning [13] does not require accurate identification of the constraints at each step of the door/drawer opening procedure as opposed to the majority of the solutions to this problem (Section 2). It uses adaptive estimates of the motion and constraint parameters that converge to the actual dynamically changing radial direction during the procedure.

The paper is organised as follows: In Section 2 we make an overview of the related work to the door opening problem. Section 3 provides description of the kinematic model of the system and the problem formulation. The proposed solution and the corresponding stability analysis are given in Section 4 followed by the simulation examples in Section 5 and the experimental results in Section 6. In Section 7 the final outcome of this work is briefly discussed.

2 Related Work and our Contributions

Pioneering work on the door opening problem is presented in [23] and [24]. Experiments on door opening with an autonomous mobile manipulator assuming a known door model were performed in [23], using the combined motion of the manipulator and the mobile platform. In [24] a method estimating the constraints describing the door motion kinematics is proposed, based on the observation that ideally the motive force should be applied along the direction of the end-effector velocity. To overcome the problems of chattering due to measurement noise and ill-definedness of the normalization for slow end-effector motion, spatial filtering is proposed, but this may cause lag and affect the system stability. The use of velocity measurements to estimate the direction of motion has inspired the recent work of [21] using a moving average filter in the velocity domain. An estimator is used to provide a velocity reference for an admittance controller. Ill-defined normalizations and estimation lags are not treated. Estimating constraints with velocity measurements is also done in [22], applying velocity and impedance control along the tangent and the radial axis of the door opening trajectory respectively.

Several position-based estimation techniques have also been proposed to estimate geometric characteristics of the mechanism rather than the motion direction. Since estimation does not guarantee identification in each control step, those methods have been coupled with controllers providing the system with the proper compliance to absorb inaccuracies of the planned trajectories. In [26], the recorded motion of the end-effector is used in a least-squares approximation to estimate the center and the radius of the motion arc, and a compliant controller is used to cancel the effects of the high forces exerted due to inaccurate trajectory planning. A similar approach is presented in [1]. An optimization algorithm using the position of the end-effector was used in [11, 12]. The algorithm produces estimates of the radius and the center of the door and, subsequently of the control directions. The velocity reference is composed of a feedforward estimated tangential velocity and radial force feedback while an equilibrium point control law enables a viscoelastic behavior of the system around an equilibrium position. In [28, 29], an inverse Jacobian velocity control law with feedback of the force error following the Task Space Formalism [4] is considered. In order to obtain the natural decomposition of the task, which is essential within this framework, the authors propose to combine several sensor modalities so that robust estimation is established. In [29], the estimation is based on the end-effector trajectory, to align the task frame with the tangent of the hand trajectory.

On the other hand, probabilistic methods that are off-line and do not consider interaction force issues have been used for more advanced estimation tasks. In [36], a probabilistic framework for learning the kinematic model of articulated objects (object's parts connectivity, degrees of freedom, kinematic constraints) is proposed. The learning procedure requires a set of motion observations of the doors. The estimates are generated in an off-line manner and can feed force/position Cartesian controllers [35]. Probabilistic methods — particle filters and extended Kalman filters — for mobile manipulation have also been applied to simultaneously estimate the position of the robot and the angle of the door using, however, an a priori defined detailed model of the door [27].

Other work on door opening exploits advanced hardware capabilities. In [31], a combination of tactile-sensor and force-torque sensor is used to control the position and the orientation of the end-effector with respect to the handle. In [18], a specific hardware configuration with clutches that disengage selected robot motors from the corresponding actuating joints and hence enable passive rotation of these joints is used. Since no force sensing is present, a magnetic end-effector was used which cannot always provide the appropriate force for keeping the grasp of the handle fixed. The DLR lightweight robot controlled via Cartesian impedance control based on joint torque measurements is used for door opening in [25]. In [20], the authors present experiments using a force/torque sensor on a custom lightweight robot to define the desired trajectory for a door opening task. In [2], a method for door opening that uses an impulsive force exerted by the robot to a swinging door is proposed. A specific dynamic model for the door dynamics is used to calculate the initial angular velocity which is required for a specific change of the door angle, and implemented on the humanoid robot HRP-2. In [7], a multi-fingered hand with tactile sensors grasping the handle is used, and the geometry of the door is estimated by observing the positions of the fingertips while slightly and slowly pulling and pushing the door in position control. In a subsequent step, the desired trajectory is derived from the estimation procedure, and is used in a position controller.

Table 1 summarizes the literature on door opening and provides a comparison to our work. In the table, the term *force control* designates work that explicitly controls or limits the interaction forces, *online, real-time* implies that the method can be used to open a door directly, at human-like velocities, without any prior learning step, *moderate hardware requirements* means that the method can be used on a simple manipulator with velocity control and a force/torque sensor, and *revolute doors* and *sliding doors* describe what types of door kinematics that can be handled by the method. *Estimate of constraints* indicates methods that produce an estimate of the current kinematic constraints of a mechanism, while *estimate of geometry* indicates methods that produce an explicit estimate of the geometry of the door mechanics themselves. *Unknown model* indicates methods that will work properly even if the model (type of mechanism, i.e. revolute or prismatic joint) is not known a priori, and *unknown parameters* indicates methods that will work if the parameters of the mechanism (i.e. hinge position or motion axis of prismatic joint) are not known a priori. Finally, *proven parameter identification* states whether proofs are provided for the convergence of estimates.

In previous work, we presented a control algorithm for estimating the center of

Table 1: Comparison of related works and this paper.

Publications	[23]	[24]	[21]	[22]	[26]	[11] [12]	[28]	[7]	[36]	[27]	[25]	[18]	[2]	proposed approach
Force control	✓	✓	✓	✓	✓	✓	✓	✓			✓	✓	✓	✓
Online, real-time	✓	✓	✓	✓	✓	✓	✓				✓	✓	✓	✓
Moderate H/W Spec.	✓	✓	✓	✓	✓	✓	✓	[1]	✓	✓	[2]	[3]	[4]	✓
Revolute Doors	✓	✓	✓	✓	✓	✓	✓	✓	✓	✓	✓	✓	✓	✓
Sliding Doors		✓	✓	✓		✓	✓		✓	✓	✓			✓
Estimate of Constraints		✓	✓	✓	✓	✓		✓	✓					✓
Estimate of Geometry					✓	✓		✓	✓					✓
Unknown Model		✓	✓	✓		✓			✓		✓		✓	✓
Unknown Parameters		✓	✓	✓	✓	✓		✓	✓				✓	✓
Proven Param. Identification														✓

[1] Multifingered hand with tactile sensors

[2] Compliant joints (torque feedback at the joint level) − DLR lightweight robot II

[3] Joint compliance by using clutches to engagedisengage motors

[4] Use of the humanoid robot HRP−2

rotation for a revolute door, exploiting the torque or velocity inputs. We proved that we can identify the constraint direction as well as achieve velocity/force tracking for smooth door opening [14, 16]. The method assumes a revolute joint and free rotation of the hand, but the center of rotation is considered uncertain, thus limiting the approach to planar problems. The proposed update law uses a projection operator to guarantee well-defined updated estimates; the use of a projection set constrains the range of uncertainties that can be dealt with. In [17], we proposed a control scheme treating both sliding doors/drawers and revolute-joint doors with arbitrary hinge orientations, by assuming grasps to be fixed and will not rotate around the handle. Furthermore, the design of the update law does not require a projection operator since it produces inherently well-defined estimates that converge to the actual values.

In the work presented here, we propose a unified controller for both revolute and prismatic mechanisms, with formulations for both fixed and non-fixed grasps, and present experimental results on a real robot that demonstrate its performance on a range of different doors and drawers. The contribution of our work compared to the existing literature is a method that simultaneausly treats all of the following:
— Our method can be applied to open both rotational and sliding doors, without requiring ill-defined normalization.
— Our method is not based on unusual hardware capabilities and can be implemented in any velocity controlled manipulator with the capability to measure or estimate the forces and torques at the end effector.
— Our method is theoretically proven to achieve identification of the motion direction simultaneously with force/velocity convergence, by explicitly considering adaptive estimates in the controller design.

3 System and Problem Description

Generally, doors and drawers can be opened by grasping the handle and moving it along its intended trajectory of motion: along a circular path for hinged mechanisms, or along a linear path for sliding doors and drawers. We now formally define the problem of door/drawer opening under uncertainty, where the position of hinges, or direction of possible sliding motion is not known a priori.

3.1 Notation and Preliminaries

We introduce the following notation:

- Bold small letters denote vectors and bold capital letters denote matrices. Hat $\hat{\cdot}$ and tilde $\tilde{\cdot}$ denote estimates and errors between control variables and their corresponding desired values/vectors respectively. Notation $\cdot^{\top}$ denotes the transpose of a vector/matrix.
- The generalized position of a frame $\{i\}$ with respect to a frame $\{j\}$ is described by a position vector ${}^{j}\mathbf{p}_{i} \in \mathbb{R}^{m}$ and a rotation matrix ${}^{j}\mathbf{R}_{i} \in SO(m)$ where

$m = 2$ or 3 for the planar and spatial case respectively. In case $\{j\} \equiv \{B\}$ where $\{B\}$ is the robot world inertial frame (typically located at the base of the robot) the left superscript is omitted. Each column of ${}^{j}\mathbf{R}_i$ is denoted by ${}^{j}\mathbf{x}_i \equiv \mathbf{R}_j^\top \mathbf{x}_i$, ${}^{j}\mathbf{y}_i \equiv \mathbf{R}_j^\top \mathbf{y}_i$, ${}^{j}\mathbf{z}_i \equiv \mathbf{R}_j^\top \mathbf{z}_i$ where $\mathbf{x}_i$, $\mathbf{y}_i$, $\mathbf{z}_i$ denote the columns of the rotation matrix $\mathbf{R}_i$ that describes the orientation of the frame $\{i\}$ with respect to the robot world inertial frame.

- The projection matrix on the orthogonal complement space of a unit three dimensional vector $\mathbf{a}$ is denoted by $\mathbf{P}(\mathbf{a})$ with $\mathbf{P}(\mathbf{a}) = \mathbf{P}^\top(\mathbf{a})$ is defined as follows:
$$\mathbf{P}(\mathbf{a}) = \mathbf{I}_3 - \mathbf{a}\mathbf{a}^\top$$
- $\mathcal{I}(\mathbf{b})$ is an element-wise integral of a vector function of time $\mathbf{b}(t) \in \mathbb{R}^n$ over the time variable t, i.e:
$$\mathcal{I}(\mathbf{b}) = \int_0^t \mathbf{b}(\tau) d\tau$$

3.2 Kinematic model of robot door/drawer opening

We consider a setting in which the end-effector has grasped the handle of a mechanism with a revolute or prismatic joint. Let $\{e\}$ and $\{h\}$ be the end-effector and the handle frame respectively. The two frames are attached on the same kinematically known position e.g. a known point of the end-effector denoted by $\mathbf{p}_e$ and represented by different rotation matrices. The orientation of the end-effector frame is strictly connected to the robot kinematics while the orientation of the handle frame is related to the kinematic constraints of the task. In case of a rotating door (revolute joint) the kinematic constraints are defined by considering a frame $\{o\}$ attached at the unknown center of the circular trajectory of the end-effector while opening the rotating door. The axis $\mathbf{z}_o$ corresponds to the axis of the rotation while $\mathbf{x}_o$, $\mathbf{y}_o$ can be arbitrarily chosen (Fig. 1a).

We make the following assumptions:

Assumption 1 *There is no relative translational motion of the end-effector with respect to the handle, i.e.* ${}^{h}\dot{\mathbf{p}}_e = 0$.

Assumption 2 *There is no relative translational and rotational motion of the end-effector with respect to the handle, i.e.* ${}^{h}\dot{\mathbf{p}}_e = 0$ *and* ${}^{h}\dot{\mathbf{R}}_e = 0$.

Assumption 2 is more restrictive since it implies a fixed grasp of the handle, while Assumption 1 is more general and can accommodate grasps that can be modeled as passive revolute joints. Obviously, Assumption 2 also implies Assumption 1, but in this work the two assumptions will be treated separately, as they correspond to two different grasp types.

In the following we state a convention in order to define the frame $\{h\}$ in both cases of revolute joints (hinged doors) and prismatic joints (sliding doors, drawers):
a) ***Revolute joints***:

- Axis $\mathbf{z}_h$ is equivalent to $\mathbf{z}_o$, i.e. $\mathbf{z}_o \equiv \mathbf{z}_h$
- Axis $\mathbf{y}_h$ is the unit vector along the line connecting the origins of $\{h\}$ and $\{o\}$ with direction towards the hinge.
- Axis $\mathbf{x}_h$ can be regarded as the allowed motion axis; it can be formed as follows: $\mathbf{x}_h = \mathbf{y}_h \times \mathbf{z}_h$

b) ***Prismatic joints***: Vector $\mathbf{x}_h$ denotes the allowed motion axis. Axes $\mathbf{z}_h$ and $\mathbf{y}_h$ can be arbitrarily chosen in order to span the two-dimensional surface to which $\mathbf{x}_h$ is perpendicular.
Examples of Fig. 1 illustrate the definition of the $\{h\}$ axes.

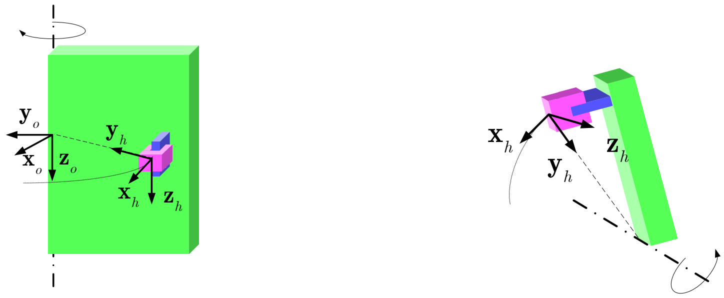

(a) Rotating mechanisms in regular doors and cupboards.

(b) Rotating mechanisms in ovens or washing machines.

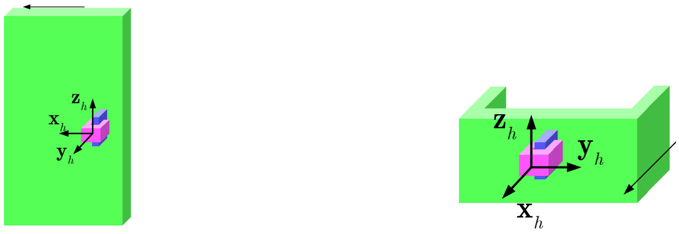

(c) Sliding mechanisms in closets.

(d) Mechanism in drawers.

Figure 1: Examples of rotating/sliding doors and drawers with revolute and prismatic joints.

For doors with a revolute joint, we can define the radial vector –which is parallel to $\mathbf{y}_h$– as the relative position of the frames $\{o\}$ and $\{e\}$ (or $\{h\}$):

$$\mathbf{r} \triangleq \mathbf{p}_o - \mathbf{p}_e, \tag{1}$$

and use it in the following equation to describe the first-order differential kinematics:

$$\mathbf{v} = \mathbf{r} \times \boldsymbol{\omega}_h \tag{2}$$

where $\mathbf{v}$ expresses the velocity of the end-effector $\dot{\mathbf{p}}_e$ or the handle velocity $\dot{\mathbf{p}}_h$ given ${}^e\dot{\mathbf{p}}_h = 0$.

Note that $\mathbf{r} = \frac{1}{\kappa}\mathbf{y}_h$ where κ denotes the curvature of the cyclic trajectory for the door opening (the inverse of the distance between the end-effector frame and the center of rotation). Thus, the inner product of (2) with $\mathbf{x}_h$ yields:

$$\omega = \kappa v \tag{3}$$

where $v \triangleq \mathbf{x}_h^\top \mathbf{v}$ denotes the end-effector/handle translational velocity magnitude and $\omega \triangleq \mathbf{z}_h^\top \boldsymbol{\omega}_h$ the rotational velocity of the handle. Although we consider a revolute joint at the hinge of the door, the constraint equation (3) can model cases of sliding doors or drawers represented by prismatic joints. Large values of radius correspond to practically zero curvature i.e. straight line trajectories for opening the mechanism and zero rotational velocity for the handle. Given the mechanism is rigid and Assumption 1 or 2, the remaining constraints regarding the translational velocity are:

$$\mathbf{P}(\mathbf{x}_h)\mathbf{v} = 0 \tag{4}$$

Constraint equation (4) implies that the end-effector/handle velocity can be parameterised as follows:

$$\mathbf{v} = v\mathbf{x}_h \tag{5}$$

Additionally Assumption 2 imposes extra constraints on the end-effector rotational velocities:

$$\boldsymbol{\omega}_e = \boldsymbol{\omega}_h \text{ with } \mathbf{P}(\mathbf{z}_h)\boldsymbol{\omega}_h = \mathbf{0} \tag{6}$$

3.3 Robot kinematic model

We consider the case of a n-DoF velocity-controlled manipulator satisfying the following assumption:

Assumption 3 *The kinematic structure and the number of DoF are sufficient for generating a 6 DoF movement of the end-effector and hence implementing the velocity for the task defined for a set of constraint's estimates including the actual constraint.*

An anthropomorphic arm with spherical wrist with $n = 6$ DoFs can satisfy Assumption 3.

For a velocity-controlled manipulator a reference generalized velocity $\mathbf{u}_{\text{ref}} \triangleq [\mathbf{v}_{\text{ref}}^\top \, \boldsymbol{\omega}_{\text{ref}}^\top]^\top \in \mathbb{R}^6$ ($\mathbf{v}_{\text{ref}} \in \mathbb{R}^3$ and $\boldsymbol{\omega}_{\text{ref}} \in \mathbb{R}^3$ denote the translational and rotational part respectively) expressed at the inertial frame can be considered as a kinematic controller which is mapped to the joint space in order to be applied at the joint velocity level as follows:

$$\dot{\mathbf{q}} = \mathbf{J}^+(\mathbf{q})\mathbf{u}_{\text{ref}} \tag{7}$$

with $\mathbf{q},\ \dot{\mathbf{q}} \in \mathbb{R}^n$ being the joint positions and velocities respectively and $\mathbf{J}(\mathbf{q})^+ = \mathbf{J}(\mathbf{q})^\top \left[\mathbf{J}(\mathbf{q})\mathbf{J}(\mathbf{q})^\top\right]^{-1}$ being the inverse or the pseudo-inverse of the manipulator Jacobian $\mathbf{J}(\mathbf{q}) \in \mathbb{R}^{6\times n}$ relating the joint velocities $\dot{\mathbf{q}}$ to the end-effector velocities $[\dot{\mathbf{p}}_e^\top\ \boldsymbol{\omega}_e^\top]^\top$. If we consider the typical Euler-Lagrange robot dynamic model, the velocity error at the joint level drives the torque (current) controller $\mathbf{u}_{\boldsymbol{\tau}}(t)$.

Assumption 4 *The actuator has sufficient torque output, external force compensation, and current control loop frequency to keep the error between commanded and actual velocity negligible. Also, the inertial dynamics of the door mechanism are sufficiently weak, such that the portion of measured forces arising from accelerating the door mechanism are negligible.*

Cases where Assumption 4 is not valid are treated in the robustness analysis of Section 4.4.

3.4 Control Objective

The task of controlling the robot to manipulate a door or a drawer, can naturally be described in the handle frame. The desired variables should be defined in the robot inertial (or end-effector frame) to be executable by the robot. Let $\mathbf{f} \in \mathbb{R}^3$ denote the interaction force exerted at the end-effector, $\boldsymbol{\tau} \in \mathbb{R}^3$ the torque around the origin of the end-effector frame and $\mathbf{f}_d$, $\boldsymbol{\tau}_d$ the corresponding desired vectors. Let $v_d(t)$ be the desired velocity along the motion axis of frame $\{h\}$. Then the desired velocity $\mathbf{v}_d(t)$ is defined along $\mathbf{x}_h$, i.e. $\mathbf{v}_d = v_d(t)\mathbf{x}_h$, and the force control objective can be achieved by projecting the desired force on the orthogonal complement space of $\mathbf{x}_h$ (constrained directions) i.e. $\mathbf{P}(\mathbf{x}_h)\mathbf{f}_d$; a small valued or zero vector $\mathbf{f}_d$ corresponds to small forces along the constraint directions. The control objective can be formulated as:

Problem 1 *Design a translational velocity control* $\mathbf{v}_{ref}$ *such that* $\mathbf{P}(\mathbf{x}_h)\mathbf{f} \to \mathbf{P}(\mathbf{x}_h)\mathbf{f}_d$ *and* $\mathbf{v} \to v_d(t)\mathbf{x}_h$*, without knowing accurately the motion axis* $\mathbf{x}_h$ *and the corresponding constraint directions* $\mathbf{P}(\mathbf{x}_h)$.

When Assumption 2 is valid, the desired rotational velocity can be defined using $v_d(t)$ along the axis $\boldsymbol{\kappa} \triangleq \kappa\mathbf{z}_h$, i.e. $\boldsymbol{\omega}_d(t) = v_d(t)\boldsymbol{\kappa}$. In this case the total interaction torque denoted by $\boldsymbol{\tau} \in \mathbb{R}^3$ is controllable and thus an additional control objective can be formulated as follows:

Problem 2 *Design a rotational velocity control* $\boldsymbol{\omega}_{ref}$ *to act in parallel to* $\mathbf{v}_{ref}$ *such that* $\boldsymbol{\tau} \to \boldsymbol{\tau}_d$ *and* $\boldsymbol{\omega} \to \kappa v_d(t)\mathbf{z}_h$ *without knowing the axis of rotation* $\mathbf{z}_h$ *and the variable* κ*. The rotation control objective is mainly set to achieve identification of* $\mathbf{z}_h$ *and* κ.

We consider that the opening task is accomplished when the observed end-effector trajectory — which coincides with the handle trajectory — has progressed far enough to enable the robot to perform a subsequent task, like picking up an object in a drawer or passing through a door. Hence, some perception system observing the progress of the opening of the mechanism is additionally required to provide the robot with the command to halt the opening procedure.

4 Control Design

In this section, we propose a solution to Problems 1 and 2 stated in Section 3.4 above. When only Assumption 1 holds, the solution to Problem 1 is given by Theorem 1, and when Assumption 2 holds, the solution to Problem 1 and 2 is given by Theorem 1 and 2. Robustness analysis is performed to derive bounds for the estimation error in case of disturbances. Proofs of the propositions and theorems of this section are given in the Appendix. First, we propose a translational velocity reference that can employ two different update laws corresponding to Assumptions 1 and 2 respectively.

4.1 Translational velocity reference with force feedback

Let $\hat{\mathbf{x}}_h(t)$ denote the online estimate of the motion direction $\mathbf{x}_h$. Dropping the argument t from $\hat{\mathbf{x}}_h(t)$ and $v_d(t)$ for notation convenience, we let $\mathbf{v}_{\text{ref}}$ be given by:

$$\mathbf{v}_{\text{ref}} = v_d \hat{\mathbf{x}}_h - \mathbf{P}(\hat{\mathbf{x}}_h)\mathbf{v}_f \tag{8}$$

where $\mathbf{v}_f$ is a PI force feedback input defined as follows:

$$\mathbf{v}_f = \alpha_f \tilde{\mathbf{f}} \ + \beta_f \mathcal{I}\left[\mathbf{P}(\hat{\mathbf{x}}_h)\tilde{\mathbf{f}}\right] \tag{9}$$

with $\tilde{\mathbf{f}} = \mathbf{f} - \mathbf{f}_d$ and α_f, β_f being positive control constants. Note that the first term of the reference velocity is the desired velocity along the estimated motion direction and it is not in general consistent with the allowable motion direction. However the second term – which is a force controller – compensates for the inconsistency owing to kinematic uncertainties and renders a reference velocity $v_{\text{ref}} \triangleq \mathbf{x}_h^\top \mathbf{v}_{\text{ref}}$ along the actual motion direction by generating forces along the constrained directions (that can be considered as Lagrange multipliers [9]).

Let $\theta(t)$ denote the angle formed between the actual vector $\mathbf{x}_h$ which is a rotating vector and its online estimate $\hat{\mathbf{x}}_h$ which is time-varying. Given that the estimate $\hat{\mathbf{x}}_h$ is a unit vector, $\cos\theta(t)$ can be defined as follows:

$$\cos\theta(t) \triangleq \mathbf{x}_h^\top \hat{\mathbf{x}}_h = {}^e\mathbf{x}_h^\top {}^e\hat{\mathbf{x}}_h \tag{10}$$

The definition is independent of the frame in which $\mathbf{x}_h$ and $\hat{\mathbf{x}}_h$ are expressed. In general, an online estimate of the vector $\hat{\mathbf{x}}_h$ provided by an adaptive estimator is not unit but in the following we are going to design an update law that produces estimates of unit magnitude. The derivative of $\theta(t)$ depends on both estimation rate and door motion velocity:

$$\frac{d}{dt}\cos\theta(t) = \mathbf{x}_h^\top \left(\dot{\hat{\mathbf{x}}}_h - v\boldsymbol{\kappa} \times \hat{\mathbf{x}}_h\right) \tag{11}$$

When the grasp imposes constraint on the rotation of the end-effector with respect to the handle (Assumption 2), the derivative of $\theta(t)$ is independent of the door motion velocity. The derivative of $\cos\theta(t)$ can be calculated as follows:

$$\frac{d}{dt}\cos\theta(t) = {}^e\mathbf{x}_h^\top\, {}^e\dot{\hat{\mathbf{x}}}_h \text{ for } {}^e\dot{\mathbf{x}}_h = \mathbf{0} \tag{12}$$

In the following, we drop out the argument of t from $\theta(t)$ for notation convenience.

The velocity error $\tilde{\mathbf{v}} \triangleq \mathbf{v} - \mathbf{v}_{\text{ref}}$ can be decomposed along $\hat{\mathbf{x}}_h$ and the corresponding orthogonal complement space as follows:

$$\tilde{\mathbf{v}} = \mathbf{P}(\hat{\mathbf{x}}_h)(\mathbf{v} + \mathbf{v}_f) + (v\cos\theta - v_d)\,\hat{\mathbf{x}}_h \tag{13}$$

In case of velocity controlled manipulators described by (7) we get $\tilde{\mathbf{v}} = \mathbf{0}$. Since the right-hand side of (13) consists of two orthogonal terms, $\tilde{\mathbf{v}} = \mathbf{0}$ implies the following closed-loop system equations:

$$\mathbf{P}(\hat{\mathbf{x}}_h)\mathbf{v}_f = -v\mathbf{P}(\hat{\mathbf{x}}_h)\mathbf{x}_h \tag{14}$$

$$v = \tfrac{1}{\cos\theta} v_d \tag{15}$$

Taking the norm of each side of (14) and substituting (15) gives:

$$\|\mathbf{P}(\hat{\mathbf{x}}_h)\mathbf{v}_f\| = |v_d \tan\theta| \tag{16}$$

From (14), (15) and (16) it is clear how the estimation error in the axis of motion affect the force errors and the velocity of the end-effector. Note that the higher the uncertainty in the motion axis θ is the higher the velocity v and the estimated constraint forces $\mathbf{P}(\hat{\mathbf{x}}_h)\mathbf{f}$ can be. In the extreme case of $|\theta(t)| = \pi/2$ which is equivalent to trying to move the mechanism along a direction which is completely mechanically constrained extremely high forces arise. Hence, the update law must at least guarantee $|\theta(t)| \neq \pi/2$, $\forall t$. Equations (14)-(16) describing the closed loop system link the physical controlled variables like velocities and forces with the uncertainty measure $\theta(t)$ and thus they are instrumental in the design of the update laws for estimating the unknown parameters described in the following subsections.

4.1.1 Update Law for the Motion Direction given Assumption 1

We propose the following update law for $\hat{\mathbf{x}}_h$[1]:

$$\dot{\hat{\mathbf{x}}}_h = -\gamma v_{\text{ref}}\mathbf{P}(\hat{\mathbf{x}}_h)\mathbf{v}_f - v_{\text{ref}}\hat{\mathbf{x}}_h \times \hat{\boldsymbol{\kappa}} \tag{17}$$

---

[1] Details on the design of the update laws can be found in the Appendix.

where γ is positive control gain for tuning the adaptation rate, $\hat{\boldsymbol{\kappa}}$ is the online estimate of the scaled rotational axis $\boldsymbol{\kappa}$ that is produced by the following appropriately designed update law:

$$\dot{\hat{\boldsymbol{\kappa}}} = \boldsymbol{\Gamma}_\kappa \hat{\mathbf{x}}_h \times \mathbf{v}_{\mathrm{ref}}, \tag{18}$$

with $\boldsymbol{\Gamma}_\kappa \in \mathbb{R}^{3\times 3}$ being a positive definite gain matrix, and $v_{\mathrm{ref}} \triangleq \mathbf{x}_h^\top \mathbf{v}_{\mathrm{ref}}$ can be calculated independently of the knowledge of the motion direction for $\hat{\mathbf{x}}_h^\top \mathbf{x}_h > 0$ as follows:

$$v_{\mathrm{ref}} = \operatorname{sgn}\left(\hat{\mathbf{x}}_h^\top \mathbf{v}_{\mathrm{ref}}\right) \|\mathbf{v}_{\mathrm{ref}}\| \tag{19}$$

The use of the update laws (17), (18) are instrumental for the stability analysis and the convergence of the estimated parameters. In the Appendix it is shown that the use of Eq. (17), (18) enable the proof of the following Propositions:

Proposition 1 *Update law (17) ensures that the norm of* $\hat{\mathbf{x}}_h(t)$ *is invariant, i.e. given* $\|\hat{\mathbf{x}}_h(0)\| = 1$, $\|\hat{\mathbf{x}}_h(t)\| = 1, \ \forall t$.

Proposition 2 *Update laws (17), (18) driven by the reference velocity* $\mathbf{v}_{ref}$ *given by (8) with a time-varying desired velocity yield to the following nonautonomous (time-dependent) nonlinear system with states* θ *and* $\tilde{\boldsymbol{\kappa}} = \hat{\boldsymbol{\kappa}} - \boldsymbol{\kappa}$ *which are well defined in the domain* $D = \{\theta \in \mathbb{R}, \tilde{\boldsymbol{\kappa}} \in \mathbb{R}^3 : |\theta| < \frac{\pi}{2}\}$:

$$\dot{\theta} = -\gamma v_d^2(t)\frac{\tan\theta}{\cos\theta} - \frac{v_d(t)}{\cos\theta}\tilde{\boldsymbol{\kappa}}^\top \mathbf{n} \tag{20}$$

$$\dot{\tilde{\boldsymbol{\kappa}}} = v_d(t)\tan\theta \boldsymbol{\Gamma}_\kappa \mathbf{n} \tag{21}$$

with $\mathbf{n}$ *being a unit vector perpendicular to the surface defined by* $\mathbf{x}_h$ *and* $\hat{\mathbf{x}}_h$*, which imply that the estimation error angle* θ *stays in* D *and converges to zero for* v_d *satisfying the persistent excitation (PE) condition (see [10]), i.e.:*

$$\int_t^{t+T_0} v_d^2(\sigma)d\sigma \geq \alpha_0 T_0 \tag{22}$$

$\forall t \geq 0$ *and for some* α_0, $T_0 > 0$.

4.1.2 Update Law for the Motion Direction given Assumption 2

Since the relative orientation of the handle frame and the end-effector is constant we can propose a simpler update law by using as a regressor the end-effector frame rotation matrix. We propose the following update law for $\hat{\mathbf{x}}_h$[1]:

$$\hat{\mathbf{x}}_h = \mathbf{R}_e {}^e\hat{\mathbf{x}}_h \tag{23}$$

$${}^e\dot{\hat{\mathbf{x}}}_h = -\gamma v_d \mathbf{R}_e^\top \mathbf{P}(\hat{\mathbf{x}}_h)\mathbf{v}_f \tag{24}$$

where γ is a positive control gain for tuning the adaptation rate. Proposition 3, 4 describe how the update law (23), (24) produces well-defined estimates that converge to the actual values. In the Appendix it is shown that the use of Eq. (24) enable the proof of the following Propositions:

Proposition 3 *Update law (24) ensures that the norm of* ${}^e\hat{\mathbf{x}}_h(t)$ *is invariant, i.e. starting with* $\|{}^e\hat{\mathbf{x}}_h(0)\| = 1$, $\|{}^e\hat{\mathbf{x}}_h(t)\| = 1, \ \forall t$.

Proposition 4 *Update laws (23), (24) driven by the reference velocity* $\mathbf{v}_{ref}$ *given by (8) with a time-varying desired velocity yield to the following nonautonomous (time-dependent) nonlinear system with state* θ *which is well defined in the domain* $D' = \{\theta \in \mathbb{R} : |\theta| < \frac{\pi}{2}\}$*:*

$$\dot{\theta} = -\gamma v_d^2(t) \tan\theta \tag{25}$$

which implies that the estimation error angle θ *stays in* D *and converges to zero for* v_d *satisfying the PE condition given by (22).*

4.1.3 Summary and force convergence results

Propositions 2 and 4 imply that given the update laws and the controller the estimates are well defined [2] and converge to their actual values. Propositions can be considered as intermediate steps for proving the stability of the overall system including aditionally the internal state introduced by the force integral in the following Theorem for Assumptions 1 and 2 (see Appendix for proof).

Theorem 1 *Consider a velocity controlled manipulator (7), grasping the handle of a sliding/rotating door or a drawer. If the robot is driven by a velocity control input* $\mathbf{v}_{ref}$ *(8) that uses a PI force feedback input* $\mathbf{v}_f$ *(16) and:*

1. *the update law (17), (18) given that Assumption 1 is valid, or*
2. *the update law (23), (24) given that Assumption 2 is valid,*

then Problem 1 will be solved, i.e., smooth opening of the moving mechanism and identification of the estimated parameters will be achieved. Analytically, the following convergence results are guaranteed: $\hat{\mathbf{x}}_h \to \mathbf{x}_h$, $\mathbf{v} \to \mathbf{x}_h v_d$, *and* $\mathbf{P}(\mathbf{x}_h)\tilde{\mathbf{f}} \to 0$, *given that* v_d *satisfies the PE condition given by (22).*

4.2 Rotational velocity reference with torque feedback

In case of Assumption 1, the rotational velocity of the end-effector can be set in order to optimize some performance index such as the manipulability index of the arm while torque cannot be controlled. On the other hand, Assumption 2 implies that rotational velocity of the end-effector is strictly connected to the the rotational velocity of the mechanism and subsequently to the translational velocity of the end-effector through the constraint (3). Hence the reference rotational velocity should be appropriately designed using the desired translational velocity v_d and exploiting torque feedback in order to fulfill the constraints (3), (6):

---

[2] The estimates are unit vectors if the initial estimate is unit and $|\theta(t)| \neq \pi/2$, $\forall t$, is true since $|\theta(t)| < \pi/2$ if $|\theta(0)| < \pi/2$.

$$\boldsymbol{\omega}_{\mathrm{ref}} = v_d \hat{\boldsymbol{\kappa}} - \boldsymbol{\omega}_\tau \tag{26}$$

where $\hat{\boldsymbol{\kappa}}$ is the online estimate of $\boldsymbol{\kappa}$ and it is appropriately designed as follows:

$$\dot{\hat{\boldsymbol{\kappa}}} = -v_d \boldsymbol{\Gamma}_\kappa \boldsymbol{\omega}_\tau \tag{27}$$

with $\boldsymbol{\Gamma}_\kappa$ being a positive definite matrix of update gains, and $\boldsymbol{\omega}_\tau$ is a PI torque feedback input defined as follows:

$$\boldsymbol{\omega}_\tau = \alpha_\tau \tilde{\boldsymbol{\tau}} \ + \beta_\tau \mathcal{I}\left(\tilde{\boldsymbol{\tau}}\right) \tag{28}$$

where $\tilde{\boldsymbol{\tau}} = \boldsymbol{\tau} - \boldsymbol{\tau}_d$.

The design of the update law (27) is instrumental for the proof of the following theorem (see Appendix):

Theorem 2 *Consider a velocity controlled manipulator (7) grasping the handle of a sliding/rotating door or a drawer according to Assumption 2. If the robot is driven by a velocity control input that consists of both* $\mathbf{v}_{ref}$ *(8) and* $\boldsymbol{\omega}_{ref}$ *(26) that uses a PI torque feedback input* $\boldsymbol{\omega}_\tau$ *(28) as well as the update law (27) to estimate the vector* $\boldsymbol{\kappa}$*, then Problem 2 will be solved, i.e., the following convergence results – additionally to those of Theorem 1 – are guaranteed:* $\tilde{\boldsymbol{\tau}} \to 0$, $\mathcal{I}(\tilde{\boldsymbol{\tau}}) \to 0$, $\hat{\boldsymbol{\kappa}} \to \boldsymbol{\kappa}$, $\boldsymbol{\omega}_e \to v_d \boldsymbol{\kappa}$*, for* v_d *satisfying the PE condition given by (22).*

4.3 Torque-controlled robot manipulators

In the aforementioned results we have considered an ideal velocity-controlled robot manipulator which is connected with the environment through rigid constraints. These assumptions allow the forces to be modeled as Lagrange multipliers related to the the range of uncertainty as shown in (16), similarly to the Lagrange multipliers used for modeling forces in the case of a torque-controlled manipulator that interacts with a rigid environment [32]. In the case of a velocity-controlled manipulator the underlying assumption is that the commanded velocity is achieved adequately fast (Assumption 4), while in the case of a torque-controlled manipulator, the actuator dynamics can be considered negligible.

The adaptive velocity controllers proposed in this paper can be readily modified and applied to the outer loop of a dynamic controller suitable for a torque-controlled manipulator as shown in our previous work [14] where the inner loop is formulated by the superposition of an appropriately designed generalized reference force, a velocity error feedback term and a term compensating for the robot dynamic model.

The reference velocity (outer loop) used in the velocity error feedback term is similar to the one proposed in this work but did not use the proportional force errors terms of (8), in order to avoid differentiation of noisy force/torque measurements while calculating the reference acceleration required in the implementation on a torque controlled robot. In general the design of dynamic (torque) controllers of robots may require a term that compensates for the dynamic model of the robot. In case of dynamic uncertainties, adaptive controllers that employ update laws for the dynamic parameters' estimation have been proposed [33]. The PE condition is complicated and the joint trajectories have to be properly chosen in order to identify the dynamic parameters online. However dynamic parameter identification is not crucial for guaranteeing the tracking error performance. In contrast to dynamic uncertainties, here we consider uncertainties of the parameters involved in the kinematic constraints. The identification of these parameters – that is prerequisite for achieving the control objectives – depends on the trajectory of the end-effector rather than on the individual joints' trajectories.

In the following section, instead of extending the analysis to the case of a torque-controlled robot manipulator, we present a robustness analysis for the performance of the system under disturbances $\boldsymbol{\delta}(t)$ arising at the velocity level that may also represent errors arising in the inner control loop.

4.4 Robustness Analysis

In this section, we present a robustness analysis for the performance of the system under disturbances $\boldsymbol{\delta}(t)$ arising at the velocity level, i.e. $\mathbf{v} = \mathbf{v}_{\text{ref}} + \boldsymbol{\delta}(t)$. These disturbances can incorporate delays at the velocity tracking control loop that would be vanishing for the case of a desired constant velocity, as well as disturbances arising due to modeling errors e.g. compliance and deformations at the grasp or at the joint of the mechanism.

The closed loop system equations (14), (15) are now affected by the disturbances as follows:

$$\mathbf{P}(\hat{\mathbf{x}}_h)\mathbf{v}_f = \mathbf{P}(\hat{\mathbf{x}}_h)\left[-v\mathbf{x}_h + \boldsymbol{\delta}(t)\right] \tag{29}$$

$$v = \tfrac{1}{\cos\theta}\left[v_d + \hat{\mathbf{x}}_h^\top \boldsymbol{\delta}(t)\right] \tag{30}$$

In the following propositions we examine the robustness of the update law (23), (24) in case of disturbances. The proofs of the propositions can be found in the Appendix.

Proposition 5 *The update laws (23), (24) driven by the reference velocity $\mathbf{v}_{ref}$ given by (8) with a time-varying desired velocity in case of disturbances (i.e. eq. (29), (30) hold) yield to the following nonautonomous (time-dependent) nonlinear system with state θ which is well defined in the domain $D' = \{\theta \in \mathbb{R} : |\theta| < \frac{\pi}{2}\}$:*

$$\dot{\theta} = -\gamma v_d^2(t)\tan\theta - \gamma v_d(t)\frac{sgn(\theta)}{\cos\theta}\mathbf{n'}^\top\boldsymbol{\delta}(t) \tag{31}$$

where $\mathbf{n'}$ *is a constrained direction (i.e.* $\mathbf{n'}^\top \mathbf{x}_h = 0$*) lying on the common plane of* $\hat{\mathbf{x}}_h$ *and* $\mathbf{x}_h$*.*

Proposition 6 *The system (31) is uniformly ultimately bounded with respect to the following region:*

$$\Omega = \{\theta \in D' : \quad |\theta| < \arcsin \lambda(t)\} \tag{32}$$

where $\lambda(t) = \frac{|\mathbf{n'}^\top \boldsymbol{\delta}(t)|}{|v_d|}$ *for* $v_d \neq 0$*.*

Variable $\lambda(t)$ denotes the range of the region of angles θ in which the estimation error converges and is well-defined for $|\mathbf{n'}^\top \boldsymbol{\delta}(t)| < |v_d|$. Notice that $\lambda(t)$ can be alternatively written as $\lambda(t) = \cos\varphi(t)\ell(t)$ where $\ell(t)$ is defined as the ratio of the magnitude of the velocity error disturbance and the commanded desired velocity i.e. $\ell \triangleq \frac{\|\boldsymbol{\delta}(t)\|}{|v_d|}$ and $\varphi(t)$ denotes the angle formed between $\mathbf{n'}$ and $\boldsymbol{\delta}(t)$. In the extreme case of a velocity disturbance being aligned with the constrained direction[3], a well-defined $\lambda(t)$ requires that the ratio $\ell(t)$ is smaller than one. If $|\varphi(t)|$ is smaller than 90 deg, the ratio $\ell(t)$ is allowed to take values bigger than one. If the disturbance is aligned with the motion direction (i.e. $\lambda(t) = 0$) convergence of the estimation error to zero is guaranteed irrespective of the magnitude of the disturbance. Notice also that in the case of a vanishing disturbance ($\lambda(t) \to 0$), the region Ω shrinks to zero, thus guaranteeing identification of the uncertain motion axis. In the case of persistent disturbances the identification error is comparable to the error arising from estimation based on inaccurate velocity measurements.

If Assumption 1 holds we can achieve a similar result by modifying the update law using a σ-modification [10]. Errors in rotational velocity can be treated in a similar fashion.

4.5 Discussion

The proposed control scheme produces estimates of the unconstrained motion direction and axis of rotation (in the case of a rotational door) using the update laws (17), (18) (Assumption 1) or (24), (27) (Assumption 2) respectively. In case of Assumption 1, the motion direction estimate converges to the actual direction but there is no proof that the scaled rotation vector converges to the actual one; note however that the rotation vector estimate is not used in the velocity reference (8) and thus its convergence do not affect stability and performance. In this case torques are not controlled and the redundant degrees of freedom can be used to enhance manipulability. In case of Assumption 2, both estimated vectors converge to the actual values and the estimates are used within velocity references (8) and (26). The velocity references enforce the robot to move with a desired velocity while controlling both forces and/or torques along the constrained directions to small values guaranteeing compliant behavior.

---

[3] Note that large velocity errors in the constraint directions would be highly unlikely, as the the constraint directions are defined as the directions in which the mechanism has significantly higher stiffness, and high velocities in these directions are effectively blocked.

By defining the handle frame according to the task constraints and involving the curvature instead of the radius and the center of rotation, the proposed method is applicable to both revolute and prismatic mechanisms. Coupling the estimation with the controller following the adaptive control framework (see e.g. [10]) makes the method inherently on-line, enabling proofs of the convergence of estimated parameters to true values and convergence of force/torque errors.

Note that no projection operators have been used in the update laws design reducing the amount of the required prior knowledge. The main condition for guaranteed performance is that the initial estimate is not perpendicular to the true value i.e. $\theta(0) \in \left(-\frac{\pi}{2}, \frac{\pi}{2}\right)$. A typical example where this condition is not satisfied could be when opening a drawer with an initial estimate corresponding to a sliding door (c.f. Fig. 2, cases (iv) and (v)). This issue can be overcome by using a moderate deviation in the initial estimate (see Section 5). The proposed method alone can not handle the case where the initial estimate is in the opposite direction of the true value, as this would generate a closing motion. This can be handled by an external monitoring system that stops the motion and retries with a different initial estimate if measured forces are too high, similar to a human who first pushes a door, and when it does not open, tries to pull it instead.

In the case of a fixed grasp we can produce explicit estimates of the physical location of the hinge of a revolute door, as reliable estimates of both radial direction and radial distance are available. If we make the assumption that a large enough radial distance (we arbitrarily choose 10 m) implies a prismatic mechanism, Algorithm 1, that can be used at any time instant continuously or in a discrete manner, will identify the hinge position. Given the center of rotation and the estimate of

Algorithm 1 Reasoning of the type of joint/Calculation of the rotation center

```
while Not Done do
    if $\|\hat{\boldsymbol{\kappa}}\| > 0.1$ then
        Rotational door
        Calculate the estimated radius $\hat{\rho} := \|\hat{\boldsymbol{\kappa}}\|^{-1}$
        Calculate the estimated radial direction:
            $\hat{\mathbf{y}}_h := \hat{\rho}\hat{\boldsymbol{\kappa}} \times \hat{\mathbf{x}}_h$
        Calculate the center of rotation $\hat{\mathbf{p}}_o := \mathbf{p}_e + \hat{\rho}\hat{\mathbf{y}}_h$.
    else
        Sliding door or drawer
    end if
end while
```

the curvature, we can estimate local variables with respect to the initial position of the end-effector such as the angular state of the door or the translation of the drawer and use them in order to provide internally – and not with an external perception system – a halt command.

5 Scenarios and Evaluation

To illustrate and demonstrate the generality of the approach, we evaluate the performance for five different mechanisms in simulation, and three mechanisms in experiments on a physical robot. The simulations consider five different scenarios covering five common cases found in domestic environments, see Fig. 2. All cases are treated with the same initial estimates and controller gains. Cases (a) and (b) are typical revolute doors with vertical axis, with the hinge to the left or to the right, respectively. Case (c) models a revolute door with axis of rotation parallel to the floor, such as is common for ovens. The radius of these door are all set to 50 cm. Case (d) models a sliding door, and case (e) a typical drawer. The common initial estimate used in all cases is that of a prismatic joint, assuming $\hat{\boldsymbol{\kappa}}(0) = \mathbf{0}$. The initial estimate of the unconstrained direction of motion is 30 deg offset from the normal direction to the plane of the door or drawer. The initial estimates are shown as red/gray arrows, and the true direction is shown as black arrows in Fig. 2. The angular values given are the initial errors of the estimates. The controller gains are chosen as follows: $\alpha_f = \alpha_\tau = 0.05$, $\beta_f = \beta_\tau = 0.005$, $\gamma = \gamma_\kappa = 2000$. The desired motion velocity is 5 cm/s, given as $v_d = 5(1 - e^{-10t})$ cm/s to avoid sharp initial transients.

Fig. 3, 4(upper) show the response of the motion axis estimation errors for update laws (17), (18) (Assumption 1 - passive revolute joint) and (24), (27) (Assumption 2 - fixed grasp) respectively – convergence to the actual axis is achieved even for larger initial errors. Note that for fixed grasps the settling time is shorter and there is less overshoot as compared to the performance for the revolute grasp, even though the same gains were used. In Fig. 3(upper) the sharp corner in the plot of the absolute value of the angle estimation error at 0.5 s corresponds to an overshoot. Fig. 3, 4(lower) depict the estimation error for the most important element of $\boldsymbol{\kappa}$. In the case of a fixed grasp (Fig. 4), this corresponds to the inverse signed distance κ between the end-effector and the hinge and the estimate $\hat{\kappa}$ is not modified when $\hat{\kappa}(0)$ coincides with κ and it converges to its actual value in all cases. In case of the passive revolute joint (Fig. 3), the convergence to actual value is also achieved, even though it is not proven theoretically, but the convergence time is twice the corresponding time for fixed grasps and a high overshoot is observed. Furthermore, some of the elements of $\boldsymbol{\kappa}$ are initially modified even when the original estimate coincides with the actual parameter, and converge with the rest of the system.

If Assumption 2 holds, it has been theoretically proven that combining estimates of the modulated rotation axis with the motion axis we can calculate the center of rotation of the rotational doors in real time using Algorithm 1; simulation gives errors of approximately 1.4 cm after 1.5 s, which is equivalent of opening the door 7.5 cm. Given the threshold of $\|\hat{\boldsymbol{\kappa}}\| > 0.1$, the revolute doors are identified as

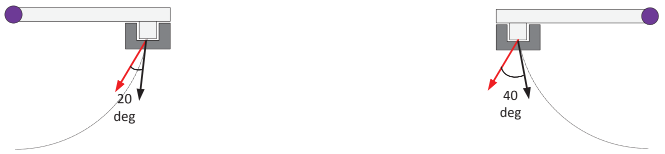

(a) Revolute door, left hinge, $\kappa = 2$. (b) Revolute door, right hinge, $\kappa = 2$.

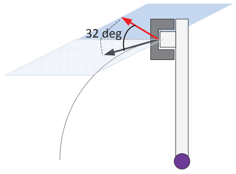

(c) Revolute door, bottom hinge, $\kappa = 2$.

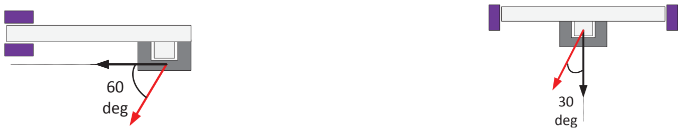

(d) Prismatic door, $\kappa = 0$. (e) Prismatic drawer, $\kappa = 0$.

Figure 2: Five different simulation cases using the same initial estimate: the angle indicates the initial error.

such after 0.2 s. The estimation error responses (Fig. 3) shows that Algorithm 1 can be used even when only Assumption 1 holds, but the identification procedure is slower (error of 3.4 cm after 4 s). Fig. 5b shows the responses of the Euclidian norms of force and torque errors ($e_f = \|\mathbf{P}(\mathbf{x}_h)\tilde{\mathbf{f}}\|$ and $e_\tau = \|\tilde{\boldsymbol{\tau}}\|$ respectively) in the case of fixed grasps. Errors converge to zero following the convergence rate of modulated rotation axis and motion axis. The same is true for the force errors in the case of a passive revolute joint grasp, as shown in Fig. 5a.

6 Experiments

To evaluate the performance of the proposed method under unmodelled system and sensor noise, the performance of the door opening controllers were also tested on a real robot setup. Our setup consists of a 7-DoF manipulator whose joints are velocity controlled. New velocity setpoints are given at 130 Hz, and maintained by internal PID current controllers running at 2 kHz. The manipulator includes a wrist mounted ATI Mini45 6-axis force-torque sensor sampled at 650 Hz, which we use for the force feedback and estimation part of our controllers. Additionally, it is equipped with a two finger parallel gripper which allows us to grasp the doors.

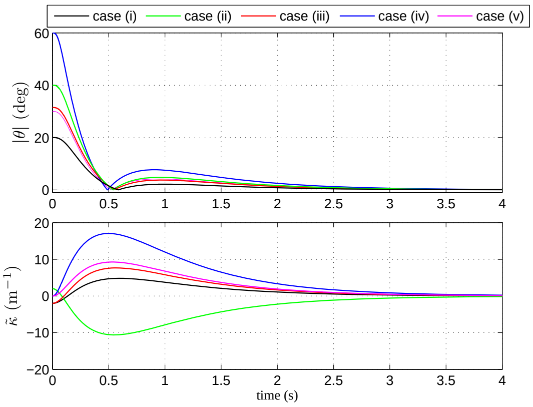

Figure 3: Estimation responses for the estimator (17), (18) (Assumption 1): (upper) estimation error response in the orientation of motion axis; (lower) estimation error response for the inverse distance between hinge and end-effector.

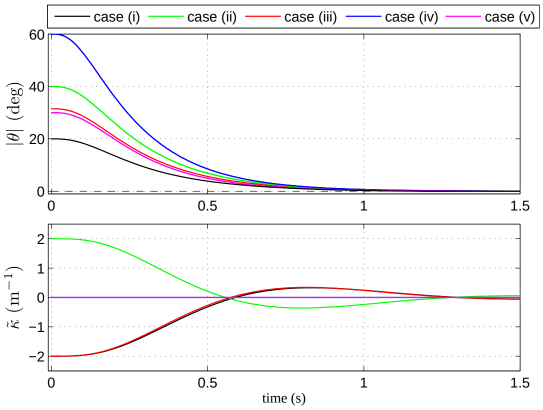

Figure 4: Estimation responses in case of the estimator (24), (27) (Assumption 2) : (upper) estimation error response in the orientation of motion axis; (lower) response of the estimation error of the inverse distance between hinge and end-effector.

The robot is approximately human-sized, and has a mass of approximately 150 kg. See [34] for a detailed description of the system.

As in the simulations, we used the door opening controllers to open and identify the kinematic parameters of doors of three different types of kinematics: a revolute door, a sliding door and a drawer, as shown in Fig. 6. Each of the experiments were initialized with a 30 deg error in the axis of motion on the motion plane.

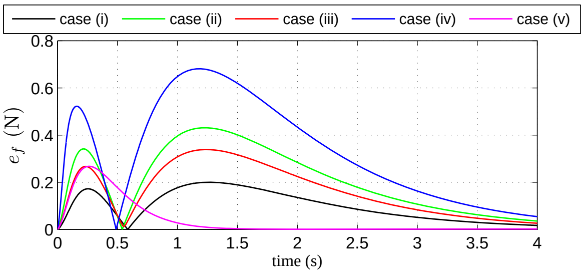

(a) Assumption 1.

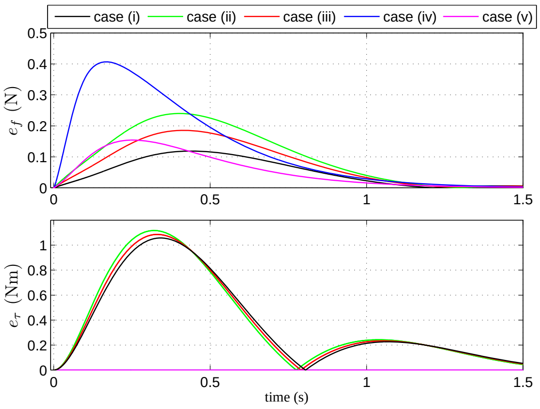

(b) Assumption 2 : (upper) norm of the projected force error, (lower) norm of the torque error.

Figure 5: Force and torque responses

For the three kinds of doors we performed experiments using fixed grasps on the doors (Assumption 2). Two of the doors — the revolute door and the drawer — were of the type typically used for kitchen cupboards, and were light-weight and fitted with significantly less rigid handles. For these, the performance of the controller evaluated both when grasping the rigid fronts of the doors directly and when grasping the less rigid handles. This allowed a test of the robustness of the system to deviations from the assumptions of rigid links in the kinematic chain. The third door was a sliding door of much larger mass, with a very rigid heavy-duty handle.

In the experiments, we set v_d to be constant for the whole trial, and thus the velocity is limited by the parts of the task where the manipulator is close to a singularity, or cannot move fast for some other reason, such as being limited by

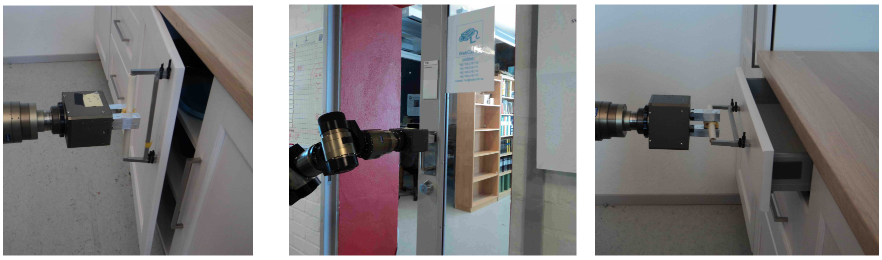

(a) Revolute door with passive handle.

(b) Sliding door.

(c) Drawer with passive handle.

Figure 6: Doors used for experimental evaluation of our controller

mass and/or friction of the heavy sliding door. Faster performance can be achived by letting v_d vary over the door opening tasks.

We also constructed alternative cylindrical handles for the revolute door and the drawer which allowed unconstrained rotation of the robot's gripper around the axis of the handle as shown in Fig. 6a. With these handles the generated grasps can be considered as passive revolute joints, and thus we can test our controllers following Assumption 1 of section 3.2. The ground truth of the axis of motion of the revolute door was obtained by manually moving the end effector to a series of points while grasping the handle, fitting a circle to the resulting trajectory and calculating the tangent of the circle at each point.

Fig. 7 shows the estimation error of the motion axis while opening a revolute door with a fixed grasp and the estimation error of the curvature $\tilde{\kappa}$, while Fig. 8 shows the corresponding norm of the projected force error and the norm of the torque error.

The results of the revolute door experiment while grasping the door directly is shown with a red dashed line. Here we see convergence to small estimation errors; less than 0.8 deg for the motion axis estimate, and 0.033m^{-1} for the curvature. In comparison, the performance when grasping the less rigid handle of the door is shown in solid blue lines in the figures. Even though the controller managed to successfully open the door and regulate the forces and torques, it incurred a 7 deg steady state error in the estimation of the motion axis and a $0.16\ \text{m}^{-1}$ error in the estimation of the inverse radius of curvature κ. In Fig. 8, we can see that the less rigid handle acts as a damper and lets the force controller converge faster.

These observations illustrate how the discrepancy between assumed and actual rigidity of the grasp on the handle and the rigidity of the handle itself with respect to the door affect the performance of our control scheme, as discussed in Section 4.4.

For the sliding door with a fixed grasp, the controller was able to operate the mechanism and we obtained the motion axis estimation error shown in Fig. 9 and force-torque response shown in Fig. 10. This door, including the handle, was much

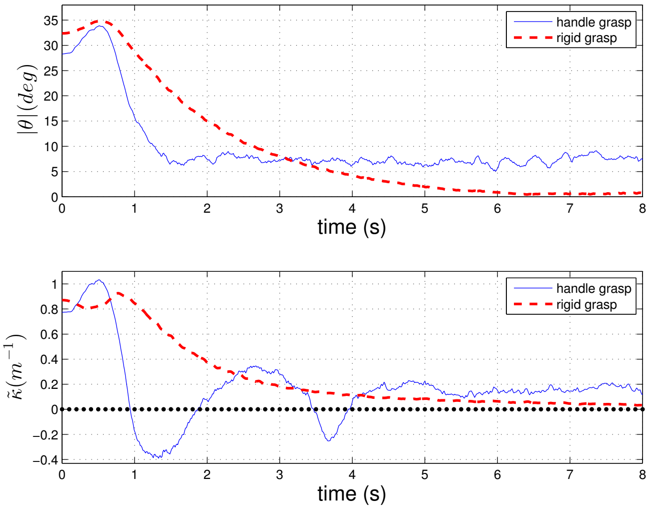

Figure 7: Estimation errors for a revolute door with fixed grasp, (upper): motion axis estimation error, (lower): inverse radius of curvature estimation error. Red dashed line show the estimation errors while grasping the door directly in a rigid manner, while the blue solid line shows the performance when grasping the less rigid handle.

more rigid than the others, thus the estimation of the motion axis shows convergence with a steady state error of less than 0.2 deg.

Fig. 11 and Fig. 12 show the performance of our controller for a drawer using fixed grasps. We observe that, similar to the revolute door case, the motion axis estimation error increases significantly from a 1.2 deg steady state error to a 6 deg error when applying a less rigid grasp, i.e. on the handle. This result illustrates that even when slightly relaxing the rigid grasp assumption, the robot can still control the doors, but the estimate is affected in terms of transient response and steady state errors.

Fig. 13 - 16 show the performance of our controller for a revolute door and a drawer each with passive revolute handles. Both mechanisms show a similar response in the estimation of the motion axis, with steady state errors of 0.9 deg and 0.4 deg respectively for the revolute door and the drawer. With this type of passive handle the controller does not exert torques on the handle and thus we obtain convergence of the motion axis estimate with low steady state errors comparable to those obtained when considering fixed grasps, as long as the rigidity assumption is fulfilled in the latter case.

In summary, we observe that our adaptive control scheme performs well as long as the doors are non-deformable and depending on how strongly the rigid grasp assumption is fulfilled in the case of fixed grasps on the doors. For typical between-

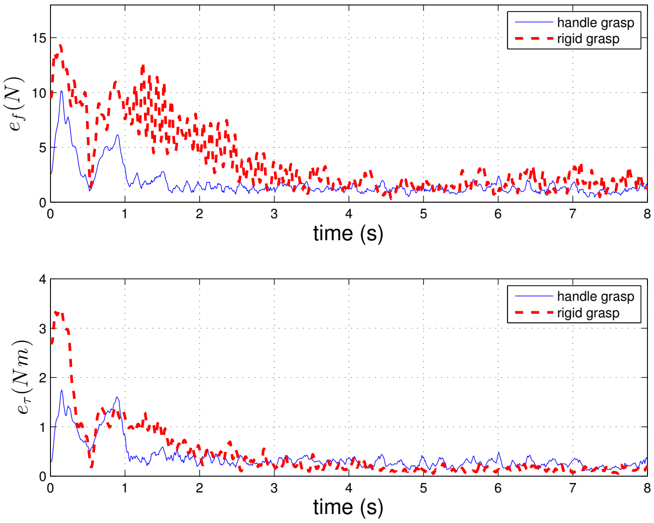

Figure 8: Force and torque responses for the revolute door experiment with fixed grasp, upper figure: norm of the projected force error, lower figure: norm of the torque error.

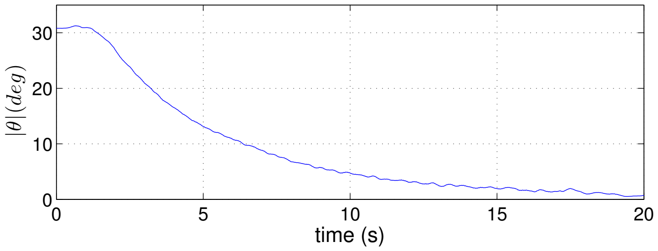

Figure 9: Sliding door with fixed grasp: motion axis estimation error.

room doors, the rigidity assumption is fulfilled, while the handles on some cupboard doors and drawers may have too low rigidity for the sensors and actuators on the robot used, causing small errors in the estimates.

7 Conclusions

We propose a unified method for manipulating different types of revolute and prismatic mechanisms. The method is model-free and can be used to identify the type and geometrical characteristics of one-joint mechanisms. By coupling estimation and action the method is inherently online and can be used in real-time applica-

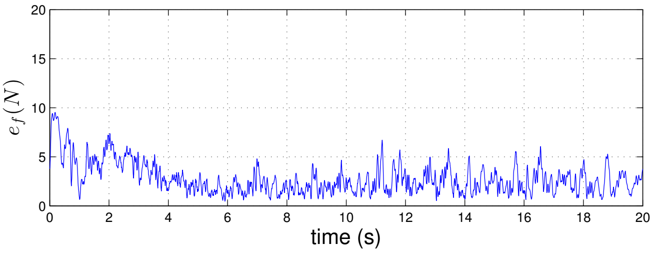

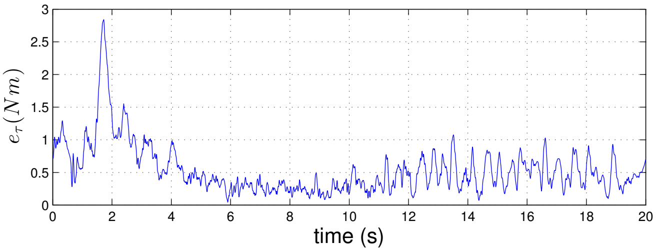

Figure 10: Force and torque responses for a sliding door with fixed grasp, upper figure: norm of the projected force error, lower figure: norm of the torque error.

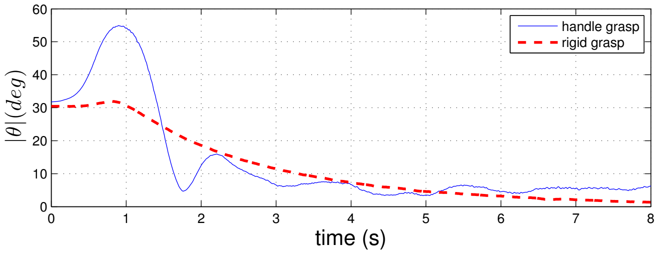

Figure 11: Motion axis estimation error for a drawer applying two types of grasps. The red dashed line shows the performance when grasping the drawer directly, and the solid blue line shows the estimation error while grasping the less rigid handle of the drawer.

tions. The method consists of a generalized velocity controller using estimates of the motion direction, the axis of rotation and update laws for the estimated vectors. The design of the overall scheme guarantees compliant behavior and convergence of the estimated vectors to their actual values.

Proof of Proposition 1: By projecting (17) along $\hat{\mathbf{x}}_h$ yields $\frac{d}{dt}\left(\frac{1}{2}\|\hat{\mathbf{x}}_h\|^2\right) = -\gamma v_{\text{ref}}\left[\mathbf{P}(\hat{\mathbf{x}}_h)\hat{\mathbf{x}}_h\right]^\top \mathbf{v}_f + v_{\text{ref}}(\hat{\mathbf{x}}_h \times \hat{\mathbf{x}}_h)^\top \hat{\boldsymbol{\kappa}} = 0$, since $\mathbf{P}(\hat{\mathbf{x}}_h)\hat{\mathbf{x}}_h = \mathbf{0}$ and $\hat{\mathbf{x}}_h \times \hat{\mathbf{x}}_h = \mathbf{0}$. $\square$

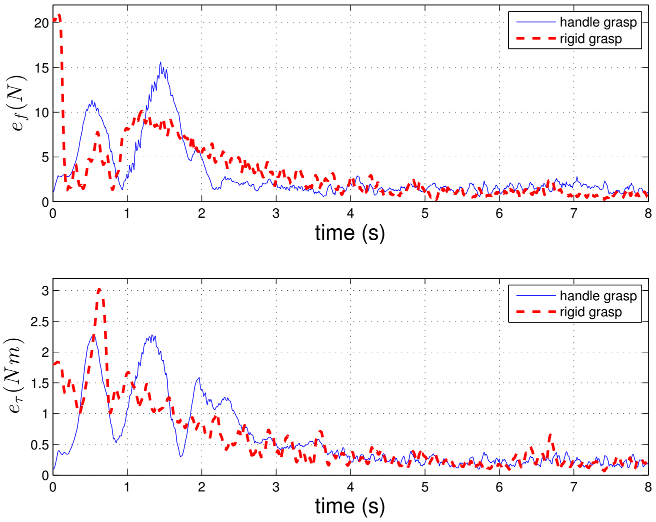

Figure 12: Force and torque responses for a drawer with fixed grasp, upper figure: norm of the projected force error, lower figure: norm of the torque error.

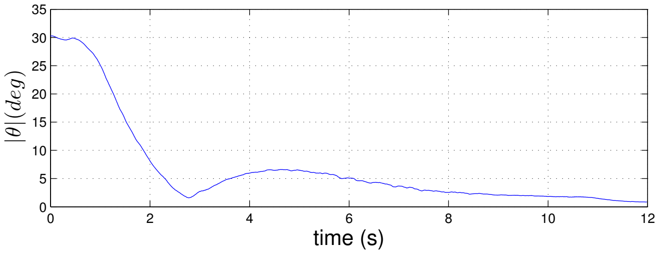

Figure 13: Motion axis estimation error for a revolute door with passive revolute handle.

Proof of Proposition 2: By projecting the update law (17) along $\mathbf{x}_h$ and subsequently substituting (11), (14), $\hat{\boldsymbol{\kappa}} = \boldsymbol{\kappa} + \tilde{\boldsymbol{\kappa}}$ and $v = v_{\text{ref}}$ (7) we get:

$$-\sin\theta\dot{\theta} = \gamma v_{\text{ref}}^2 \mathbf{x}_h^\top \mathbf{P}(\hat{\mathbf{x}}_h)\mathbf{x}_h - v_{\text{ref}}\mathbf{x}_h^\top(\hat{\mathbf{x}}_h \times \tilde{\boldsymbol{\kappa}})$$

Taking into account (15), $\mathbf{x}_h^\top \mathbf{P}(\hat{\mathbf{x}}_h)\mathbf{x}_h = \sin^2\theta$ and $\mathbf{x}_h^\top(\hat{\mathbf{x}}_h \times \tilde{\boldsymbol{\kappa}}) = -\tilde{\boldsymbol{\kappa}}^\top(\hat{\mathbf{x}}_h \times \mathbf{x}_h)$ yields

$$-\sin\theta\dot{\theta} = \gamma v_d^2 \tan^2\theta + \frac{v_d}{\cos\theta}\tilde{\boldsymbol{\kappa}}^\top(\hat{\mathbf{x}}_h \times \mathbf{x}_h) \tag{33}$$

As both $\mathbf{x}_h$ and $\hat{\mathbf{x}}_h$ are unit (see Proposition 1) we can write the cross product $(\hat{\mathbf{x}}_h \times \mathbf{x}_h)$ as $\sin\theta\mathbf{n}(t)$ with $\mathbf{n}(t)$ being a unit vector perpendicular to the plane defined

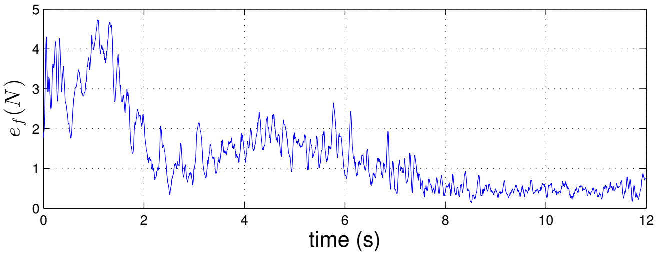

Figure 14: Revolute door experiment with passive revolute handle. Force response: norm of the projected force error.

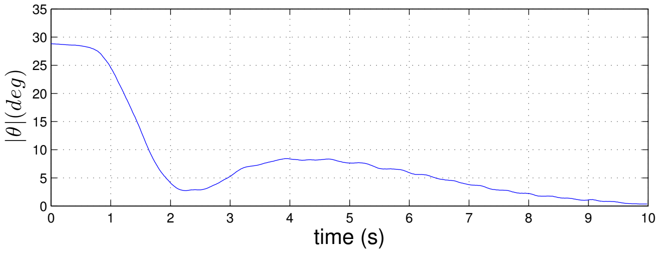

Figure 15: Motion axis estimation error for a drawer with passive revolute handle.

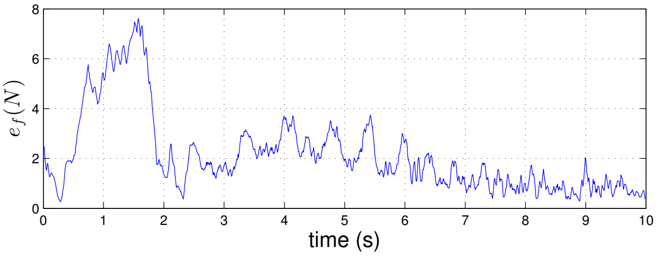

Figure 16: Drawer experiment with passive revolute handle. Force response: norm of the projected force error.

by $\mathbf{x}_h$ and $\hat{\mathbf{x}}_h$. Hence the non-trivial solution of (33) is given by the differential equation (20). Given $\dot{\hat{\boldsymbol{\kappa}}} = \dot{\tilde{\boldsymbol{\kappa}}}$, $\mathbf{v} = \mathbf{v}_{\text{ref}} = \mathbf{x}_h v = \mathbf{x}_h v_{\text{ref}}$ and $(\hat{\mathbf{x}}_h \times \mathbf{x}_h) = \sin\theta \mathbf{n}(t)$ we can easily transform (18) to (21).

In order to examine the stability of the nonlinear nonautonomous system we consider the following positive definite function in the domain D

$$W(\theta, \tilde{\boldsymbol{\kappa}}) = U(\theta) + \frac{1}{2}\tilde{\boldsymbol{\kappa}}^\top \boldsymbol{\Gamma}_\kappa^{-1}\tilde{\boldsymbol{\kappa}},\ U(\theta) = 1 - \cos\theta \tag{34}$$

Differentiating $W(\theta, \tilde{\boldsymbol{\kappa}})$ with respect to time along the system trajectories (20), (21) we get:

$$\dot{W} = -\gamma v_d^2 \tan^2 \theta \tag{35}$$

Since $W(\theta, \tilde{\boldsymbol{\kappa}})$ is locally positive definite and $\dot{W} \leq 0$ which implies $W(\theta, \tilde{\boldsymbol{\kappa}}) \leq W(\theta(0), \tilde{\boldsymbol{\kappa}}(0))$ we get that $\tilde{\boldsymbol{\kappa}}$ is bounded and $U(\theta) \leq W(\theta(0), \tilde{\boldsymbol{\kappa}}(0))$. The latter implies that:

$$\cos\theta \geq \cos\theta(0) - \frac{1}{2}\tilde{\boldsymbol{\kappa}}(0)^\top \boldsymbol{\Gamma}_\kappa^{-1} \tilde{\boldsymbol{\kappa}}(0) \tag{36}$$

which practically means that starting with $\theta(0) \in \left(-\frac{\pi}{2}, \frac{\pi}{2}\right)$, $\theta(t) \in \left(-\frac{\pi}{2}, \frac{\pi}{2}\right)$, $\forall t$ if $\boldsymbol{\Gamma}_\kappa$ is chosen such that:

$$\cos\theta(0) - \frac{1}{2}\tilde{\boldsymbol{\kappa}}(0)^\top \boldsymbol{\Gamma}_\kappa^{-1} \tilde{\boldsymbol{\kappa}}(0) > 0 \tag{37}$$

Since $\theta(0)$ and $\tilde{\boldsymbol{\kappa}}(0)$ are unknown, appropriately large value for $\boldsymbol{\Gamma}_\kappa$ can guarantee that the aforementioned condition is satisfied. Consequently, (14) and (15) implies that $\mathbf{P}(\hat{\mathbf{x}}_h)\mathbf{v}_f$ and v are bounded. Furthermore, the boundedness of $\mathbf{P}(\hat{\mathbf{x}}_h)\mathbf{v}_f$ implies that the update law rate $\dot{\hat{\mathbf{x}}}_h$ is bounded and subsequently $\dot{\theta}$ is bounded. Thus $\ddot{W}$ is bounded and according to Barbalat's Lemma $\dot{W} \to 0$. If v_d satisfies the PE condition then $\dot{W} \to 0$ implies $\theta \to 0$.

□

Proof of Proposition 3: Projecting (24) along ${}^e\hat{\mathbf{x}}_h$ yields $\frac{d}{dt}\left(\frac{1}{2}\|{}^e\hat{\mathbf{x}}_h(t)\|^2\right) = -\gamma v_d \left[\mathbf{P}(\hat{\mathbf{x}}_h)\mathbf{R}_e {}^e\hat{\mathbf{x}}_h\right]^\top \mathbf{v}_f = 0$ (since $\mathbf{P}(\hat{\mathbf{x}}_h)\hat{\mathbf{x}}_h = 0$). Note that $\hat{\mathbf{x}}_h$ has also invariant magnitude since it is derived by expressing ${}^e\hat{\mathbf{x}}_h$ at the robot inertia frame by using the rotation matrix $\mathbf{R}_e$. □

Proof of Proposition 4:

By projecting the update law (24) along $\mathbf{x}_h$ and subsequently substituting (12), (14), (15) we get:

$$-\sin\theta\dot{\theta} = \gamma \frac{v_d^2}{\cos\theta}\mathbf{x}_h^\top \mathbf{P}(\hat{\mathbf{x}}_h)\mathbf{x}_h \tag{38}$$

Taking into account $\mathbf{x}_h^\top \mathbf{P}(\hat{\mathbf{x}}_h)\mathbf{x}_h = \sin^2\theta$ we can readily see that the non-trivial solution of (38) is given by the differential equation (25). Differentiating the following positive definite Lyapunov function in the domain D':

$$U(\theta) = -\log(\cos\theta) \tag{39}$$

we get:

$$\dot{U} = -\gamma v_d^2 \tan^2\theta \tag{40}$$

Note that (40) implies $U(\theta) \leq U(\theta(0))$, which implies that starting with $\theta(0) \in \left(-\frac{\pi}{2}, \frac{\pi}{2}\right)$, $U(\theta)$ remains bounded $\forall t$. Since function $U(\theta)$ is a logarithmic barrier function, its boundedness implies that $\theta(t) \in \left(-\frac{\pi}{2}, \frac{\pi}{2}\right)$, $\forall t$. Consequently (14), (15) and (24) implies that $\mathbf{P}(\hat{\mathbf{x}}_h)\mathbf{v}_f$, v and the update law rate $\dot{\hat{\mathbf{x}}}_h$ are bounded. Eq. (40) implies also the exponential convergence of the angle error to zero (details can be found in [17]) given that v_d satisfies the PE condition. □

Proof of Theorem 1: We extend the positive function $W(\theta, \tilde{\boldsymbol{\kappa}})$ (proof of Proposition 2, Eq. (34)) or the function $U(\theta)$ (proof of Proposition 4, Eq. (39)) by adding a quadratic term of $\mathcal{I}\left[\mathbf{P}(\hat{\mathbf{x}}_h)\tilde{\mathbf{f}}\right]$ and we consider the following Lyapunov-like function:

$$V = \alpha_f \beta_f \mathcal{I}^2\left[\mathbf{P}(\hat{\mathbf{x}}_h)\tilde{\mathbf{f}}\right] + \frac{1}{\gamma} W(\theta, \tilde{\boldsymbol{\kappa}}) \tag{41}$$

By differentiating (41), completing the squares $\alpha_f^2 \left\|\mathbf{P}(\hat{\mathbf{x}}_h)\tilde{\mathbf{f}}\right\|^2$, $\beta_f^2 \left\|\mathcal{I}\left[\mathbf{P}(\hat{\mathbf{x}}_h)\tilde{\mathbf{f}}\right]\right\|^2$, substituting (16) and (35) (or (40) in case of U given by (39) is used in (41)) we get:

$$\dot{V} = -\alpha_f^2 \left\|\mathbf{P}(\hat{\mathbf{x}}_h)\tilde{\mathbf{f}}\right\|^2 - \beta_f^2 \left\|\mathcal{I}\left[\mathbf{P}(\hat{\mathbf{x}}_h)\tilde{\mathbf{f}}\right]\right\|^2$$

Hence, $V(t) \leq V(0)$, $\forall\ t$ which additionally to the boundedness results of Proposition 2 or Proposition 4 implies that $\mathcal{I}[\mathbf{P}(\hat{\mathbf{x}}_h)\tilde{\mathbf{f}}]$ is bounded. The boundedness of $\mathbf{P}(\hat{\mathbf{x}}_h)\mathbf{v}_f$ and $\mathcal{I}[\mathbf{P}(\hat{\mathbf{x}}_h)\tilde{\mathbf{f}}]$, implies that $\mathbf{P}(\hat{\mathbf{x}}_h)\tilde{\mathbf{f}}$ is bounded. Differentiating (14), (15) and using the boundedness of $\mathcal{I}[\mathbf{P}(\hat{\mathbf{x}}_h)\tilde{\mathbf{f}}]$, $\mathbf{P}(\hat{\mathbf{x}}_h)\mathbf{v}_f$ and $\dot{\hat{\mathbf{x}}}_h$, it can be easily shown that $\frac{d}{dt}\left[\mathbf{P}(\hat{\mathbf{x}}_h)\mathbf{v}_f\right]$ is bounded. Hence, the second derivative of V is bounded allowing the use of Barbalat's Lemma in order to prove that $\dot{V} \to 0$ and consequently $\mathcal{I}\left[\mathbf{P}(\hat{\mathbf{x}}_h)\tilde{\mathbf{f}}\right]$, $\mathbf{P}(\hat{\mathbf{x}}_h)\tilde{\mathbf{f}} \to 0$. Note that the aforementioned convergence results are referred to the estimated motion space defined by $\hat{\mathbf{x}}_h$. Taking into account Proposition 2 or 4 that implies the convergence of θ to zero or $\hat{\mathbf{x}}_h \to \mathbf{x}_h$ for v_d satisfying the PE condition, we get $\mathcal{I}\left[\mathbf{P}(\mathbf{x}_h)\tilde{\mathbf{f}}\right]$, $\mathbf{P}(\mathbf{x}_h)\tilde{\mathbf{f}} \to 0$ □

Proof of Theorem 2: First, we will reform $\boldsymbol{\omega}_{\text{ref}}$ by adding/subtracting the term $\boldsymbol{\kappa}(v - v_d)$, using (15) and substituting $\hat{\boldsymbol{\kappa}} = \boldsymbol{\kappa} + \tilde{\boldsymbol{\kappa}}$ as follows:

$$\boldsymbol{\omega}_{\text{ref}} = \boldsymbol{\kappa} v + \tilde{\boldsymbol{\kappa}} v_d - \boldsymbol{\omega}_\tau + v_d \left(\tfrac{\cos\theta - 1}{\cos\theta}\right) \boldsymbol{\kappa} \tag{42}$$

For design purposes we consider the following positive definite function:

$$V = \alpha_\tau \beta_\tau \|\mathcal{I}\left(\tilde{\boldsymbol{\tau}}\right)\|^2 + \frac{1}{2}\tilde{\boldsymbol{\kappa}}^\top \boldsymbol{\Gamma}_\kappa^{-1} \tilde{\boldsymbol{\kappa}} + \frac{\xi}{\gamma} U(\theta) \tag{43}$$

with $U(\theta)$ being defined in (39) and ξ being a positive constant. By differentiating (43) with respect to time and substituting $\dot{\tilde{\boldsymbol{\kappa}}} = \dot{\hat{\boldsymbol{\kappa}}}$, $\boldsymbol{\omega} = \boldsymbol{\omega}_{\text{ref}}$ given by (42), (40) and the rotational constraints (3), (6) we get:

$$\begin{aligned} \dot{V} = & -\alpha_\tau^2 \|\tilde{\boldsymbol{\tau}}\|^2 - \beta_\tau^2 \|\mathcal{I}(\tilde{\boldsymbol{\tau}})\|^2 + v_d \left(\tfrac{\cos\theta - 1}{\cos\theta}\right) \boldsymbol{\omega}_\tau^\top \boldsymbol{\kappa} \\ & - \xi v_d^2 \tan^2\theta + \tilde{\boldsymbol{\kappa}}^\top \left(\boldsymbol{\Gamma}_\kappa^{-1} \dot{\hat{\boldsymbol{\kappa}}} + v_d \boldsymbol{\omega}_\tau\right) \end{aligned} \tag{44}$$

In order to cancel the last term of the right side part of (44) we set $\dot{\hat{\boldsymbol{\kappa}}} = -v_d \boldsymbol{\Gamma}_\kappa \boldsymbol{\omega}_\tau$ which corresponds to the update law (27). By using (27) and the inequality:

$$\boldsymbol{\omega}_\tau^\top \boldsymbol{\kappa} \left(\frac{\cos\theta - 1}{\cos\theta} \right) v_d \leq \frac{\|\boldsymbol{\omega}_\tau\|^2}{4} + \|\boldsymbol{\kappa}\|^2 v_d^2 \left(\tfrac{\cos\theta - 1}{\cos\theta} \right)^2 \tag{45}$$

we can upper-bound $\dot{V}$ (44) as follows:

$$\begin{aligned} \dot{V} \leq &- \alpha_\tau^2 \|\tilde{\boldsymbol{\tau}}\|^2 - \beta_\tau^2 \|\mathcal{I}(\tilde{\boldsymbol{\tau}})\|^2 + \frac{\|\boldsymbol{\omega}_\tau\|^2}{4} \\ &- \xi v_d^2 \tan^2\theta + \|\boldsymbol{\kappa}\|^2 v_d^2 \left(\tfrac{\cos\theta - 1}{\cos\theta} \right)^2 \end{aligned} \tag{46}$$

Expanding $\|\boldsymbol{\omega}_\tau\|^2$ – using (28)– and setting $\xi > \|\boldsymbol{\kappa}\|^2$, we get:

$$\dot{V} \leq - \tfrac{\alpha_\tau^2}{2} \|\tilde{\boldsymbol{\tau}}\|^2 - \tfrac{\beta_\tau^2}{2} \|\mathcal{I}(\tilde{\boldsymbol{\tau}})\|^2 - 2\|\boldsymbol{\kappa}\|^2 v_d^2 \left(\tfrac{1 - \cos\theta}{\cos\theta} \right) \tag{47}$$

Since $\cos\theta \leq 1$ and $\theta(t) \in \left(-\frac{\pi}{2}, \frac{\pi}{2} \right)$ provided that $\theta(0) \in \left(-\frac{\pi}{2}, \frac{\pi}{2} \right)$ (Proposition 4), the derivative of function V can be upper-bounded as follows:

$$\dot{V} \leq -\tfrac{\alpha_\tau^2}{2} \|\tilde{\boldsymbol{\tau}}\|^2 - \tfrac{\beta_\tau^2}{2} \|\mathcal{I}(\tilde{\boldsymbol{\tau}})\|^2$$

Hence, $V(t) \leq V(0)$, $\forall\, t$ which implies that $\mathcal{I}(\tilde{\boldsymbol{\tau}})$ and $\tilde{\boldsymbol{\kappa}}$ are bounded. Hence, by taking into account the constraints (3), (6) for the closed loop system $\boldsymbol{\omega} = \boldsymbol{\omega}_{\text{ref}}$ (42), it is clear that $\tilde{\boldsymbol{\tau}}$ is bounded and hence $\dot{\hat{\boldsymbol{\kappa}}}$ is bounded. Using the aforementioned boundedness results as well as those implied by Proposition 4 and Theorem 1, it can be easily proved by differentiating $\dot{V}$ that $\ddot{V}$ is bounded. Hence, applying Barbalat's Lemma we get that $\tilde{\boldsymbol{\tau}} \to 0$, $\mathcal{I}(\tilde{\boldsymbol{\tau}}) \to 0$. Using the aforementioned convergence results as well as $\theta \to 0$, it can be shown that $\hat{\boldsymbol{\kappa}} \to \boldsymbol{\kappa}$ provided that v_d satisfies the PE condition and hence $\boldsymbol{\omega}_e \to v_d \boldsymbol{\kappa}$. □

Proof of Proposition 5: By projecting the update law (24) along $\mathbf{x}_h$ and subsequently substituting (12), (29), (30) and $\mathbf{x}_h^\top \mathbf{P}(\hat{\mathbf{x}}_h)\mathbf{x}_h = \sin^2\theta$ we get:

$$-\sin\theta\dot{\theta} = \gamma \frac{v_d^2}{\cos\theta} \sin^2\theta + \gamma v_d \left(\frac{\hat{\mathbf{x}}_h}{\cos\theta} - \mathbf{x}_h \right)^\top \boldsymbol{\delta}(t)$$

Note that vector $\frac{\hat{\mathbf{x}}_h}{\cos\theta} - \mathbf{x}_h$ is perpendicular to $\mathbf{x}_h$ since $\left(\frac{\hat{\mathbf{x}}_h}{\cos\theta} - \mathbf{x}_h \right)^\top \mathbf{x}_h = 0$ while its magnitude is equal to $|\tan\theta|$. By defining a unit vector $\mathbf{n}'(t)$ parallel to $\frac{\hat{\mathbf{x}}_h}{\cos\theta} - \mathbf{x}_h$ we can easily get:

$$-\sin\theta\dot{\theta} = \gamma \frac{v_d^2}{\cos\theta} \mathbf{x}_h^\top \mathbf{P}(\hat{\mathbf{x}}_h)\mathbf{x}_h + \gamma v_d |\tan\theta| \delta(t) \tag{48}$$

The nontrivial solution of (48) is given by (31). □

Proof of Proposition 6: Differentiating (39) with respect to time and substituting (31), we get that $\dot{U}(\theta)$ is upper-bounded as follows:

$$\dot{U}(\theta) \leq -\gamma v_d^2 \frac{|\tan\theta|}{\cos\theta} \left(|\sin\theta| - \lambda(t)\right) \tag{49}$$

From (49) and Theorem 4.18 of [19] regarding uniform ultimate boundedness we can find that the region in which the estimation error converges is given by (32). ☐

References

[1] Saleh Ahmad, Hongwei Zhang, and Guangjun Liu. Multiple working mode control of door opening with a mobile modular and reconfigurable robot. *IEEE/ASME Trans. on Mechatronics*, 18(3):833–844, 2013.

[2] H. Arisumi, J.-R. Chardonnet, and K. Yokoi. Whole-body motion of a humanoid robot for passing through a door - opening a door by impulsive force. In *IEEE/RSJ International Conference on Intelligent Robots and Systems*, pages 428–434, oct. 2009.

[3] H. Bruyninckx. *Kinematic Models for Robot Compliant Motion with Identification of Uncertainities.* PhD thesis, KU Leuven, Department of Mechanical Engineering, 1995.

[4] H. Bruyninckx and J. De Schutter. Specification of force-controlled actions in the “task frame formalism”-a synthesis. *IEEE Trans. on Robotics and Automation*, 12 (4):581–589, Aug 1996.

[5] C. C. Cheah, S. Kawamura, and S. Arimoto. Stability of hybrid position and force control for robotic kinematics and dynamics uncertainties. *Automatica*, 39:847–855, 2003.

[6] C.C. Cheah, C. Li, and J.J.E. Slotine. Adaptive tracking control for robots with unknown kinematic and dynamic properties. *The International Journal of Robotics Research*, 25(3):283–296, 2006.

[7] Woojin Chung, Changju Rhee, Youngbo Shim, Hyungjin Lee, and Shinsuk Park. Door-opening control of a service robot using the multifingered robot hand. *IEEE Trans. on Industrial Electronics*, 56(10):3975–3984, oct. 2009.

[8] Joris De Schutter, Tinne De Laet, Johan Rutgeerts, Wilm Decrè, Ruben Smits, Erwin Aertbeliën, Kasper Claes, and Herman Bruyninckx. Constraint-based task specification and estimation for sensor-based robot systems in the presence of geometric uncertainty. *The International Journal of Robotics Research*, 26(5):433–455, 2007.

[9] S. Erhart and S. Hirche. Adaptive force/velocity control for multi-robot cooperative manipulation under uncertain kinematic parameters. In *2013 IEEE/RSJ International Conference on Intelligent Robots and Systems (IROS)*, pages 307–314, Nov 2013.

[10] P. A. Ioannou and J. Sun. *Robust Adaptive Control.* Upper Saddle River, NJ:Prentice Hall, 1996.

[11] A. Jain and C.C. Kemp. Pulling open novel doors and drawers with equilibrium point control. In *IEEE-RAS International Conference on Humanoid Robots*, pages 498–505, dec. 2009.

[12] A. Jain and C.C. Kemp. Pulling open doors and drawers: Coordinating an omni-directional base and a compliant arm with equilibrium point control. In *IEEE International Conference on Robotics and Automation*, pages 1807–1814, 2010.

[13] Y. Karayiannidis and Z. Doulgeri. Adaptive control of robot contact tasks with on-line learning of planar surfaces. *Automatica*, 45(10):2374–2382, 2009.

[14] Yiannis Karayiannidis, Christian Smith, Petter Ögren, and Danica Kragic. Adaptive force/velocity control for opening unknown doors. In *IFAC Symposium on Robot Control*, Dubrovnik, Croatia, Sep 2012.

[15] Yiannis Karayiannidis, Christian Smith, Francisco Viña, and Danica Kragic. Online kinematics estimation for active human-robot manipulation of jointly held objects. In *IEEE/RSJ International Conference on Intelligent Robots and Systems*, pages 4872–4878, 2013.

[16] Yiannis Karayiannidis, Christian Smith, Francisco Viña, Petter Ögren, and Danica Kragic. 'Open Sesame!' - Adaptive Force/Velocity Control for Opening Unknown Doors. In *IEEE/RAS Conference on Intelligent Robots and Systems*, Vilamoura, Portugal, Oct 2012.

[17] Yiannis Karayiannidis, Christian Smith, Francisco Viña, Petter Ögren, and Danica Kragic. Model-free robot manipulation of doors and drawers by means of fixed-grasps. In *IEEE International Conference on Robotics and Automation*, pages 4470–4477, 2013.

[18] C.C. Kessens, J.B. Rice, D.C. Smith, S.J. Biggs, and R. Garcia. Utilizing compliance to manipulate doors with unmodeled constraints. In *IEEE/RSJ International Conference on Intelligent Robots and Systems*, pages 483–489, oct. 2010.

[19] H. Khalil. *Nonlinear Systems*. Prentice Hall, third edition, 2002.

[20] D.W. Kim and G.-T. Kang, J.-H.and Park. Door-opening behaviour by home service robot in a house. *International Journal of Robotics and Automation*, 25(4):271–284, 2010.

[21] E. Lutscher, M. Lawitzky, G. Cheng, and S. Hirche. A control strategy for operating unknown constrained mechanisms. In *IEEE International Conference on Robotics and Automation*, pages 819–824, may 2010.

[22] D. Ma, H. Wang, and W. Chen. Unknown constrained mechanisms operation based on dynamic hybrid compliance control. In *IEEE International Conference on Robotics and Biomimetics*, pages 2366–2371, dec. 2011.

[23] K. Nagatani and S.I. Yuta. An experiment on opening-door-behavior by an autonomous mobile robot with a manipulator. In *IEEE/RSJ International Conference on Intelligent Robots and Systems*, volume 2, pages 45–50, aug 1995.

[24] G. Niemeyer and J.-J.E. Slotine. A simple strategy for opening an unknown door. In *IEEE International Conference on Robotics and Automation*, volume 2, pages 1448–1453, apr 1997.

[25] C. Ott, B. Bäuml, C. Borst, and G. Hirzinger. Employing cartesian impedance control for the opening of a door: A case study in mobile manipulation. In *IEEE/RSJ International Conference on Intelligent Robots and Systems, Workshop on mobile manipulators: Basic techniques, new trends & applications*, 2005.

[26] L. Peterson, D. Austin, and D. Kragic. High-level control of a mobile manipulator for door opening. In *IEEE/RSJ International Conference on Intelligent Robots and Systems*, volume 3, pages 2333–2338, 2000.

[27] A. Petrovskaya and A. Y. Ng. Probabilistic mobile manipulation in dynamic environments with application to opening doors. In *International Joint Conference on Artifical Intelligence*, pages 2178–2184, Hydrabad, India, January 2007.

[28] M. Prats, S. Wieland, T. Asfour, A.P. del Pobil, and R. Dillmann. Compliant interaction in household environments by the Armar-III humanoid robot. In *IEEE-RAS International Conference on Humanoid Robots*, pages 475–480, dec. 2008.

[29] Mario Prats, Angel p. del Pobil, and Pedro J Sanz. *Robot Physical Interaction through the combination of Vision, Tactile and Force Feedback - Applications to Assistive Robotics*, volume 84 of *Springer Tracts in Advanced Robotics*, chapter Physical Interaction: When Only Force Is Available, pages 55–77. Springer, 2013.

[30] M. H. Raibert and J. J. Craig. Hybrid position/force control of manipulators. *Journal of Dynamic Systems, Measurement and Control, Trans. of the ASME*, 103(2):126–133, 1981.

[31] A.J. Schmid, N. Gorges, D. Goger, and H. Worn. Opening a door with a humanoid robot using multi-sensory tactile feedback. In *IEEE International Conference on Robotics and Automation*, pages 285–291, may 2008.

[32] B. Siciliano, L. Sciavicco, and L. Villani. *Robotics: Modelling, Planning and Control*. Advanced Textbooks in Control and Signal Processing. Springer, 2009. ISBN 9781846286414.

[33] J.J.E. Slotine and W. Li. *Applied Nonlinear Control*. Prentice Hall, 1991. ISBN 9780130408907.

[34] Christian Smith and Yiannis Karayiannidis. Optimal command ordering for serial link manipulators. In *IEEE-RAS International Conference on Humanoid Robots*, pages 255–261, 2012.

[35] J. Sturm, A. Jain, C. Stachniss, C.C. Kemp, and W. Burgard. Operating articulated objects based on experience. In *IEEE/RSJ International Conference on Intelligent Robots and Systems*, pages 2739–2744, 2010.

[36] J. Sturm, C. Stachniss, and W. Burgard. A probabilistic framework for learning kinematic models of articulated objects. *Journal of Artificial Intelligence Research*, 41:477–526, 2011.

[37] T. Yoshikawa. *Foundations of Robotics*. Cambridge, MA:MIT Press, 1990.

Paper B

Online Contact Point Estimation for Uncalibrated Tool Use

Published in
IEEE International Conference on Robotics and Automation, 2014

Online Contact Point Estimation for Uncalibrated Tool Use

Yiannis Karayiannidis, Christian Smith, Francisco E. Viña B., and Danica Kragic

Abstract

One of the big challenges for robots working outside of traditional industrial settings is the ability to robustly and flexibly grasp and manipulate tools for various tasks. When a tool is interacting with another object during task execution, several problems arise: a tool can be partially or completely occluded from the robot's view, it can slip or shift in the robot's hand - thus, the robot may lose the information about the exact position of the tool in the hand. Thus, there is a need for online calibration and/or recalibration of the tool. In this paper, we present a model-free online tool-tip calibration method that uses force/torque measurements and an adaptive estimation scheme to estimate the point of contact between a tool and the environment. An adaptive force control component guarantees that interaction forces are limited even before the contact point estimate has converged. We also show how to simultaneously estimate the location and normal direction of the surface being touched by the tool-tip as the contact point is estimated. The stability of the the overall scheme and the convergence of the estimated parameters are theoretically proven and the performance is evaluated in experiments on a real robot.

1 Introduction

The ability to robustly grasp and manipulate tools intended for human use and employ these for various tasks (as in Fig. 1) remains one of the big challenges for robots working outside of traditional industrial settings. The application areas range from flexible industrial robots working with tools intended for human use to domestic service robots that perform household chores [11]. In order to provide the input for the control loop guiding the execution of a task, the knowledge of the position of the tool-tip is necessary.

In contrast to classical industrial or other robots with fixed and a priori known tools, it is not realistic to assume that service robots have precise beforehand calibrations of the positions of the tool-tips. Even if they did, the tool may slip and move relative to the gripper while it is being used. Therefore, there is a need for online calibration and/or recalibration of the position of the tip of the tool the robot

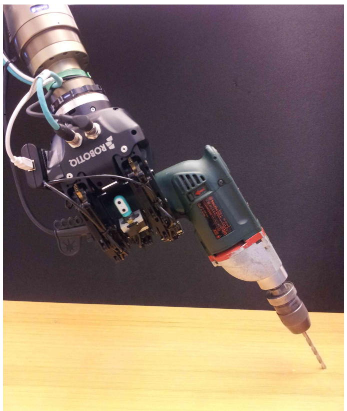

Figure 1: Robot manipulating a tool intended for human use.

is using. Current approaches mostly rely on vision-based methods for calibrating the pose and are therefore not applicable in scenarios where the tools or relevant parts of it are occluded.

In this paper, we present an online tool-tip calibration method that uses force/torque measurements and an adaptive estimation scheme to find the point of contact between a tool and the environment. This estimation can be carried out in real-time while the robot is using the tool to perform some arbitrary task, and does not require any predefined model of the shape, size or initial position of the tool being used.

An adaptive force control component guarantees that interaction forces are limited even before the contact point estimate has converged. We also show how to simultaneously estimate the location and normal direction of the surface being touched by the tool-tip as the contact point is estimated.

The paper has the following structure: Section 2 reviews the state of the art in related work, Section 3 formalizes the problem in terms of statics and kinematics, Section 4 describes the proposed approach and motivates it theoretically, giving stability and convergence proofs, while Section 5 describes the experimental implementation of the method on a real robot and the experimental results. Finally, conclusions are presented in Section 6.

2 Related Work

The problem of resolving uncertainties in the end-effector or the tool positioning is well-studied and has been a relevant topic in robotics since the advent of the first manipulators. Early work focused on solving the problem of calibrating the position of the manipulators and end-effectors themselves [20], and this has been extended to also include objects grasped by the robot [4].

Some works treat the problem without explicitly modelling the position of a tool or its point of interaction with the environment, but focus rather on robust performance of a well-defined task under positioning uncertainties. Examples of this includes work by Bruyninckx *et al.* that estimates the alignment error between the peg and the hole for an insertion task [3], work by Hovland and McCarragher that uses a neural network approach to estimate the contact states between two work pieces [7], and work by Koeppe and Hirzinger that learns the appropriate interaction forces for a peg-in-hole task [13].

Some work treats tool-tip position estimation as a calibration problem that can be performed offline prior to using the tool. Yang *et al.* use an iterative least squares approach to calibrate the relationship between tool-tip position and joint angles, using measurements from a known external reference [23]. Cheah *et al.* use adaptive control for tracking a kinematically uncertain manipulator chain, including a tool grasped by the end-effector, but only estimate the kinematics — the position of the end-effector and the tool are measured externally [4].

Others use a particle filter approach to fit a model to the object pose by collecting measurements from touching the object before grasping it [5, 18]. Hebert *et al.* use a fusion approach with vision, force/torque measurements and proprioception to estimate the position of an object with a known model, held in the end-effector [6]. Păiş *et al.* learn relations between a held object and an external tool it interacts with using gaussian mixture models [19].

Atkeson *et al.* have proposed a method for estimating inertial parameters of a grasped object based on force/torque measurements [1], and Kubus *et al.* have used sensor fusion combining measurements of acceleration, velocities, position, forces, and torques to estimate inertial parameters and principal moments of inertia of a grasped object, fitting parameters to estimate object pose [15]. Both these approaches require free motion in a prespecified trajectory, and can not be applied to estimate the contact point of a tool online as it is being used.

Muto and Shimokura have shown a method for estimating contact points given a known tool fixed in the end-effector, using force measurements [17]. Lei *et al.* propose a method that learns model parameters to estimate the position and external force load on a specific non-rigid grinding tool, using proprioception and force/torque measurements [16].

The literature on vision-based object pose estimation and tracking is far too vast to summarize here, but some examples of tool pose estimation based on computer vision methods include work by Kemp and Edsinger who use visual gradients to detect tool-tip positions [12], Krainin *et al.* who simultaneously build an object model and track it in the robot hand [14], and Beetz *et al.*, who use repeated visual template matching to find the location of a spatula in the robot hand [2].

In our previous work, we have shown how an adaptive estimator, integrating proprioception and force/torque measurements can be used to estimate the location of hinges on doors, or the direction of unconstrained motion for drawers that the robot is opening [10], and to estimate slopes on surfaces the robot is in contact with [9]. We have also shown how to learn manipulation affordances and slippage behaviors of held objects by using combined measurements of wrist-based force/torque measurements and grasp forces [22].

In the present paper, we build on these ideas and propose an adaptive controller that estimates the point of contact of the tool with the environment, along with estimating the contact surface normal. This enables the robot to execute a task with the held tool while performing the estimation. The proposed controller limits the interaction forces, to avoid damage to the tool or workpiece while estimates are converging. The proposed method uses force/torque measurements from a wrist-mounted sensor, it is inherently online and fast enough to react to changes, and can thus track the contact point even if it moves relative to the robot hand while executing the task.

3 Kineto-Statics Formulation

Before describing the proposed method for estimating the contact point and the surface normal, we define notation and formalize the relevant first-order differential kinematics and the statics. We assume a system that consists of a robot which performs a task with its tool on a surface; the task requires motion control of the tool contact point and control of the contact forces of the tool on a surface.

3.1 Notation

First, we introduce the following notation and definitions that will be used throughout this paper:

Bold small letters denote vectors and bold capital letters denote matrices. $\mathbf{I}_\nu$, $\mathbf{O}_\nu \in \mathbb{R}^{\nu \times \nu}$ denote an identity and a square matrix of zeros respectively while $\mathbf{0}_\nu \in \mathbb{R}^\nu$ denotes a column vector of zeros. Hat $\hat{\cdot}$ and tilde $\tilde{\cdot}$ denote estimates and the errors between control variables and their corresponding desired values/vectors respectively. $\mathbf{R}_a$ denotes a rotation matrix that describes the orientation of a frame with respect to the global frame. A left superscript (e.g. ${}^a\mathbf{b}$) denotes the frame (e.g. $\{a\}$) in which a three-dimensional vector (e.g. $\mathbf{b} \in \mathbb{R}^3$) is expressed, e.g. ${}^a\mathbf{b} = \mathbf{R}_a^\top \mathbf{b}$, and it is omitted in case of the global frame. The projection matrix on the orthogonal complement space of a unit three dimensional vector $\mathbf{a}$ is denoted by $\mathbf{P}(\mathbf{a}) \triangleq \mathbf{I}_3 - \mathbf{a}\mathbf{a}^\top$. $\mathbf{S}(\mathbf{b})$ denotes the skew-symmetric matrix produced by $\mathbf{b} \in \mathbb{R}^3$ to perform a cross product operation with any three-dimensional vector $\mathbf{a} \in \mathbb{R}^3$ i.e. $\mathbf{b} \times \mathbf{a} = \mathbf{S}(\mathbf{b})\mathbf{a}$.

3.2 First Order Differential Kinematics

Consider a robot end-effector equipped with a force/torque sensor on its wrist that is grasping a tool which is in contact with a surface, as shown in Fig. 2. We denote with $\{e\}$ a frame attached at a kinematically known position of the end-effector (e.g. center of force/torque sensor) denoted by $\mathbf{p}_e$. We assume that the contact between the tool and the surface is modeled as a contact point that can slide along the surface when the end-effector is moving. At the contact point position $\mathbf{p}_c$, we attach a frame $\{c\}$ with orientation described by $\mathbf{R}_c = [\mathbf{n}_c\ \mathbf{o}_c\ \mathbf{a}_c]$, with $\mathbf{n}_c$ being a unit vector which is normal to the surface while $\mathbf{o}_c$, $\mathbf{a}_c$ being vectors that span the flat surface and can be arbitrarily chosen. Let $\mathbf{r}$ be the relative position of $\{e\}$ and $\{c\}$ defined as follows:

$$\mathbf{r} = \mathbf{p}_c - \mathbf{p}_e \tag{1}$$

Note that ${}^e\mathbf{r} \triangleq \mathbf{R}_e^\top \mathbf{r}$ is constant if we assume that the end-effector is rigidly grasping the tool. Assuming additionally that only sliding motion is performed i.e. $\dot{\mathbf{p}}_c = \dot{\mathbf{p}}_e$ then $\mathbf{r}$ is constant too and the velocity of the end-effector frame is constrained as follows:

$$\mathbf{n}_c^\top \dot{\mathbf{p}}_e = 0 \tag{2}$$

Note that the assumption of pure sliding motion that simplifies the estimation of the surface slope is not necessary for the main objective of this work which is the contact point estimation. Differentiating (1) implies that the contact point velocity is related to the end-effector velocity as follows:

$$\dot{\mathbf{p}}_c = \mathbf{J}_t \begin{bmatrix} \dot{\mathbf{p}}_e \\ \boldsymbol{\omega}_e \end{bmatrix}, \text{ with } \mathbf{J}_t \triangleq \begin{bmatrix} \mathbf{I}_3 & -\mathbf{S}(\mathbf{r}) \end{bmatrix} \in \mathbb{R}^{3\times 6} \tag{3}$$

being the tool Jacobian matrix and $\boldsymbol{\omega}_e$ being the end-effector rotational velocity i.e. $\mathbf{S}(\boldsymbol{\omega}_e) = \dot{\mathbf{R}}_e \mathbf{R}_e^\top$. By commanding zero rotational velocity and assuming only sliding motion, we can omit the tool Jacobian when mapping the contact point velocities to the joint space. This means that the first order inverse kinematics are given by:

$$\dot{\mathbf{q}} = \mathbf{J}^+ \begin{bmatrix} \mathbf{u} \\ \mathbf{0}_3 \end{bmatrix} \tag{4}$$

where $\mathbf{u}$ is a commanded end-effector or contact point velocity control law and $\mathbf{J}^+$ is the right pseudo-inverse of the end-effector Jacobian with $\mathbf{J}^+ \triangleq \mathbf{J}^\top(\mathbf{J}\mathbf{J}^\top)^{-1}$.

3.3 Statics

While the end-effector presses with the tool on the surface, the normal force arising (with magnitude denoted by f_n) can – in case of rigid contact – be regarded as a Lagrange multiplier of the controlled system associated to the constraint (2). While the contact point is moving along the surface following the motion of the end-effector, tangential forces $\mathbf{f}_t$ arise owing to dynamic friction components that depend on the sliding velocity of the contact point. The total contact force applied at the contact point is mapped to the end-effector as a wrench consisting of a force vector $\mathbf{f}_c$ and a torque vector $\boldsymbol{\tau}_c$:

$$\mathbf{f}_c = \mathbf{n}_c f_n + \mathbf{f}_t, \tag{5}$$

$$\boldsymbol{\tau}_c = \mathbf{r} \times \mathbf{f}_c. \tag{6}$$

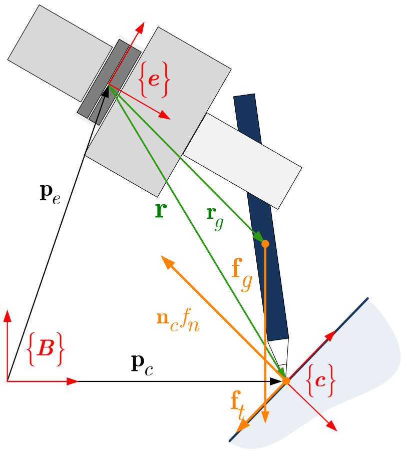

Figure 2: A robot end-effector equipped with a force/torque sensor on its wrist that is grasping a tool which is in contact with the surface. Frames are illustrated with red lines. Forces are depicted with orange. Absolute position vectors with respect to the base frame $\{B\}$ are depicted with black lines. Relative positions with respect to the end-effector (sensor) frame are depicted with green lines.

The total force $\mathbf{f}_m$ and torque $\boldsymbol{\tau}_m$ measured by the force/torque sensor (assuming noise-free measurements, and no acceleration of the end-effector) is given by:

$$\mathbf{f}_m = \mathbf{f}_c + \mathbf{f}_g, \tag{7}$$

$$\boldsymbol{\tau}_m = \mathbf{r} \times \mathbf{f}_c + \mathbf{r}_g \times \mathbf{f}_g, \tag{8}$$

where $\mathbf{f}_g$ is the gravity force acting at the center of mass of the object and $\mathbf{r}_g$ is the position of the center of mass with regard to $\mathbf{p}_e$. Note that if $\mathbf{f}_g$ and $\mathbf{r}_g$ are known, gravity compensation can be performed by subtracting them from (7) and (8) to obtain $\mathbf{f}_c$ and $\boldsymbol{\tau}_c$, and thus we can use (5) and (6) to identify $\mathbf{r}$ as proposed in Section 4.1. This gravity compensation can be achieved either by assuming an object with known mass and position with respect to the end-effector, or by considering identification of the gravity effects $\mathbf{f}_g$ and $\mathbf{r}_g$ in a prior free-motion phase where the only force acting on the object is inertial, and $\mathbf{f}_c = \mathbf{0}_3$. In the latter case, proper rotation of the object by the end-effector can generate signals that can be used in the algorithm in Section 4.1 to identify $\mathbf{r}_g$ to allow compensation for the gravity during the main contact phase. In case of a lightweight tool, such that $\mathbf{f}_g \ll \mathbf{f}_c$, we can assume that the effects of gravity are within the limits of the measurement errors, and do not need to be compensated for.

4 Methodology

In this section we propose the adaptive laws for estimating the contact point and the surface orientation as well as the force/motion control which is based on these estimates. The overall control scheme effectiveness is theoretically justified and the formal proofs of the results are given in the Appendix.

4.1 Contact Point Estimation

First we design the adaptive law for estimating ${}^e\mathbf{r}$ assuming that ${}^e\mathbf{r}$ is piecewise constant or slowly varying compared to the rate of the estimation. An example of an estimation rate that can be achieved is demonstrated in Section 5. The estimates can also be used to estimate $\mathbf{r} \triangleq \mathbf{R}_e {}^e\mathbf{r}$ in the global frame. The proposed adaptive law utilizes measurements of forces and torques expressed in the end-effector frame, which is assumed to coincide with the force/torque sensor frame, as this can trivially be achieved through known transformations. The law is given by the following equations:

$$ {}^e\dot{\hat{\mathbf{r}}} = -\boldsymbol{\Gamma}_r \left[\mathbf{L}_r(t) {}^e\hat{\mathbf{r}} - \mathbf{c}_r(t) \right] \tag{9}$$

with

$$ \dot{\mathbf{L}}_r = -\beta_r \mathbf{L}_r - \mathbf{S}({}^e\mathbf{f})\mathbf{S}({}^e\mathbf{f}) \qquad \text{with } \mathbf{L}_r(0) = \mathbf{O}_3 \tag{10}$$

$$ \dot{\mathbf{c}}_r = -\beta_r \mathbf{c}_r + \mathbf{S}({}^e\mathbf{f}){}^e\boldsymbol{\tau} \qquad \text{with } \mathbf{c}_r(0) = \mathbf{0}_3 \tag{11}$$

where $\boldsymbol{\Gamma}_r$ is a positive definite matrix affecting the speed of convergence, β_r is a positive design constant acting as forgetting factor and ${}^e\mathbf{f}$, ${}^e\boldsymbol{\tau}$ are either the measured force and torque after gravity compensation used to estimate ${}^e\mathbf{r}$ during the contact phase, or the measured force and torque owing to gravity used to estimate the center of mass ${}^e\mathbf{r}_g$ in the free-motion phase.

Proposition 7 *The adaptive estimation law (9)-(11) guarantees that:*

(i) the torque estimation error, the estimate ${}^e\hat{\mathbf{r}}$ and its derivative are bounded i.e. ${}^e\boldsymbol{\tau} - {}^e\hat{\boldsymbol{\tau}}$, ${}^e\hat{\mathbf{r}}$, ${}^e\dot{\hat{\mathbf{r}}} \in \mathcal{L}_\infty$,

(ii) the torque estimation error and and the estimation rate ${}^e\dot{\hat{\mathbf{r}}}$ are square integrable, i.e. ${}^e\boldsymbol{\tau} - {}^e\hat{\boldsymbol{\tau}}$, ${}^e\dot{\hat{\mathbf{r}}} \in \mathcal{L}_2$,

(iii) $\lim_{t\to\infty} {}^e\hat{\boldsymbol{\tau}} = {}^e\boldsymbol{\tau}$ and $\lim_{t\to\infty} \|\dot{\hat{\mathbf{r}}}\| = 0$, and

(iv) if $\mathbf{S}({}^e\mathbf{f})$ is persistently excited (PE) ${}^e\hat{\mathbf{r}}$ converges exponentially to ${}^e\mathbf{r}$. By choosing $\boldsymbol{\Gamma}_r = \gamma_r \mathbf{I}$, with γ_r being positive constant, the speed of convergence can be arbitrarily increased by increasing γ_r.

The proposed estimator (9)-(11) is an integral adaptive control law since its design is based on the minimization of an integral cost function of the error between the actual and the estimated torque [8]; the proof of the Proposition 7 is following the proof of the integral adaptive control for identifying the parameters in a multiple inputs-single output parametric model and is based on the use of a quadratic Lyapunov function $V({}^e\tilde{\mathbf{r}}) = \frac{1}{2}{}^e\tilde{\mathbf{r}}^\top \mathbf{\Gamma}_r^{-1}{}^e\tilde{\mathbf{r}}$.

As is demonstrated in Section 5, convergence to the actual parameters can be achieved by varying the direction of $\mathbf{f}_e$ in order to span some surface in the Cartesian space, which is an identification condition arising from the problem formulation.

The contact point estimate $\hat{\mathbf{p}}_c$ can be calculated using proprioception and the estimate ${}^e\mathbf{r}$ produced by exploiting force/torque measurements:

$$\hat{\mathbf{p}}_c = \mathbf{p}_e + \mathbf{R}_e{}^e\hat{\mathbf{r}} \tag{12}$$

Note that it is also possible to use the contact point estimation together with an accurate model of the grasped tool to determine which of a possible set of points is in contact. In this case, we can additionally infer the orientation of the tool given that the grasping point is obtained through tactile sensing.

The adaptive law can also be used to identify the center of mass in case of free-space motion. The parameters are identified exponentially fast given that ${}^e\mathbf{f} = \mathbf{R}_e^\top \mathbf{f}$ is PE. Note that $\mathbf{f} = \mathbf{f}_g$ is constant and thus the identification is excited by the rotational motion of the object.

4.2 Surface Normal Estimation

In order to estimate the surface normal direction we design the following adaptive law:

$$\dot{\hat{\mathbf{n}}}_c = -\gamma_n \bar{\mathbf{P}}(\hat{\mathbf{n}}_c)\mathbf{L}_n(t)\hat{\mathbf{n}}_c \tag{13}$$

$$\dot{\mathbf{L}}_n = -\beta_n \mathbf{L}_n + \frac{1}{1+\|\dot{\mathbf{p}}_e\|^2}\dot{\mathbf{p}}_e\dot{\mathbf{p}}_e^\top \qquad \text{with } \mathbf{L}_n(0) = \mathbf{O}_3 \tag{14}$$

where γ_n is a positive constant for tuning the speed of convergence and β_n is a positive forgetting factor.

Proposition 8 *The adaptive law (13)-(14) guarantees that:*

(i) the norm of the estimate $\hat{\mathbf{n}}_c(t)$ is invariant i.e. given that $\|\hat{\mathbf{n}}_c(0)\| = 1$, $\|\hat{\mathbf{n}}_c(t)\| = 1, \forall t > 0$,

(ii) if $\vartheta(0) \in (-\frac{\pi}{2}, \frac{\pi}{2})$ then $\vartheta(t) \in (-\frac{\pi}{2}, \frac{\pi}{2}), \forall t > 0$ where ϑ is the angle formed between $\mathbf{n}_c$ and $\hat{\mathbf{n}}_c$,

(iii) $\lim_{t\to\infty} \|\dot{\hat{\mathbf{n}}}_c\| = 0$, and

(iv) if $\dot{\mathbf{p}}_e$ is persistently excited (PE) ϑ converges to zero exponentially which implies that $\hat{\mathbf{n}}_c$ converges exponentially to $\mathbf{n}_c$ with a rate that can be tuned by γ_n.

The proposed estimator (13)-(14) is an integral adaptive control – in contrast to those used in our previous work [10], [9]– with normalized input but here is modified in order to produce unit and well-defined estimates of the normal direction as the problem in hand requires. The proof of Proposition 8 can be found in the Appendix, and is based on defining the Lyapunov function in the domain of the *estimation error angle* ϑ formed between $\mathbf{n}_c$ and $\hat{\mathbf{n}}_c$.

Measurements of the contact force $\mathbf{f}_c$ alone cannot in general be used together with (5) to identify the surface normal if the contribution from the tangential force $\mathbf{f}_t$ due to friction is unknown. However, we can use the force measurements in order to initialize the proposed estimator when contact is detected i.e. $\hat{\mathbf{n}}_c(0) = \mathbf{f}(0)/\|\mathbf{f}(0)\|$. Given that the gravity is compensated in $\mathbf{f}(0)$, the initial angle error will be within the cone of friction which implies that $|\vartheta(0)| < \pi/2$ and consequently that the estimator is properly initialized. If there is no rotational motion of the end-effector, the sliding velocity of the tool-tip on the surface is equal to the end-effector velocity, and thus the latter can be directly used to estimate the surface normal direction, independent of the accuracy of the contact point estimate.

4.3 Force/motion Control

The control objective is to follow a velocity trajectory $\mathbf{v}_d(t)$ and to press upon the surface with a desired force f_d. In this way, we can perform a meaningful task and simultaneously generate signals ${}^e\mathbf{f}$ and $\dot{\mathbf{p}}_e$. In particular, the motion along the surface not only generates $\dot{\mathbf{p}}_e$ that span the orthogonal complement of the normal direction required in (13) but gives rise to tangential forces owing to dynamical friction that can be added to the normal interaction forces, see (5), in order to generate an appropriate signal ${}^e\mathbf{f}$ to excite (9) by spanning a surface in the Cartesian space.

The velocity control design is based on decomposing the motion and force control directions according to hybrid force/motion control methodology by using however the estimates $\hat{\mathbf{n}}_c$ – like the kinematic loop of [9]. The proposed kinematic controller is given by the following equation:

$$\mathbf{u} = \bar{\mathbf{P}}(\hat{\mathbf{n}}_c)\mathbf{v}_d - \hat{\mathbf{n}}_c v_f \tag{15}$$

where v_f is a PI control loop of the estimated force error $\tilde{\hat{f}}_n = \hat{f}_n - f_d$. Note that the estimated $\hat{f}_n$ can be calculated based on force measurements and the online estimates $\hat{\mathbf{n}}_c$. In particular:

$$v_f = \alpha_I \int_0^t (\hat{f}_n - f_d) d\tau + \alpha_P(\hat{f}_n - f_d), \quad \hat{f}_n = \hat{\mathbf{n}}_c^\top \mathbf{f} \tag{16}$$

with α_I and α_P are positive control gains.

The velocity trajectory $\mathbf{v}_d(t)$ can be either defined a priori in a feedforward fashion or designed appropriately by using feedback of control errors such as end-effector or contact point position errors. A simple way to define $\mathbf{v}_d(t)$ is the following:

$$\mathbf{v}_d(t) = \dot{\mathbf{p}}_d - \alpha(\mathbf{p} - \mathbf{p}_d) \tag{17}$$

where α is positive control gain and $\mathbf{p}$ can be either the end-effector position or the contact point estimate depending on the definition of the desired position $\mathbf{p}_d$. Note that $\mathbf{p}_d$ can be defined as follows:

1. directly and a priori in the robot workspace e.g. by using vision and mapping a desired trajectory from the image space to robot space. In this case the feedback control is designed using the contact point position which is however based on estimates obtained by (9) i.e. $\mathbf{p} := \hat{\mathbf{p}}_c$.

2. locally at the surface as $\xi_d \in \mathbb{R}^2$ and then mapped online to the robot workspace through a transformation $(\mathbf{p}_e(0), \hat{\mathbf{R}}_c)$. Details on the motivation behind this selection and the construction of $\hat{\mathbf{R}}_c$ can be found in [9]. In this case the design of $\mathbf{v}_d(t)$ is based on $\mathbf{p}_e$ instead of $\hat{\mathbf{p}}_c$. This can be explained by the following observation: the objective of drawing a circle with center around the initial contact point is equivalent of drawing a virtual circle around the end-effector's initial position.

In more complicated scenarios where both sliding and rolling motion of the tool take place the estimated contact point position must be used in $\mathbf{v}_d(t)$ even when the target is defined based on local coordinates.

Analysis of the closed loop when $\mathbf{u}$ (15)–(17) is applied (briefly sketched in the Appendix) yields to the following theorem:

Theorem 3 *The control law (15)–(17) applied as a translational velocity controller to a robot firmly grasping a tool which is in contact with a flat surface, together with the adaptive laws (9) and (13) used for estimating the contact parameters such as contact point position and surface orientation ensure the boundedness of the contact force and the velocity along the unconstrained directions as well as the convergence of the force/motion errors to zero and the identification of the uncertain parameters given that* $\mathbf{u}$ *and* ${}^e\mathbf{f}$ *are persistently excited.*

5 Experiments

Our adaptive control framework for tool and surface calibration was evaluated with a robot setup consisting of a 7-DOF velocity controlled manipulator controlled at 130 Hz. The manipulator also includes a wrist mounted ATI Mini45 6-axis force-torque sensor used for the force feedback control and the contact point estimator.

For more details on the experimental setup, see e.g. [21]. The end-effector velocities used for the estimation of the surface normal were calculated using joint velocities filtered through joint position measurements.

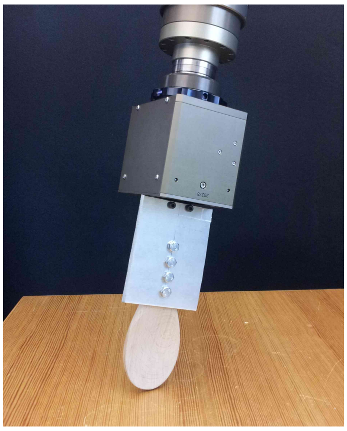

Figure 3: Experimental setup used for evaluating our adaptive control scheme for contact point and surface normal estimation.

To perform our experiments we attached a tool rigidly to the robot's gripper as shown in Fig. 4. Attaching the tool rigidly to the end-effector allowed us to have a consistent ground truth with which to compare the controller's estimation of the contact point. Furthermore, we tested the controller over a flat table which was previously calibrated to obtain the ground truth of the surface normal. A circular trajectory of 4 cm radius and 5 second period was commanded to the manipulator during the experiment.

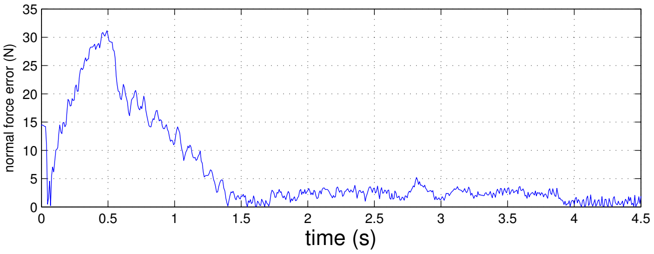

Figure 4: Normal force error $|\tilde{f}_n|$.

Fig. 4 shows the normal force error $|\tilde{f}_n| = |f_n - f_d|$ which indicates that the adaptive controller manages to regulate the normal contact force.

Fig. 5 and 6 show the estimation errors of the contact point and the surface normal respectively. The contact point converges with an error of approximately 5 mm, which, given the 30.8 cm distance from the force-torque sensor to the tool-tip is within the error margins of the setup. Moreover, the surface normal estimate converges with an approximately 1.5 degree error with respect to the ground truth

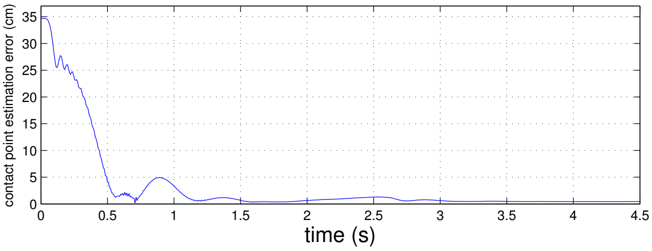

Figure 5: Contact point estimation error.

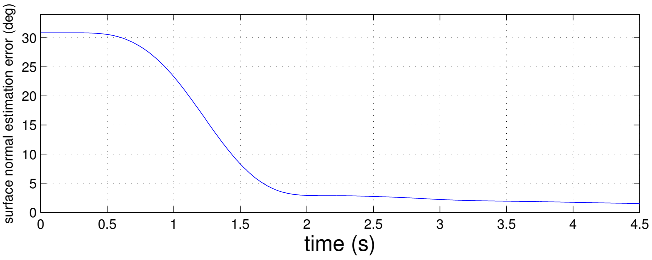

Figure 6: Surface normal estimation error.

normal.

For a set of contact forces that share the same direction and only vary in magnitude, the contact point estimate $\hat{\mathbf{p}}_c$ will converge to a point on a line passing through the actual contact point $\mathbf{p}_c$, parallel to the force direction. As the direction of contact forces vary, $\hat{\mathbf{p}}_c$ will converge to the intersection point of a set of such lines, which will be $\mathbf{p}_c$. In the experimental convergence of $\hat{\mathbf{p}}_c$, as seen in Fig. 5, we see an initial convergence to a point on such a line after approx 0.1 s, and then, as the direction of the contact force starts to change as the tool-tip slides on the surface, we see convergence to the intersection point, or $\mathbf{p}_c$. For the setup in the experiment we see that we have good convergence for forces that spread over approximately 14 degrees with respect to the surface normal. For faster convergence with the same setup, we would need contact forces spanning that angle variation in shorter time.

6 Conclusions

In this paper, we have proposed a method for simultaneous online estimation of the point of contact of a tool held by a robot, and the normal of the surface it is interacting with. The method is based on adaptive estimation and a hybrid force/motion controller, and uses force and torque measurements from a wrist-mounted sensor.

The fast convergence of the contact point estimate makes it suitable for real time tracking of the endpoint of a tool that may slip and move in the robot's hand as it is being used for a task execution. The method also guarantees stable control of contact forces even before the estimates converge. For non-contact motion, the method can be used to estimate the center of mass of the end-effector and/or a grasped object. This enables tool use with unmodelled and/or uncalibrated tools.

The strength of the method lies in the fact that it uses force and torque measurements and it is therefore complimentary to vision based approaches where occluded or bad lighting conditions make affect the estimation. An interesting future extension is to combine the proposed method with other methods for object tracking. One possibility is to combine it with model based vision methods or tactile sensors to use the tracked contact point to improve pose tracking of an object.

7 Appendix

Proof of Proposition 2: (i) Note that $\frac{d}{dt}\left(\|\hat{\mathbf{n}}_c\|^2\right) = -\gamma_n[\bar{\mathbf{P}}(\hat{\mathbf{n}}_c)\hat{\mathbf{n}}_c]^\top \mathbf{L}_n(t)\hat{\mathbf{n}}_c = 0$; thus the norm of the estimate is invariant and consequently bounded. (ii) Note that (14) and the constraint (2) implies:

$$\frac{d}{dt}\left(\mathbf{L}_n\mathbf{n}_c\right) = -\beta_n\mathbf{L}_n\mathbf{n}_c$$

which in turn, for $\mathbf{L}_n(0) = \mathbf{O}_3$, implies that $\mathbf{n}_c$ belongs in the nullspace of $\mathbf{L}_n$. Note also that $\mathbf{L}_n$ is positive semidefinite. Consider the following Lyapunov function:

$$V(\theta) = -\ln(\cos\vartheta), \quad V : (-\tfrac{\pi}{2}, \tfrac{\pi}{2}) \to \mathbb{R} \tag{18}$$

Its time derivative along the systems trajectories (13)-(14) is given by:

$$\dot{V}(\theta, t) = -\gamma_n\tilde{\mathbf{n}}_c^\top\mathbf{L}_n(t)\tilde{\mathbf{n}}_c \tag{19}$$

From (18) and (19) we conclude that $V(\theta)$ is bounded which implies $\vartheta(t) \in (-\frac{\pi}{2}, \frac{\pi}{2}), \forall t > 0$ for $\vartheta(0) \in (-\frac{\pi}{2}, \frac{\pi}{2})$. (iii) Clearly (i) and (ii) imply that $\hat{\mathbf{n}}_c \in \mathcal{L}_\infty$. Furthermore, since $\frac{1}{1+\|\dot{\mathbf{p}}_e\|^2}\dot{\mathbf{p}}_e\dot{\mathbf{p}}_e^\top$ is bounded by construction, (14) implies that $\mathbf{L}_n$ and $\dot{\mathbf{L}}_n$ are bounded too. By integrating both sides of (19) in $t \in [0, \infty)$ and taking into account that $V(\infty)$ is bounded from (ii), we get that $\mathbf{L}_n^{1/2}\tilde{\mathbf{n}}_c \in \mathcal{L}_2$. The update law (13) implies: (a) $\|\dot{\hat{\mathbf{n}}}_c\| \leq \gamma_n\|(\mathbf{L}_n^\top)^{1/2}\|\|\mathbf{L}_n^{1/2}\tilde{\mathbf{n}}_c\|$ which implies that $\dot{\hat{\mathbf{n}}}_c \in \mathcal{L}_\infty \bigcap \mathcal{L}_2$ as well as (b) $\ddot{\hat{\mathbf{n}}}_c$ given the boundedness of $\dot{\hat{\mathbf{n}}}_c$ and $\dot{\mathbf{L}}_n$. Clearly (a) and (b) yield $\lim_{t\to\infty}\|\dot{\hat{\mathbf{n}}}_c\| = 0$. (iv) The PE condition is satisfied given that there exists α_0, T_0 such that $\int_t^{t+T_0}\dot{\mathbf{p}}_e\dot{\mathbf{p}}_e^\top d\tau \geq \alpha_0\mathbf{I}_3$. Using the integral expression of $\mathbf{L}_n = \int_0^t \exp(-\beta_n(t-\tau))\frac{1}{1+\|\dot{\mathbf{p}}_e\|^2}\dot{\mathbf{p}}_e\dot{\mathbf{p}}_e^\top d\tau$ implied by (14), it can be found that $\mathbf{L}_n(t) \geq \lambda\exp(-\beta_n T_0)\mathbf{I}_3$ given that the PE condition is satisfied. Then we consider a quadratic Lyapunov function $U = \frac{1}{2}\|\tilde{\mathbf{n}}_c\|^2$ which in our case depends only on the estimation error angle i.e. $U = 1 - \cos\vartheta$. It can be easily proved that $\dot{U} \leq -2\lambda\gamma_n \exp(-\beta_n T_0) U$

$$U(t) \leq \exp\left(-2\lambda\gamma_n e^{-\beta_n T_0} t\right) U(T_0) \tag{20}$$

Note also that $\frac{4}{\pi^2}\|\vartheta\|^2 \leq U(\theta) \leq \frac{1}{2}\|\vartheta\|^2$ and thus (21) implies that the angle between the actual and the estimated vector $\hat{\mathbf{n}}_c$, converges exponential to zero as follows:

$$|\vartheta(t)| \leq \tfrac{\pi\sqrt{2}}{4} \exp\left(-\lambda\gamma_n e^{-\beta_n T_0} t\right) |\vartheta(T_0)| \tag{21}$$

Proof of Theorem 1: Let us consider the case of a bounded input $\mathbf{v}_d$. This assumption is valid even when $\mathbf{v}_d$ is defined using feedback given that $\mathbf{p}_d$, $\dot{\mathbf{p}}_d$ are bounded and by considering a bounded robot workspace. Saturation on the position error can be used in order to construct a bounded $\mathbf{v}_d$. Substituting the control law in to the system first order differential kinematics (4) we get: $\dot{\mathbf{p}}_e = \mathbf{u}$. By projecting the aforementioned equation along the surface normal we get: $v_f = \frac{1}{\cos\vartheta}\mathbf{n}_c^\top \bar{\mathbf{P}}(\hat{\mathbf{n}}_c)\mathbf{v}_d$. Since $\hat{\mathbf{n}}_c$ is bounded and $\vartheta \neq \pi/2$ from (i) and (ii) of Proposition 8, v_f is bounded. The boundedness of v_f implies $\dot{\mathbf{p}}_e$ is bounded and additionally that $\int_0^t (\hat{f}_n - f_d) d\tau$, $\hat{f}_n$ are bounded. Hence ${}^e\mathbf{f}$ is bounded and thus the update law for ${}^e\hat{\mathbf{r}}$ (9)-(11) is well-defined. The boundedness of $\mathbf{p}_e$ can be proved by using the boundedness of the estimates ${}^e\hat{\mathbf{r}}$, $\hat{\mathbf{n}}_c$ and their derivatives ${}^e\dot{\hat{\mathbf{r}}}$, $\dot{\hat{\mathbf{n}}}_c$. Ultimate bounds can also be found by exploiting $\lim_{t\to\infty} {}^e\dot{\hat{\mathbf{r}}} = \mathbf{0}_3$, $\lim_{t\to\infty} \dot{\hat{\mathbf{n}}}_c = \mathbf{0}_3$ (Proposition 7 and 8); analytic derivations are omitted. Given that ${}^e\mathbf{f}$, $\dot{\mathbf{p}}_e$ (or $\mathbf{v}_d$) satisfy the PE condition the estimation error converges to zero exponentially fast and thus v_f converges exponential fast to zero which implies $\int_0^t (\hat{f}_n - f_d) d\tau \to 0$ and $f_n \to f_d$. Furthermore, $\dot{\mathbf{p}}_e \to \bar{\mathbf{P}}(\mathbf{n}_c)\mathbf{v}_d$ with implies that $\bar{\mathbf{P}}(\mathbf{n}_c)(\mathbf{p} - \mathbf{p}_d) \to \mathbf{0}_3$.

References

[1] C.G. Atkeson, C.H. An, and J.M Hollerbach. Rigid body load identification for manipulators. In *24th conf on Decision and Control*, pages 996–1003, Fort Lauderdale, Fl, Dec 1985.

[2] M. Beetz, U. Klank, I. Kresse, A. Maldonado, L. Mosenlechner, D. Pangercic, Thomas Ruhr, and M. Tenorth. Robotic roommates making pancakes. In *IEEE-RAS International Conference on Humaoid Robots*, pages 529–536, 2011.

[3] H. Bruyninckx, S. Dutre, and J. De Schutter. Peg-on-hole: a model based solution to peg and hole alignment. In *IEEE International Conference on Robotics and Automation*, volume 2, pages 1919–1924, 1995.

[4] C.C. Cheah, C. Liu, and J.E. Slotine. Adaptive jacobian tracking control of robots with uncertainties in kinematic, dynamic and actuator models. *Automatic Control, IEEE Transactions on*, 51(6):1024–1029, 2006.

[5] C. Corcoran and R. Platt. A measurement model for tracking hand-object state during dexterous manipulation. In *IEEE International Conference on Robotics and Automation*, pages 4302–4308, 2010.

[6] P. Hebert, N. Hudson, J. Ma, and J. Burdick. Fusion of stereo vision, force-torque, and joint sensors for estimation of in-hand object location. In *IEEE International Conference on Robotics and Automation*, pages 5935–5941, 2011.

[7] G.E. Hovland and Brenan J. McCarragher. Combining force and position measurements for the monitoring of robotic assembly. In *IEEE/RSJ International Conference on Intelligent Robots and Systems*, volume 2, pages 654–660, 1997.

[8] P. A. Ioannou and J. Sun. *Robust Adaptive Control*. Upper Saddle River, NJ:Prentice Hall, 1996.

[9] Yiannis Karayiannidis and Zoe Doulgeri. Adaptive control of robot contact tasks with on-line learning of planar surfaces. *Automatica*, 45(10):2374–2382, 2009.

[10] Yiannis Karayiannidis, Christian Smith, Francisco Viña, Petter Ögren, and Danica Kragic. Model-free robot manipulation of doors and drawers by means of fixed-grasps. In *IEEE International Conference on Robotics and Automation*, pages 4470–4477, 2013.

[11] C.C. Kemp, A. Edsinger, and E. Torres-Jara. Challenges for robot manipulation in human environments [grand challenges of robotics]. *IEEE Robotics Automation Magazine*, 14(1):20–29, 2007.

[12] Charles C. Kemp and Aaron Edsinger. Robot manipulation of human tools: Autonomous detection and control of task relevant features. In *5th IEEE International Conference on Development and Learning (ICDL-06*, 2006.

[13] R. Koeppe and G. Hirzinger. Sensorimotor compliant motion from geometric perception. In *IEEE International Conference on Intelligent Robots and Systems*, volume 2, pages 805–811, 1999.

[14] Michael Krainin, Peter Henry, Xiaofeng Ren, and Dieter Fox. Manipulator and object tracking for in hand model acquisition. In *Workshop on Best Practice in 3D Perception and Modeling for Mobile Manipulation at the Int. Conf. on Robotics & Automation (ICRA), Anchorage, Alaska*, 2010.

[15] Daniel Kubus, Torsten Krüger, and Friedrich M. Wahl. On-line rigid object recognition and pose estimation based on inertial parameters. In *EEE/RSJ International Conference on Intelligent Robots and Systems*, pages 1402–1408, San Diego, CA, 2007.

[16] Yang Lei and Scott F. Miller. Pose estimation and machining efficiency of an endoscopic grinding tool. *The International Journal of Advanced Manufacturing Technology*, pages 1–11, 2013.

[17] S. Muto and K. Shimokura. Teaching and control of robot contour-tracking using contact point detection. In *IEEE International Conference on Robotics and Automation*, pages 674–681, 1994.

[18] Anna Petrovskaya, Oussama Khatib, Sebastian Thrun, , and Andrew Y. Ng. Touch based perception for object manipulation. In *Robotics Science and Systems Conference, Robot Manipulation Workshop*, Atlanta, GA, 2007.

[19] Lucia Pãiş, Keisuke Umezawa, Yoshihiko Nakamura, and Aude Billard. Learning robot skills through motion segmentation and constraints extraction. *ACM/IEEE International Conference on Human-robot Interaction, Workshop on Collaborative Manipulation*, 2013.

[20] Zvi S. Roth, B. Mooring, and B. Ravani. An overview of robot calibration. *IEEE Journal of Robotics and Automation*, 3(5):377–385, 1987.

[21] Christian Smith and Yiannis Karayiannidis. Optimal command ordering for serial link manipulators. In *IEEE-RAS International Conference on Humanoid Robots*, pages 255–261, 2012.

[22] Francisco Viña, Yasemin Bekiroglu, Christian Smith, Yiannis Karayiannidis, and Danica Kragic. Predicting slippage and learning manipulation affordances through gaussian process regression. In *IEEE-RAS International Conference on Humanoid Robots*, 2013.

[23] Guilin Yang, I-Ming Chen, Song Huat Yeo, and Wee Kiat Lim. Simultaneous base and tool calibration for self-calibrated parallel robots. *Robotica*, 20:367–374, 7 2002.

Paper C

Predicting Slippage and Learning Manipulation Affordances through Gaussian Process Regression

Published in
IEEE-RAS International Conference on Humanoid Robots, 2013

Predicting Slippage and Learning Manipulation Affordances through Gaussian Process Regression

Francisco E. Viña B., Yasemin Bekiroglu, Christian Smith,
Yiannis Karayiannidis and Danica Kragic

Abstract

Object grasping is commonly followed by some form of object manipulation – either when using the grasped object as a tool or actively changing its position in the hand through in-hand manipulation to afford further interaction. In this process, slippage may occur due to inappropriate contact forces, various types of noise and/or due to the unexpected interaction or collision with the environment.

In this paper, we study the problem of identifying continuous bounds on the forces and torques that can be applied on a grasped object before slippage occurs. We model the problem as kinesthetic rather than cutaneous learning given that the measurements originate from a wrist mounted force-torque sensor. Given the continuous output, this regression problem is solved using a Gaussian Process approach.

We demonstrate a dual armed humanoid robot that can autonomously learn force and torque bounds and use these to execute actions on objects such as sliding and pushing. We show that the model can be used not only for the detection of maximum allowable forces and torques but also for potentially identifying what types of tasks, denoted as *manipulation affordances*, a specific grasp configuration allows. The latter can then be used to either avoid specific motions or as a simple step of achieving in-hand manipulation of objects through interaction with the environment.

1 Introduction

Interaction with and manipulation of objects are essential abilities of robots operating in realistic environments. As humans, robots may need to grasp objects for simple tasks such as moving them from one position to another. More complex tasks, such as using objects as tools, requires a more advanced ability of manipulating an object in the hand so to achieve a suitable grasp configuration. In this process of achieving and loosing contacts with the object in the hand, events such as slippage commonly occur. The knowledge of contacts and slippage provides important information about the status of the task one is executing.

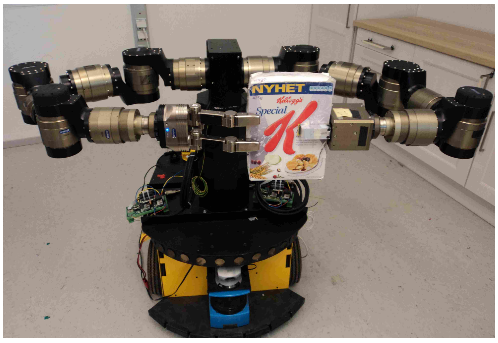

Figure 1: A dual arm robot setup for estimating maximal allowable forces and torques for a grasp.

For both humans and robots, sense of touch is paramount for safe and flexible interaction with objects and the environment. As reviewed in [8], components of tactile perception in humans depend on the sensory inputs within muscles, tendons and joints (kinesthetic) and stimulus mediated by receptors in the skin (cutaneous). Most of the research in robotic tactile sensing addressed the problem of finger-object interactions and grasp stability assessment. If the contact locations as well as the friction coefficients of the contacting surfaces are known, the problem can be formulated in terms of the Grasp Wrench Space (GWS) [4, 10]. However, it is difficult to construct the GWS in practice since it requires the exact values of those parameters.

Besides planning stable grasps, the robot should also acquire knowledge of the maximum forces and torques that can be applied on the object before slippage occurs. Various methods have been proposed for detecting slippage [8, 12, 13, 17]. Apart from addressing the problem at the signal processing level in terms of cutaneous tactile sensing, general machine learning methods have proven adequate for analysis in cases where noise and imperfect models are inherent to the problem, [2, 9].

Our work follows the direction of using kinesthetic sensing for slip detection in combination with machine learning techniques. Autonomous learning and a physical model of the friction forces are used to estimate the maximum static friction forces and torques on objects the robot is interacting with. We approach the problem through Gaussian Process regression, resulting in a model that can predict forces and torques that a grasp can tolerate before the held object starts slipping. As such, the model can also be used to identify the affordances of a specific grasp such as, for example, what type of in-hand rotation can be applied to an object while still keeping the object in the hand.

The learned bounds can be used as constraints at the control level to avoid certain motions and thus prevent slippage of the grasped object while executing the task. In addition, the approach also identifies in which directions the object might translate or rotate in the hand and thus be exploited in tool use and in-hand manipulation to actively change the pose of the object in the hand – either through specific motion or interaction with the environment. This is also commonly done by humans, for example prior to putting a key in a keyhole we may change its orientation between the fingers by pushing the key toward a surface.

Thus, differently from commonly addressed *grasp affordances* [11], we facilitate the system to identify *manipulation affordances*. Our method uses force-torque and proprioceptive feedback different from commonly used tactile or skin sensors which in practice can be fragile and easily damaged. However, when possible, the cutaneous and kinesthetic methods can be integrated resulting in a more biologically inspired approach [8]. Our approach also takes advantage of the dual arm capabilities of humanoid robots since the training actions can be executed autonomously through dual arm manipulation procedures. Fig. 1 shows our dual-arm robot as an example of a platform that can be used to implement the method we propose in this paper.

The paper is organized as follows: Section 2 presents the related work, Section 3 our learning framework, including the friction model and the use of Gaussian Process regression while in Section 4 we proceed to describe how our system learns manipulation affordances from doing regression on the static friction. Finally, we provide our experimental results in Section 5 as well as the conclusions, discussion on the results and future directions in Section 6.

2 Related Work

Early works studying the physics of robotic grasping and contact between rigid bodies are reviewed in [4]. The review addressed the basic closure properties of grasps, force and form closure, which describe the equilibrium conditions of an object grasped by a robotic hand by assuming frictional and frictionless point contacts respectively. Given that friction forces play a central role in robotic grasping, some of the works reported in the literature have focused on studying their properties [5, 17]. These studies cover not only the translational Coulomb friction, but also the rotational friction. Moreover, by combining different sensor modalities (tactile and force-torque) it is shown in [17] that it is possible to detect and control both translational and rotational slippage.

Besides modeling the physics of grasping and the friction forces, quantifying the quality of grasps in terms of the capability to counteract external disturbances has been one of the main research questions in the grasping community. In order to plan stable grasps with robotic hands, many grasp planners have been proposed in the literature which optimize these quality measures [6, 7, 10]. These planners are constructed in terms of approximations of wrench spaces or heuristic algorithms that consider a subset of a wrench space.

The main drawback of these methods is that these require precise 3D models of the object as well as prior knowledge of the friction coefficient and the location of the contact points of the robot's hand. To cope with this problem, [20] proposes a set of manipulation actions to estimate properties such as weight, stiffness and friction in order to set appropriate grasping forces.

In order to overcome the uncertainties and problems with modeling errors in grasping, learning approaches have also been proposed. Example works of [1, 2, 9] consider learning of grasp stability and grasp affordances. Our previous work on grasp stability assessment performs learning mainly through tactile (cutaneous), proprioceptive and visual feedback in order to predict the stability of the grasp prior to lifting and manipulating the object [1, 2]. In [9] the proposed system learns grasp affordances which are defined as hand-object relative poses that lead to successful grasps on a particular object. These affordance densities are learned through exploration and visual features. The main strength of these learning approaches originates from the fact that these do not require prior knowledge of physical contact parameters as the system is trained using supervised learning without explicitly modeling the physics of grasping.

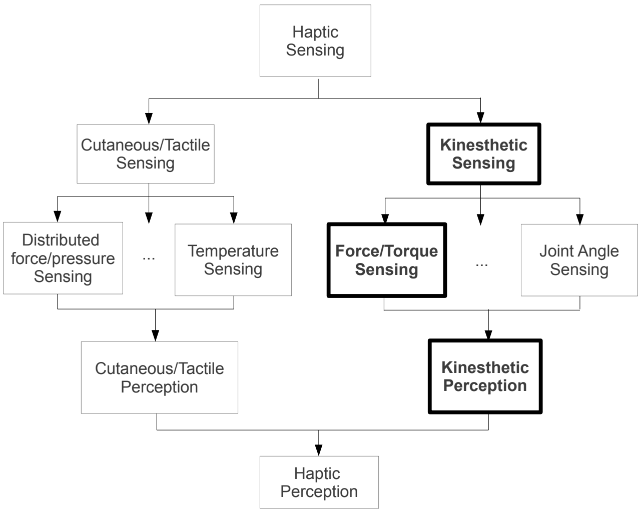
Haptic Sensing
Cutaneous/Tactile Sensing
Kinesthetic Sensing
Distributed force/pressure Sensing
...
Temperature Sensing
Force/Torque Sensing
...
Joint Angle Sensing
Cutaneous/Tactile Perception
Kinesthetic Perception
Haptic Perception

Figure 2: Cutaneous and kinesthetic components of haptic sensing and perception [8, 21]. Highlighted in bold are the kinesthetic components which we consider in our approach.

Our work makes use of the physics models of friction described in the seminal work of [5, 17]. However, instead of employing geometrical, analytical or signal processing based approaches [6, 7, 10, 13, 17] we follow a kinesthetic learning approach for predicting slippage. In this sense, our work follows more closely approaches in which the robot first interacts with objects and assesses their contact and friction properties prior to executing tasks [20]. Our method also follows the motivation behind learning based approaches in order to deal with the issue of modeling errors and uncertainties in grasping [1, 2, 9].

Within the broader scope of *haptic* sensing, which consists of both cutaneous and kinesthetic sensing as shown in Fig. 2, our approach falls under the subcategory of kinesthetic sensing and perception while most of the related work discussed so far including our own work on grasp stability assessment cover mostly the domain of cutaneous/tactile sensing [1, 2, 12, 13].

3 Physics and Learning Model

The main objective of our system is learning the maximum static friction forces and torques for various grasp configurations through force-torque sensing. In this section we present the modeling aspects of our framework, beginning with a description of the friction model used and the selection of input features for training. We finalize the section with a brief overview of Gaussian Process regression and explain how we apply it within our work.

3.1 Friction Model

According to the Coulomb friction model, when an external force is applied parallel to the surface of contact between two bodies, there is a reaction friction force f_f which relates to the normal force f_n according to the following inequality

$$f_f \leq \mu_s f_n \tag{1}$$

where μ_s is the static coefficient of friction. This equation holds until the external force exceeds the maximum static friction force. The object then starts slippping when Eq. (1) becomes an equality. From this point, a dynamic friction force with a lower friction coefficient starts acting on the object as depicted in Fig. 3. The peak of this curve corresponds to the maximum static friction force f_{slip} given by

$$f_{slip} = \mu_s f_n \tag{2}$$

The static torsional friction typically displays a nonlinear behavior given by

$$\tau_{slip} = \beta_s f_n^{4/3} \tag{3}$$

where β_s depends on geometric and elasticity factors of the contact [17]. However, slippage still occurs at the point in which the friction torque reaches its maximum value, which we denote as τ_{slip}.

In order to achieve a more general physical model for prediction, we take into consideration the effect of both rotational and translational friction forces as discussed in [14, 17]. When an object is subject to both rotational and translational shears, the translational and rotational friction components become correlated as shown in Fig. 4. The curve $f_t = h(\tau_n)$, where f_t is the component of the force tangent to the contacting surfaces and τ_n the component of the torque in the normal

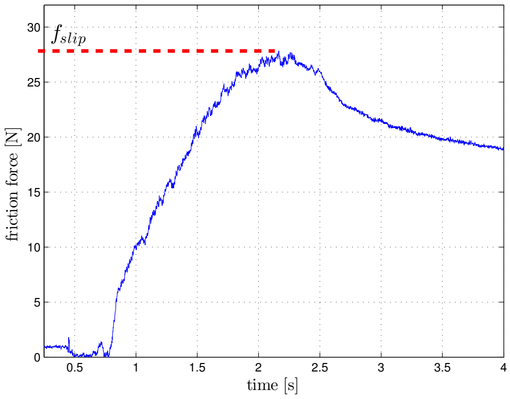

Figure 3: Translational friction force exerted on an object held in a robot hand. The peak of the signal, f_{slip} denotes the maximum static friction force at which the object begins to slip.

direction, represents the boundary at which the object starts slipping due to the loads exerted on the object. If the tangential force f_t applied on the object is above the curve for a given applied torque τ_n, then the object will slip and the grasp is thus unstable.

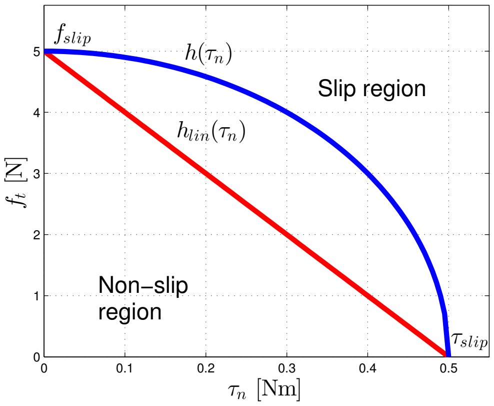

Figure 4: Slippage boundaries: $f_t = h(\tau_n)$ represents the boundary for slippage of objects under combined translational and rotational shear while $f_t = h_{lin}(\tau_n)$ represents a linear approximation of h as proposed in [17].

A number of mathematical approximations have been formulated in the literature to describe this slippage boundary. We will use the linear approximation described in [17] that defines a conservative bound on the magnitude of the forces and torques that cause slippage on an object. This linear bound is denoted by

$f_t(\tau_n) = h_{lin}(\tau_n)$ in Fig. 4 and can be expressed using the following equation:

$$\frac{f_t}{\mu_s} + \frac{\tau_n}{\beta_s} = f_n \tag{4}$$

3.2 Learning Framework

Our goal is to learn the mapping between a set of input features (X) and the resulting maximum friction forces and torques (Y), which is a regression problem due to the continuous outputs. While there are several types of regression techniques that could be used within our framework, we have chosen Gaussian Process (GP) regression which can capture the nonlinearity in the data and provide estimates for uncertainty in the predictions.

3.2.1 Gaussian Processes

Given a dataset $\mathcal{D} = \{\mathbf{x}_i, y_i\}_{i=1}^n$ with n observations where $\mathbf{x}_i \in \Re^N$ and $y_i \in \Re$ is a scalar output, regression analysis aims at learning a model for the relationship $y = f(\mathbf{x}) + \varepsilon$ which is composed of a latent function of the input and a noise component ε. As a result of this learning, given a new input $\mathbf{x}^*$, the aim is to obtain the predictive distribution for y^*.

A GP [18] defines a distribution over functions and is parametrized by a mean and a covariance function as

$$GP \sim (m(\mathbf{x}), k(\mathbf{x}, \mathbf{x}')) \tag{5}$$

The mean function is assumed to be zero. The covariance function expresses how similar two outputs, $f(\mathbf{x}_i)$ and $f(\mathbf{x}_j)$ are given the inputs $\mathbf{x}_i$ and $\mathbf{x}_j$. Our covariance function is based on the squared exponential, which is given by

$$k(\mathbf{x}_i, \mathbf{x}_j) = \sigma_f^2 \exp[-\frac{(\mathbf{x}_i - \mathbf{x}_j)^2}{2l^2}] + \sigma_n^2 \delta(\mathbf{x}_i, \mathbf{x}_j). \tag{6}$$

The hyperparameters of the covariance function, (σ_f, σ_n, l), are optimized based on $\mathcal{D}$, where σ_f denotes the signal variance, σ_n is for the noise variance and l is the length-scale which determines how relevant an input is, i.e., if l has a large value the covariance will be independent of that input.

We are interested in the conditional probability $p(y^*|\mathcal{D}, \mathbf{x}^*)$ as we want to find how likely is a certain prediction for y^*, given the data and the new input. Based on a trained GP model, the estimate for y^* is given by the mean value at the test point with the confidence being the variance. The interested reader can refer to the literature [18] for additional details on Gaussian Processes.

3.2.2 Feature Selection

As an input to the regressor, we need a set of informative features X, that can reliably represent the behavior of the maximum static friction forces and torques. In our case, we have selected the x component of the hand H pose with respect to the object O as shown in Fig. 5

$$X = \left[\begin{array}{c} {}^{O}x_H \end{array} \right] \tag{7}$$

We have selected this feature for illustration purposes, yet more features can easily be incorporated into the system, such as for example the joint angles of the fingers and their grasping force which can modify the friction forces present in a grasp. If more features are incorporated into the system, a preprocessing stage with dimensionality reduction would be necessary [19].

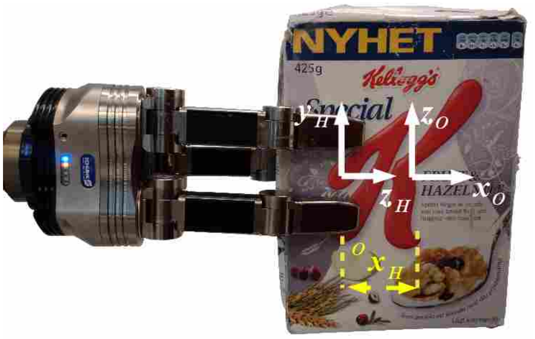

Figure 5: Grasp preshape used for training on the maximum static friction forces and torques, with the corresponding reference frames of the hand and the object used for training.

The outputs Y of the regression system are the maximum static friction force and torque

$$Y = \left[\begin{array}{c} f_{slip} \\ \tau_{slip} \end{array} \right] \tag{8}$$

which can be measured through force-torque sensors by interacting with the object. We isolate the components of Y and train two GPs, one for the translational friction f_{slip} and one for the rotational friction τ_{slip}. In our case, we learn friction forces f_{slip} in the $y_H - z_H$ plane and friction torques τ_{slip} around the x_H axis of the tip of the hand reference frame as shown in Fig. 5, given that these are the directions in which the object can move within the hand. Forces and torques around the remaining axes are trivial to learn since they will be constrained by the operational safety limits of the hand, given the geometry of the grasp.

4 Towards Learning Manipulation Affordances

Once the robot has interacted with an object and learned the maximum friction forces $Y = [f_{slip}, \tau_{slip}]^T$ for a range of grasp configurations, it can use this information to infer what type of motions the object can withstand given the current grasp. The details of the training data generation for learning are provided in the next section.

For a given wrench $\boldsymbol{w}^*$ measured by the robot while executing a task, the robot can detect how close the object is to slipping according to the model discussed in Section 3.1. In order for the object to remain fixed in the robot's hand the measured force should lie below the torque dependent slippage boundary $h(\tau)$

$$f_t^* < h(\tau_n^*) \tag{9}$$

where f_t^* and τ_n^* are the tangential force and normal torque components of the wrench measured by the robot.

In the training stage we isolate the translational and rotational components of the friction and thus we can approximate $h(\tau_n)$ linearly with $h_{lin}(\tau_n)$ by joining the end points $(f_t, \tau_n) = (f_{slip}, 0)$ and $(f_t, \tau_n) = (0, \tau_{slip})$. In the case of a linear approximation the following condition ensures a stable grasp in terms of zero relative motion between the object and the hand ${}^H\mathbf{v}_O = \mathbf{0}$:

$$\begin{aligned} f_t^* &< h_{lin}(\tau_n^*) \\ f_t^* &< -\tfrac{f_{slip}}{\tau_{slip}}\tau_n^* + f_{slip} \end{aligned} \tag{10}$$

Thus, our approach makes it possible to identify stable grasps through identification of forces and torques that can be applied on an object before slippage occurs. In a broader sense, the methodology also identifies directions of motion constraints – that is, in which directions the object is more likely to translate or rotate.

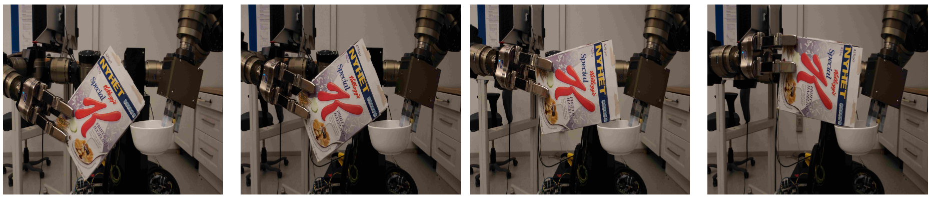

Figure 6: Example scenario of a pouring task with rotational slippage.

In the case of the grasp studied in this work, see Fig. 5, the model would inform that the object can translate in the $y_H - z_H$ plane and rotate around the x_H axis. Moreover, if a large torque is detected around the x_H axis with relatively low forces in the $y_H - z_H$ plane then we can expect the object to rotate around

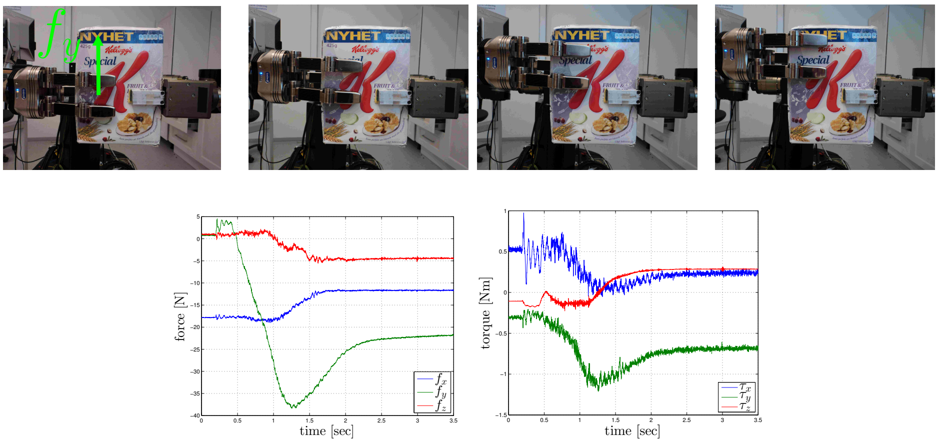

Figure 7: Sliding action for training on the maximum static linear friction f_{slip} and its corresponding force and torque profiles.

the fingertips rather than translate once the force-torque measurements reach the slippage boundary of Eq. (4).

This knowledge is necessary for manipulation tasks where a predicted slippage of the object may be facilitated to complete a task. An example scenario is shown in Fig. 6, in which the robot exploits the rotational slippage to pour the contents of the cereal box into the bowl by letting the box rest against an edge of the bowl and allowing it to rotate slightly in the hand while the manipulator moves upwards.

5 Experimental evaluation

Our experimental setup consists of a dual arm robot as shown in Fig. 1. Each manipulator has 7 DOF and these are equipped with ATI Mini45 6-DOF force/torque sensors mounted at the wrists and they are sampled at a 650 Hz frequency. We start by describing the training data collection process.

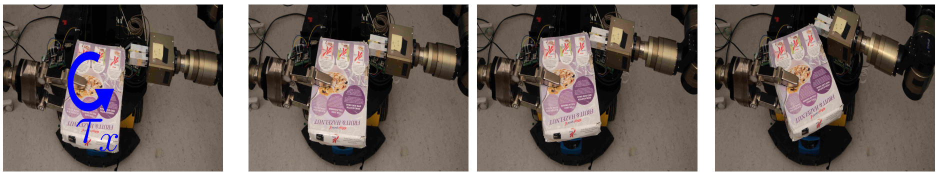

Figure 8: Pushing action for training on the maximum static rotational friction τ_{slip}.

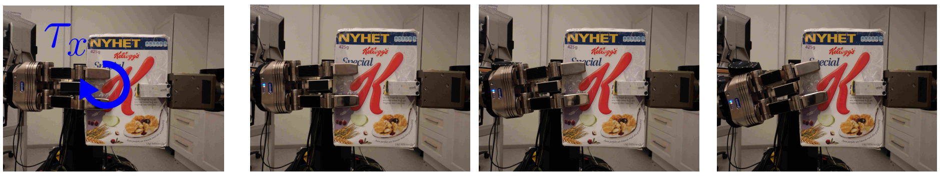

Figure 9: Rotational motion for training on the maximum static rotational friction τ_{slip}.

5.1 Training Data Collection

For collecting training data autonomously with the robot we use three dual arm manipulation procedures: one sliding action for measuring the maximum static linear friction f_{slip} and the other two are a rotational motion and pushing action for measuring the rotational friction τ_{slip}.

Fig. 7 shows an illustration of the sliding action along with the forces and torques measured during the execution. In this case the robot holds the object firmly with the parallel gripper shown on the right while the hand on the left, which is the one we train for, slides up in the y_H direction of the hand. The y-component of the force signal f_y measured in the force-torque sensor of the arm is then similar to the one shown in Fig. 3, and f_{slip} is obtained from the peak of the signal.

For obtaining training data for the maximum static friction torque τ_{slip}, we used the pushing action shown in Fig. 8. This action is performed by grasping the object with the hand we train for, while the parallel gripper shown on the right pushes the object on a corner so that the object rotates around the x_H axis of the tip of the robotic hand. We selected this action given that we expect collisions with the environment to be a source of rotational slippage when the robot performs tasks with the object.

For verification purposes we also trained a separate GP for τ_{slip} by applying a different type of training action as shown in Fig. 9. This training action consists of performing a rotational motion with the grasping hand while the object is kept on a fixed grasp with the parallel gripper shown on the right. Even though in this case we also train for τ_{slip} as with the pushing action, we can expect different outcomes from the learning given that each training action represents a different kind of interaction with the environment. The pushing action gives τ_{slip} for tasks in which the object is grasped by the robot's hand and it collides with the environment while being grasped by the robot hand, whereas the rotational motion models a task in which the object is fixed with respect to the environment and the robot's hand rotates around the object.

5.2 Experimental results

We collected 14 training examples for the friction force and 10 training examples for the torque by varying the relative pose between the robot hand and the manipulated object along one dimension as described in Section 5.1. To learn the Gaussian

Processes and obtain the hyperparameters we used Rasmussen and Nickisch's Gaussian Process Regression and Classification Toolbox [18]. The hyperparameters were calculated by maximizing a Gaussian likelihood function.

Fig. 10 shows the resulting learned Gaussian Process for f_{slip}. This plot shows the mean function of the learned GP (solid blue line) which follows the training points, along with the two standard deviation confidence bounds (dashed red lines) enveloping it. Given this result, we take the lower confidence bound as stability boundary for f_{slip} given that the Gaussian Process predicts that 95% of the points of the process will lie above this boundary.

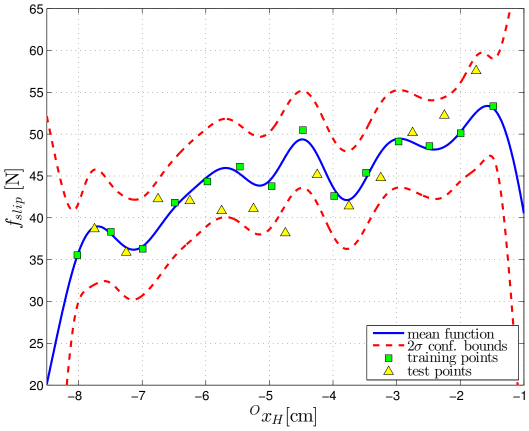

Figure 10: Learned GP of f_{slip} with two-standard deviation confidence bounds. The solid blue line is the mean function of the GP while the dashed red lines are the confidence bounds. The green square markers correspond to the training data, while the yellow triangular markers correspond to the test set.

For testing and validating the learned GP, we manually pushed the object while it was being grasped by the robot in different configurations compared to the ones used for training. Fig. 10 confirms that the sliding action performed on the object is valid for training f_{slip} as most of the test points lie above the lower confidence bound of the Gaussian Process.

Fig. 11 shows the learned Gaussian Process for τ_{slip} when using the pushing action. Once again, we manually pushed the object while it was grasped by the robot in order to collect the test points shown in the figure. These test points show that the pushing action and the learned Gaussian Process succeeded in capturing the behavior of τ_{slip} with respect to the object to hand relative pose.

Fig. 12 shows the result of learning τ_{slip} by using the rotational motion, while we collected test points by manually pushing the object as in the previous case. The clear offset between the learned GP and the test points shows that the training and testing actions are not anymore physically consistent. In the case of the rotational

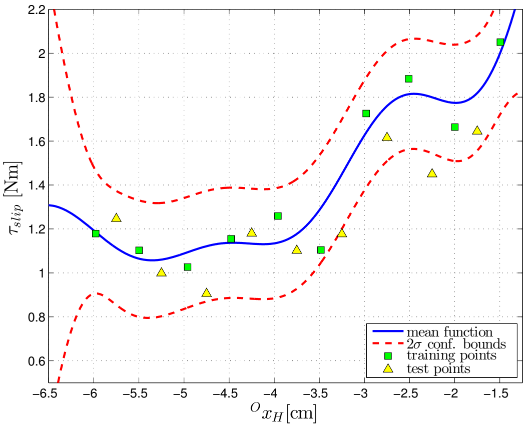

Figure 11: Learned GP of τ_{slip} trained by using the pushing action shown in Fig. 8.

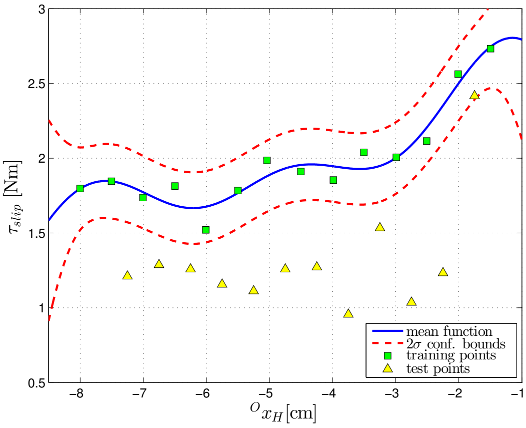

Figure 12: Learned GP of τ_{slip} with two-standard deviation confidence bounds trained with the rotational motion shown in Fig. 9.

training motion, the interaction between the active robot hand and the object involves both forces and torques, while pushing actions, performed either by the robot hand or manually by ourselves for testing, exert only forces on the object. This result can thus be used to inform the system that the action is not proceeding according to the model and provide the basis for replanning. This is something we plan to adress in the subsequent work.

6 Conclusions and Future Work

In this work we have presented a learning framework for prediction of slippage of grasps through kinesthetic perception which provides a basis for learning manipulation affordances. Our method uses Gaussian Process regression and the training is performed by isolating the translational and rotational components of the friction. The novelty of the approach lies on using a machine learning approach together with a physical model of the friction to determine continuous bounds on the forces and torques that a grasped object can withstand before slipping for a set of different object-hand relative poses. The experimental results show that our system is able to generate reliable predictions which agree with tests performed by manually pushing the object in the hand of the robot for previously unencountered grasp configurations.

Future directions of work include expanding our sensor modalities from kinesthetic perception to cover a wider spectrum of haptic perception (see Fig. 2) by use of tactile sensing. We also aim to incorporate into our system the estimation of the axis of rotation of the object in the hand of the robot as it can improve the results shown here. We have assumed a constant axis of rotation around the fingertips of the hand that might not correspond precisely with the actual axis around which the object rotates when it is manipulated. In order to cope with this issue, we aim to use adaptive control techniques previously used for estimating the kinematic constraints of hinged doors [15] and treat the object as a virtual hinge. We are also interested in coupling this work with probabilistic grasp assessment techniques and object categorization as demonstrated in our previous work in [3, 16].

References

[1] Y. Bekiroglu, J. Laaksonen, J.A. Jorgensen, V. Kyrki, and D. Kragic. Assessing grasp stability based on learning and haptic data. *IEEE Transactions on Robotics*, 27(3): 616–629, june 2011.

[2] Yasemin Bekiroglu, Renaud Detry, and Danica Kragic. Learning tactile characterizations of object- and pose-specific grasps. In *2011 IEEE/RSJ International Conference on Intelligent Robots and Systems*, pages 1554–1560, Sept. 2011.

[3] Yasemin Bekiroglu, Dan Song, Lu Wng, and Danica Kragic. A Probabilistic Framework for Task-Oriented Grasp Stability Assessment. In *IEEE International Conference on Robotics and Automation*, 2013.

[4] A. Bicchi and V. Kumar. Robotic grasping and contact: a review. In *Proc. IEEE International Conference on Robotics and Automation*, volume 1, pages 348 –353 vol.1, 2000.

[5] Antonio Bicchi, J Kenneth Salisbury, and David Brock. Experimental evaluation of friction characteristics with an articulated robotic hand. *Experimental Robotics II*, pages 153–167, 1993.

[6] C. Borst, M. Fischer, and G. Hirzinger. Grasping the dice by dicing the grasp. In *Proc. IEEE International Conference on Intelligent Robots and Systems*, volume 4, pages 3692 – 3697 vol.3, oct. 2003.

[7] Ch. Borst, M. Fischer, and G. Hirzinger. Grasp planning: how to choose a suitable task wrench space. In *Proc. IEEE International Conference on Robotics and Automation*, volume 1, pages 319 – 325 Vol.1, april-1 may 2004.

[8] R.S. Dahiya, G. Metta, M. Valle, and G. Sandini. Tactile sensing - from humans to humanoids. *IEEE Transactions on Robotics*, 26(1):1–20, 2010.

[9] R. Detry, E. Baseski, M. Popovic, Y. Touati, N. Kruger, O. Kroemer, J. Peters, and J. Piater. Learning object-specific grasp affordance densities. In *IEEE 8th International Conference on Development and Learning*, pages 1–7, 2009.

[10] C. Ferrari and John Canny. Planning optimal grasps. In *IEEE International Conference on Robotics and Automation*, pages 2290–2295 vol.3, 1992.

[11] J.J. Gibson. *The theory of affordances.* In: Shaw R, Bransford J, editors. Perceiving, acting and knowing: towards an ecological psychology. Hillsdale, NJ: Erlbaum., 1977.

[12] B. Heyneman and M.R. Cutkosky. Biologically inspired tactile classification of object-hand and object-world interactions. In *Proc. IEEE International Conference on Robotics and Biomimetics*, 2012.

[13] R.D. Howe and M.R. Cutkosky. Sensing skin acceleration for slip and texture perception. In *Proc. IEEE International Conference on Robotics and Automation*, pages 145–150, 1989.

[14] R.D. Howe, I. Kao, and M.R. Cutkosky. The sliding of robot fingers under combined torsion and shear loading. In *Proc. IEEE International Conference on Robotics and Automation*, pages 103 –105 vol.1, apr 1988.

[15] Yiannis Karayiannidis, Christian Smith, Francisco Viña, Petter Ögren, and Danica Kragic. Model-free robot manipulation of doors and drawers by means of fixed-grasps. In *IEEE International Conference on Robotics and Automation*, 2013.

[16] Marianna Madry, Dan Song, and Danica Kragic. From Object Categories to Grasp Transfer Using Probabilistic Reasoning. In *IEEE International Conference on Robotics and Automation*, 2012.

[17] C. Melchiorri. Slip detection and control using tactile and force sensors. *IEEE/ASME Transactions on Mechatronics*, 5(3):235 –243, sep 2000.

[18] C E Rasmussen and C K I Williams. *Gaussian processes for machine learning.* MIT Press, 2006.

[19] Dan Song, Carl Henrik Ek, Kai Hübner, and Danica Kragic. Multivariate discretization for Bayesian Network structure learning in robot grasping. In *IEEE ICRA*, pages 1944–1950, 2011.

[20] T. Sugaiwa, G. Fujii, H. Iwata, and S. Sugano. A methodology for setting grasping force for picking up an object with unknown weight, friction, and stiffness. In *IEEE-RAS International Conference on Humanoid Robots*, pages 288 –293, dec. 2010.

[21] Jan BF Van Erp, Ki-Uk Kyung, Sebastian Kassner, Jim Carter, Stephen Brewster, Gerhard Weber, and Ian Andrew. Setting the standards for haptic and tactile interactions: ISO's work. In *Haptics: Generating and Perceiving Tangible Sensations*, pages 353–358. Springer, 2010.

Paper D

In-hand Manipulation Using Gravity and Controlled Slip

Published in
IEEE/RSJ International Conference on Intelligent Robots and Systems, 2015

In-hand Manipulation Using Gravity and Controlled Slip

Francisco E. Viña B., Yiannis Karayiannidis, Karl Pauwels,
Christian Smith and Danica Kragic

Abstract

In this work we propose a sliding mode controller for in-hand manipulation that repositions a tool in the robot's hand by using gravity and controlling the slippage of the tool. In our approach, the robot holds the tool with a pinch grasp and we model the system as a link attached to the gripper via a passive revolute joint with friction, i.e., the grasp only affords rotational motions of the tool around a given axis of rotation. The robot controls the slippage by varying the opening between the fingers in order to allow the tool to move to the desired angular position following a reference trajectory. We show experimentally how the proposed controller achieves convergence to the desired tool orientation under variations of the tool's inertial parameters.

1 Introduction

Many tasks robots are expected to do require complex interactions with objects. Although significant contributions have been achieved in the area of grasping, in-hand manipulation remains one of the open challenges [1]. In tasks that require tool use, the robot is expected to pick-up a tool and also choose a grasp that is suitable for the task. For example, a task such as hammering requires the robot to apply large forces with the tool in a given direction. Thus, the robot must ensure that it applies enough grasping force in a right direction and that the tool is correctly positioned in the hand to avoid undesired displacements while executing the task. However, even if the robot plans the grasp correctly, once it picks the tool up from a table or a shelf the resulting grasp configuration may be different to the planned one due to imprecise sensing, motion planning and control. Moreover, the grasp configuration can change as the robot performs the task due to externally applied forces such as unplanned collisions with the environment.

Thus, the robot must be capable of evaluating the state of the grasp, that is, its suitability for the task. The evaluation can result in the confirmation that the grasp configuration is still acceptable for performing the task or that an adjustment of the grasping force or repositioning of the tool is needed. Repositioning the tool in the hand can be done by regrasping: placing the tool on a fixed surface and picking it up again from a different position [17]. On the other hand, if the robot's hand is dexterous and/or individual fingers have multiple degrees of freedom, the robot can coordinate their motion in such a way that the tool moves to the desired position. This is known as in-hand manipulation using the *intrinsic* dexterity of the robot's hand. If, however, the hand has a rather simple kinematic structure, it is perhaps more feasible to employ *extrinsic* dexterity, i.e. use resources that are external to the robot hand's embodiment [4]. The robot may for instance push the tool against an external object or it may loosen the grip so that the tool falls to a desired position due to gravity.

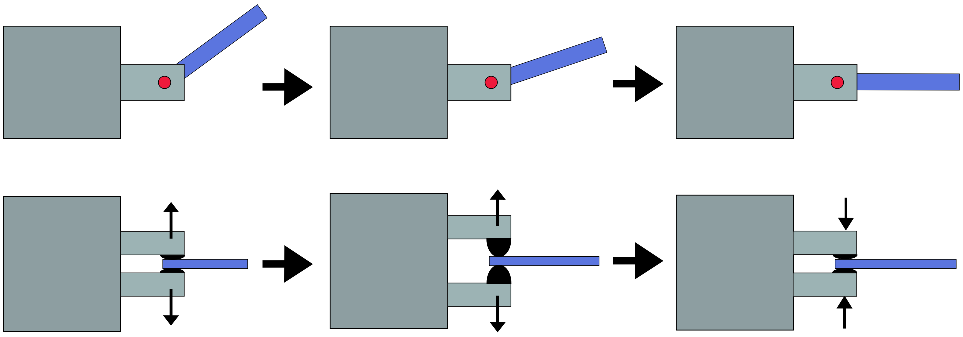

Figure 1: In-hand manipulation control using extrinsic dexterity by means of gravity and controlled slip. The top row depicts a side view of the gripper with the fixed axis of rotation marked with a red circle. The bottom row depicts a top view of the gripper as the robot opens and closes the fingers to allow the tool to fall to the desired configuration due to the gravitational pull.

The main contribution of our work is the design of a sliding mode control law for in-hand manipulation which uses an extrinsic resource, gravity, for reorienting a tool in the robot's hand by regulating the friction exerted by the grasp. We assume that the robot has already performed a pinch grasp on the tool, such that the motion of the object is constrained to one rotational degree of freedom as shown in Fig. 1. We thus consider that the tool is attached to the robot hand via a passive revolute joint with friction. Furthermore, the controller regulates this friction by controlling the opening between the fingers of the hand. We show experimentally how the proposed control law achieves convergence to the desired angular trajectory of the tool with robustness to variations in the inertial parameters of the system.

One of the main differences between our work and the previous works on friction control comes from the fact that they focused mainly on friction compensation for servo motors or translation of objects on a surface. When working with robotic in-hand manipulation a number of challenges arise that we can enumerate as follows

1. The friction control literature mainly deals with friction *compensation*. The general approach in those studies is to estimate the friction parameters and

use them in an additive compensation term in the control signal while in our case we actively regulate the friction through the grasping force and use gravity as actuation for the system.

2. The friction parameters of servo motors can be identified and used for compensating friction in the controller. Normally these parameters are considered fixed in the control law. In contrast, a robot may use different kinds of tools depending on the task, and each of these tools could potentially exhibit different friction characteristics.

3. In-hand manipulation is subject to loss of controllability since the manipulated tool can fall out of the robot's hand if not enough friction is applied at the contact.

This paper is organized as follows: Section 2 contains the related work, Section 3 derives the dynamic model of the system, Section 4 describes our proposed sliding mode controller and Section 5 shows our experimental results. Finally, we present our conclusions and planned future work in Section 6.

2 Related Work

Early works on regrasping focused on pick-and-place operations where the robot would release an object on a surface and pick it up from a different position. For instance, Tournassoud *et al.* identified sets of stable grasps and placements of polyhedral objects on a table and combined these in a discrete sequence of pick and place actions taking into account kinematic constraints of the manipulator [17].

Works in the intrinsic dexterity-based in-hand manipulation literature have studied planning and control aspects when coordinating multiple degrees of freedom of multifingered hands to move the manipulated object along a specified trajectory. Cole *et al.* designed a control scheme which coordinates sliding motions of two planar fingers over an object assuming Coulomb sliding friction at the contacts [3]. Han *et al.* proposed an in-hand manipulation framework that combines rolling and finger gaiting [6]. Hertkorn *et al.* formulated a planning framework which also takes into consideration kinematic and dynamic constraints of the task [7]. Okamura *et al.* formulated a survey of different dexterous manipulation techniques that have been proposed in the literature, as well as a summary of the main kinematic, contact and dynamic models used in those techniques [10].

On the other hand, the work of Brock provides one of the earliest analysis of controlled slip and how it can be useful for dexterous extrinsic manipulation [2]. The author studied how to determine the possible directions of motion of a grasped object and the effect of grasping forces and externally applied forces on the motion of the object. This knowledge is then used by the robot to reposition a grasped object by controlling the slippage when it comes in contact with other objects in the environment.

Dafle *et al.* presented a strong case for the benefits of extrinsic dexterity for in-hand manipulation [4]. Even though the robot used in the study is equipped with a rather simple gripper, the authors demonstrated that it is still physically possible to reposition the object in the hand of the robot by taking advantage of resources external to the robot's hand such as gravity, use of external objects for support and inertial forces due to the manipulator's acceleration. The authors show this by implementing a discrete set of preprogrammed manipulation actions and combining them via a graph. In contrast with [4], our work focuses on one specific manipulation scenario but instead of using discrete preprogrammed actions we design a continuous closed loop control law to move the tool to the target position.

Senoo *et al.* used high speed manipulators and vision systems to manipulate objects within the robot's hand [14, 15]. The authors demonstrated that the high speed feedback and control allow them to perform fine in-hand manipulation using both intrinsic and extrinsic dexterity. In [15] the authors also proposed in-hand manipulation via a passive joint. However, these approaches are custom tailored for specialized high-speed hardware while in our case we use standard commercially available hardware.

Kappler *et al.* developed a high level representation framework of pregrasping manipulation actions that enable a robot to slide objects on a tabletop to positions which are suitable for generating more robust grasps [8].

Given that our in-hand manipulation control scheme relies on slippage control it is worth mentioning some of the previous works on friction modeling and control. This topic has been extensively studied in the control community given the widespread presence of friction in different kinds of mechanical systems. Olsson *et al.* provide a detailed survey of friction models and friction compensation schemes [11]. De Wit *et al.* proposed the LuGre friction model and designed friction compensation control schemes for this model [5]. Xie proposed an adaptive controller with sliding mode observer to estimate the friction parameters of a servo motor and perform position control with an unknown load [19].

Friction control is also a topic of interest in the design of Antilock Braking Systems (ABS) in vehicles. Ünsal et. al. designed a sliding mode control law for the braking torque applied on a vehicle's wheel [18]. The main difference with our work is that the control objective consists in maximizing the tractive force exerted by the road on the wheels by regulating the wheel slip with respect to the road.

The contribution of our work is the design of a closed loop sliding mode control law which uses gravity and controlled slip. We track the position of the tool using a vision tracking system and control the slip by varying the opening between the gripper's fingers. We show experimentally that the proposed control law converges to the desired orientation of the tool despite changes in its inertial parameters.

3 Modeling

In our in-hand manipulation controller we assume a 1 DOF parallel gripper with soft fingertips that performs a pinch grasp on a tool as shown in Fig. 1. We assume that the pinch grasp affords only rotational motions around a fixed axis of rotation, which we assume is known a priori. The position of the tool with respect to the robot's hand can thus be described by the angle $\theta(t)$ with respect to the horizontal axis.

The control objective is to change the angular position of the tool to a desired set point $\theta_d(t_f)$ following a specified trajectory $\theta_d(t)$. We assume that the manipulator is static and we only actuate the opening d between the fingers of the parallel gripper to control the grasping force applied on the tool, and hence the magnitude of the friction torque. We assume that the state of the tool $\mathbf{x}(t) = [\theta(t), \dot{\theta}(t)]^\top$ can be observed through sensor measurements.

Furthermore, we operate the gripper in such a way that the tool only rotates and does not fall out of the robot's hand. As one increases the opening d between the fingers the object will first experience rotational slippage and then a combination of rotational and translational slippage until it falls out of the robot's hand as depicted in Fig. 2.

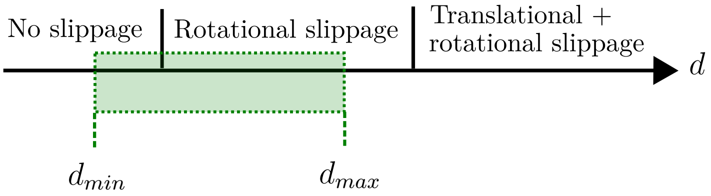

Figure 2: Slippage of an object grasped via a pinch grasp according to the separation d between the fingers of the parallel gripper. The object is assumed to be initially at rest.

We assume that the bounds $[d_{min}, d_{max}]$ are given beforehand, where d_{min} is a lower bound designed to avoid damages to the tool and/or gripper and to ensure that the friction torque is large enough to stop the object at the desired position $\theta_d(t_f)$, and d_{max} is set small enough to allow some safety margin and avoid translational motions of the tool but large enough to ensure that the gravitational torque can overcome the stiction torque.

3.1 Sliding friction model

Our proposed control scheme uses the sliding friction torque at the contact between the tool and the gripper to control the rotational motion of the tool.

We model the friction torque τ_f at the axis of rotation as Coulomb and viscous friction [11]

$$\tau_f(f_n, \dot{\theta}) = -\mu \operatorname{sgn}(\dot{\theta}) f_n - \sigma\dot{\theta} \tag{1}$$

where μ is the Coulomb sliding friction coefficient, f_n the normal force applied by the fingers of the gripper, $\dot{\theta}$ the angular velocity of the tool, $\mathrm{sgn}(\cdot)$ is the sign function and σ the viscous friction coefficient. From Eq. (1) we obtain a relation between the applied normal force and the resulting friction torque.

3.2 Deformation model

In principle the robot can control the friction torque described in Eq. (1) if measurements of the normal force f_n are available e.g. via tactile sensors.

However, we assume that such hardware capabilities are not available in our system and we control the normal force instead via the separation of the gripper fingers assuming a linear deformation model

$$f_n(x) = k(x - x_0) \tag{2}$$

where k is the stiffness of the fingers, x_0 is the position of zero deformation at which the fingers initiate contact with the tool and x is the position of the fingers. Replacing $x = -d$ and $-kx_0 = f_0$, the deformation model (2) can be rewritten as a function of the finger separation d

$$f_n(d) = f_0 - kd \tag{3}$$

3.3 Dynamic model

Since we assume that the tool moves along one rotational degree of freedom, it suffices to analyze the rotational dynamics of the system which is given by

$$I\ddot{\theta} = \tau_g + \tau_f \tag{4}$$

where I is the tool's moment of inertia with respect to the rotation axis, $\ddot{\theta}$ the tool's angular acceleration, τ_g the torque generated by the gravitational pull on the tool's center of mass and τ_f the torsional friction generated at the contact between the tool and the gripper.

Substituting the friction and deformation models (1) and (3) into (9) and adding the expression for the gravity induced torque we obtain the following dynamic model

$$I\ddot{\theta} = -mgl\cos\theta - \mu\,\mathrm{sgn}(\dot{\theta})(f_0 - kd) - \sigma\dot{\theta} \tag{5}$$

where m is the tool's mass, l the distance from the axis of rotation to the tool's center of mass and g the gravity.

4 Sliding mode control design

To design a sliding mode control law we rewrite the dynamic model described by Eq. (5) as

$$\ddot{\theta} = h(\theta, \dot{\theta}) + b(\dot{\theta})u_d \tag{6}$$

where we denote u_d the gripper position control signal, i.e., the separation between the fingers of the gripper commanded by the controller. $h(\theta, \dot{\theta})$, $b(\dot{\theta})$ are given by

$$h(\theta, \dot{\theta}) = -\frac{mgl\cos(\theta)}{I} - \frac{\sigma\dot{\theta}}{I} - \frac{\mu f_0 \operatorname{sgn}(\dot{\theta})}{I} \tag{7a}$$

$$b(\dot{\theta}) = \frac{\mu \operatorname{sgn}(\dot{\theta})k}{I} \tag{7b}$$

The robot can determine the value of $\operatorname{sgn}(\dot{\theta})$ given the initial orientation of the tool with respect to gravity so that Eq. (7a) and (7b) become continuous functions of the state $\mathbf{x}(t) = [\theta(t), \dot{\theta}(t)]^\top$.

It is important to note the modeling uncertainties in Eq. (6). Even though the mass and center of mass can be estimated online by the robot just before running the controller by using a force-torque sensor, this estimate is subject to measurement errors arising from e.g. sensor noise. The moment of inertia and the friction and deformation model parameters are in general more difficult to estimate and require some form of pre-manipulation of the tool. Furthermore, in our formulation we have used a simplified friction model which ignores phenomena such as stiction, the Stribeck effect, hysteresis and stick-slip motion [5]. These observations make sliding mode control a natural choice since it is a robust control law when confronted with modeling imprecisions [16].

For the control law we define the first order sliding surface $s(t)$

$$s(t) = \dot{\tilde{\theta}}(t) + \lambda\tilde{\theta}(t) \tag{8}$$

where $\tilde{\theta}(t) = \theta(t) - \theta_d(t)$ and $\dot{\tilde{\theta}}(t) = \dot{\theta}(t) - \dot{\theta}_d(t)$ are the angle and angular velocity errors respectively with respect to a desired state trajectory and the control bandwidth λ is a positive constant. We design the reference trajectory $\mathbf{x}_d(t) = [\theta_d(t), \dot{\theta}_d(t)]^\top$ as the output of a second order critically damped system with unit DC gain with a trapezoidal angular velocity profile as input.

We can then formulate a sliding mode control law for the gripper position as follows [16]

$$u_d(t) = \hat{b}^{-1}\left(\hat{u}_d(t) - k_s \mathrm{sat}\left(\frac{s(t)}{\phi}\right)\right) \tag{9}$$

where $\hat{b}$ is an estimate of b in Eq. (7b) given the best available knowledge of the parameters, k_s is a positive switching control gain, ϕ is a constant parameter describing the boundary layer of the control signal whose purpose is to smooth the switching behavior of the control signal generated by the saturation function $\mathrm{sat}(\cdot)$. This function is defined as

$$\mathrm{sat}(z) = \begin{cases} z & \text{if } |z| \leq 1 \\ \mathrm{sgn}(z) & \text{otherwise} \end{cases} \tag{10}$$

The nominal control signal $\hat{u}_d(t)$ is designed such that the dynamics of the sliding surface becomes $\dot{s} = 0$ assuming perfect knowledge of the system parameters. This yields

$$\hat{u}_d = -\hat{h} + \ddot{\theta}_d - \lambda\dot{\tilde{\theta}} \tag{11}$$

where we have dropped the time argument (t) for notational convenience. In this expression $\hat{h}$ is an approximation of h given approximate estimates of the inertial, friction and deformation parameters in Eq. (7a).

In order to implement the position based control law (9) in our system we couple an additional proportional velocity control law for the fingers

$$u_v = -k_v\tilde{d} \tag{12}$$

where $\tilde{d} = d - u_d$ is the gripper position error, k_v a positive proportional control gain and u_v is the velocity that we command to the fingers of the gripper.

5 Experimental evaluation

We implemented the sliding controller proposed in Section 4 on the 2-finger parallel gripper shown in Fig. 3. The gripper is equipped with semispherical rubber fingertips which allows us to execute pinch grasps on the tool and control the grasping force due to the deformation of the rubber.

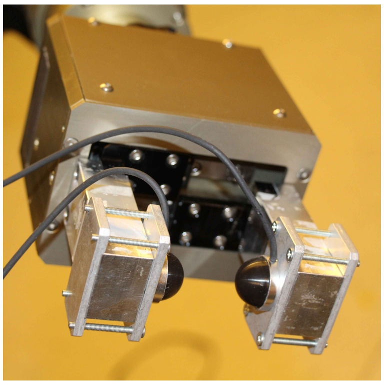

Figure 3: Parallel gripper with soft semispherical fingertips used in the experiments.

We used the model-based visual tracking system *Simtrack* together with a standard 30fps RGB-D camera to estimate the angular position $\theta(t)$ of the tool [13]. We then fed this signal to a Kalman filter to obtain estimates of the angular velocity $\dot{\theta}(t)$.

At each iteration of the control loop we calculated the maximum gripper velocity so that the gripper position would remain within the bounds $[d_{min}, d_{max}]$ defined in Section 3 until the next control iteration. We then saturated the gripper velocity $u_v(t)$ from the controller if it exceeded this maximum velocity.

Experiment	$I[\mathrm{kg} * \mathrm{cm}^2]$	m [g]
1	10.64	52.83
2	14.27	68.50
3	17.90	84.17

Table 1: Inertial parameters (moment of inertia and mass) of the tool used in the experiments.

$I[\mathrm{kg} * \mathrm{cm}^2]$	30
m [g]	100
l [cm]	12
μ	0.05
σ	0.2
f_0 [N]	175.0
k [N/m]	3871.0
λ	2.0
ϕ	0.05
k_s	600.0
k_v	4.0

Table 2: Sliding mode controller parameters and gains.

We executed three experiments where we varied the inertial characteristics of the tool as shown in Table 1 with the controller parameters shown in Table 2. We determined the parameters by trial and error and we kept them fixed throughout the experiments. Fig. 4 illustrates an example run of our sliding mode controller.

Fig. 5 shows the experimental results of our proposed controller. In the first experiment the robot grasped a 52.83g tool and controlled the gripper position to allow the object to fall to the zero degree position following the reference trajectory $\theta_d(t)$. Despite the modeling uncertainties, the sliding controller managed to move the tool to the desired angular position as shown in Fig. 5a with a steady state error of approximately 0.5 degrees. However, we also see that the controller had difficulty in achieving tracking convergence around $t = 2.2$s and $t = 5$s. This is due to unmodeled friction phenomena such as the Stribeck effect, which makes the friction coefficient increase as the rotational velocity decreases. The tool abruptly

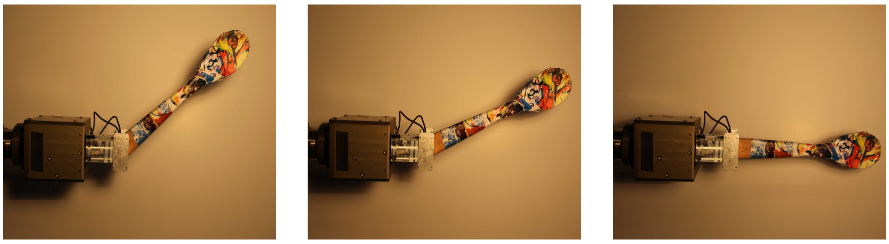

Figure 4: Side view of an example run of the sliding mode controller with our experimental setup.

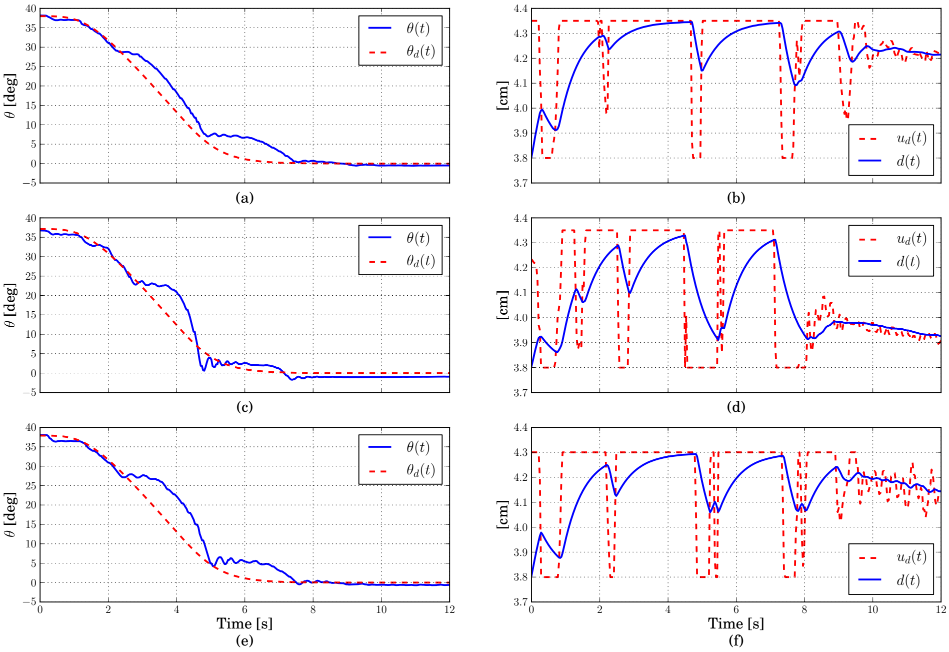

Figure 5: Experimental results of the proposed sliding mode controller. Each row corresponds to each of the experiments 1-3 from Table 1. The left column shows the angular position $\theta(t)$ of the tool and reference angular position trajectory $\theta_d(t)$ for each experiment while the right column shows the corresponding position control signal $u_d(t)$ and gripper position $d(t)$.

stopped and continued to move once the separation between the fingers was increased enough.

Fig. 5b shows the switching control signal $u_d(t)$ in the first experiment. The figure also shows the resulting separation of the fingers $d(t)$ measured from the gripper encoders after feeding the position control signal to the gripper velocity controller of Eq. (12). This figure highlights some of the difficulties when using friction as a control input for in-hand manipulation. First, even though we used soft fingertips which can deform and vary the friction torque, we see that the gripper can only operate in a limited range ($d_{max} - d_{min} = 5.5$mm). Secondly, comparing with Fig. 5a we notice that e.g. between $t = 2.2$s and $t = 5$s the tool can abruptly transition between zero velocity and a large angular velocity with small motions of the fingers of approximately 1mm.

For the second experiment we attached a 15.67g mass to the tool at a 15 cm distance from the axis of rotation, which represents a 30% increase in the mass and roughly a 34% increase in the moment of inertia. Fig. 5c shows the angular position of the tool for this second experiment while Fig. 5d shows the respective control signal.

Once again, the controller converged to the desired position, albeit with a larger steady state error of 1 degree. Furthermore, one can notice the larger control effort when compared to the previous experiment.

We then performed the third experiment by attaching two 15.67g masses to the tool 15cm away from the axis of rotation. This raised the mass by 60% and the moment of inertia by roughly 68% (see Table 1). The results of the experiment are shown in Fig. 5e and Fig. 5f.

As shown in Fig. 5f we reduced the maximum finger separation d_{max} by 0.5mm with respect to the previous experiments in order to avoid loosing grip of the tool. We observe that this relatively small change in d_{max} has a critical impact on the controller performance and that the steady state error is 0.5 degrees. Furthermore, the control signal converged to a larger finger separation d than the previous experiment since by lowering d_{max} the gripper induced higher friction torque on the tool, resulting in lower angular accelerations.

6 Conclusions and Future Work

We have proposed a sliding mode controller for in-hand manipulation with extrinsic dexterity which uses gravity and slippage control to reorient a tool in the robot's hand. In the derivation of the control law we assume a pinch grasp so that the tool can be modeled as a link attached to the gripper through a passive revolute joint with friction and a fixed axis of rotation. We performed experiments by tracking the position of the tool using a model based vision tracking system and controlling the separation of the fingers of a parallel gripper. The proposed control law converges to the desired angular position despite changes in the inertial characteristics of the tool and uncertainties in the friction and deformation models.

As future work we plan to use more accurate dynamic friction models such as the LuGre-like model mentioned in [12] in order to analyze more rigorously the friction characteristics of the problem and propose more robust control schemes that could potentially improve the tracking performance. Even though we showed in our experiments the robustness of the control law to changes in the inertial parameters of the tool, we have yet to design a control law that can accommodate more appropriately for variations in the friction characteristics of the tool.

We also plan to incorporate tactile sensing to measure and control directly the grasping forces. Furthermore, one of the limitations of our controller is the limited control frequency due to the vision tracking system. One possibility to improve the controller performance is to incorporate optical sensors at the fingertips to obtain more local and faster estimates of the pose of the tool [9].

This work can also be extended by replacing gravity with inertial forces generated by accelerating the manipulator. Additionally, we will generalize the ideas presented in this work to apply closed loop control in other in-hand manipulation scenarios by e.g. using external support objects and dual-arm manipulation.

References

[1] J. Bohg, A. Morales, T. Asfour, and D. Kragic. Data-driven grasp synthesis – a survey. *IEEE Transactions on Robotics*, 30(2):289–309, April 2014.

[2] D.L. Brock. Enhancing the dexterity of a robot hand using controlled slip. In *IEEE International Conference on Robotics and Automation*, pages 249–251 vol.1, Apr 1988.

[3] A.A. Cole, Ping Hsu, and S.S. Sastry. Dynamic control of sliding by robot hands for regrasping. *IEEE Transactions on Robotics and Automation*, 8(1):42–52, Feb 1992.

[4] N.C. Dafle, A. Rodriguez, R. Paolini, Bowei Tang, S.S. Srinivasa, M. Erdmann, M.T. Mason, I. Lundberg, H. Staab, and T. Fuhlbrigge. Extrinsic dexterity: In-hand manipulation with external forces. In *IEEE International Conference on Robotics and Automation*, pages 1578–1585, May 2014.

[5] C.C. De Wit, H. Olsson, K.J. Åström, and P. Lischinsky. A new model for control of systems with friction. *IEEE Transactions on Automatic Control*, 40(3):419–425, Mar 1995.

[6] L. Han and J.C. Trinkle. Dextrous manipulation by rolling and finger gaiting. In *IEEE International Conference on Robotics and Automation*, volume 1, pages 730–735 vol.1, May 1998.

[7] K. Hertkorn, M.A. Roa, and C. Borst. Planning in-hand object manipulation with multifingered hands considering task constraints. In *IEEE International Conference on Robotics and Automation*, pages 617–624, May 2013.

[8] D. Kappler, L. Chang, M. Przybylski, N. Pollard, T. Asfour, and R. Dillmann. Representation of pre-grasp strategies for object manipulation. In *IEEE-RAS International Conference on Humanoid Robots*, pages 617–624, Dec 2010.

[9] A. Maldonado, H. Alvarez, and M. Beetz. Improving robot manipulation through fingertip perception. In *IEEE/RSJ International Conference on Intelligent Robots and Systems*, pages 2947–2954, Oct 2012.

[10] A.M. Okamura, N. Smaby, and M.R. Cutkosky. An overview of dexterous manipulation. In *IEEE International Conference on Robotics and Automation*, volume 1, pages 255–262 vol.1, 2000.

[11] Henrik Olsson, Karl J Åström, C Canudas De Wit, Magnus Gäfvert, and Pablo Lischinsky. Friction models and friction compensation. *European journal of control*, 4(3):176–195, 1998.

[12] G. Palli, Gianni Borghesan, and Claudio Melchiorri. Modeling, identification, and control tendon-based actuation systems. *IEEE Transactions on Robotics*, 28(2):277–290, April 2012.

[13] Karl Pauwels and Danica Kragic. Simtrack: A simulation-based framework for scalable real-time object pose detection and tracking. In *IEEE/RSJ International Conference on Intelligent Robots and Systems*, Hamburg, Germany, 2015.

[14] T. Senoo, Y. Yamakawa, Satoru Mizusawa, A. Namiki, M. Ishikawa, and M. Shimojo. Skillful manipulation based on high-speed sensory-motor fusion. In *IEEE International Conference on Robotics and Automation*, pages 1611–1612, May 2009.

[15] T. Senoo, D. Yoneyama, A. Namiki, and M. Ishikawa. Tweezers manipulation using high-speed visual servoing based on contact analysis. In *IEEE International Conference on Robotics and Biomimetics*, pages 1936–1941, Dec 2011.

[16] J.J.E. Slotine and W. Li. *Applied Nonlinear Control*. Prentice Hall, 1991. ISBN 9780130408907.

[17] P. Tournassoud, T. Lozano-Perez, and E. Mazer. Regrasping. In *IEEE International Conference on Robotics and Automation*, volume 4, pages 1924–1928, Mar 1987.

[18] C. Ünsal and P. Kachroo. Sliding mode measurement feedback control for antilock braking systems. *IEEE Transactions on Control Systems Technology*, 7(2):271–281, Mar 1999.

[19] Wen-Fang Xie. Sliding-mode-observer-based adaptive control for servo actuator with friction. *IEEE Transactions on Industrial Electronics*, 54(3):1517–1527, June 2007.

Paper E

Adaptive Control for Pivoting with Visual and Tactile Feedback

Published in
IEEE International Conference on Robotics and Automation, 2016

Adaptive Control for Pivoting with Visual and Tactile Feedback

Francisco E. Viña B., Yiannis Karayiannidis, Christian Smith and Danica Kragic

Abstract

In this work we present an adaptive control approach for pivoting, which is an in-hand manipulation maneuver that consists of rotating a grasped object to a desired orientation relative to the robot's hand. We perform pivoting by means of gravity, allowing the object to rotate between the fingers of a one degree of freedom gripper and controlling the gripping force to ensure that the object follows a reference trajectory and arrives at the desired angular position. We use a visual pose estimation system to track the pose of the object and force measurements from tactile sensors to control the gripping force. The adaptive controller employs an update law that accommodates for errors in the friction coefficient, which is one of the most common sources of uncertainty in manipulation. Our experiments confirm that the proposed adaptive controller successfully pivots a grasped object in the presence of uncertainty in the object's friction parameters.

1 Introduction

Humans are capable of in-hand manipulation, i.e., repositioning grasped objects in the hand, by sliding, rolling and/or pushing the objects through precisely coordinated motions of the fingers. This is possible among other reasons due to the high mechanical complexity of the human hand and because humans are able to simultaneously control the motion of the fingers with great precision. Replicating this *intrinsic dexterity* in robots is to some degree achievable by equipping robots with hands that are composed of multiple fingers and actuators. However, most robot platforms today have rather simple grippers with few degrees of freedom given that they are generally more robust, cost efficient, easy to control and also because they simplify grasp planning and execution. At first sight such grippers may not seem capable of performing regrasps by only actuating the fingers, raising the question of whether they are actually suitable for in-hand manipulation.

This apparent lack of dexterity can however be compensated by the use of *extrinsic dexterity*, i.e., by leveraging resources external to the robot such as external

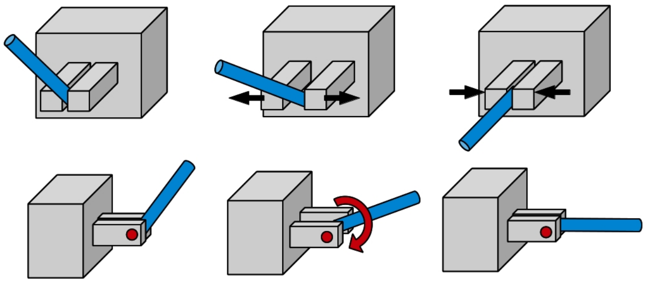

Figure 1: Pivoting with gravity by controlling the gripping force exerted by a two finger pinch grasp. The top row shows how the robot opens and closes the gripper to control the object's rotational motion induced by gravity. The object rotates around a fixed axis of rotation connecting the two fingers as shown in the bottom row.

contacts, gravity and inertial forces that can enable the robot to perform meaningful manipulation tasks. Extrinsic dexterity essentially enables roboticists to trade off complexity in gripper hardware design and control with more clever and active use of the robot's environment through an effective combination of control, interactive perception and motion planning.

Numerous examples of how a robot can make effective use of extrinsic dexterity for in-hand manipulation have been shown in the literature [3, 5, 10, 18]. These can include e.g. pushing the grasped object against an external pusher to make the object slip in a controlled manner within the gripper. Other examples include accelerating the manipulator such that inertial forces drag the object to a specified location within the gripper, and allowing the object to slip within the robots hand due to the object's weight.

In this paper we address a specific regrasp action known as *pivoting*, in which the objective is to rotate a grasped object to a desired angular position relative to the robot's hand. We perform pivoting by using extrinsic dexterity as shown in Fig. 1, allowing the gravitational torque generated on the grasped object's center of mass to rotate the object, while using the gripping force of a 1 DOF parallel jaw gripper as a braking mechanism to control the object's trajectory.

One of the major challenges of pivoting as well as other in-hand manipulation actions is how to account for imperfect knowledge of the grasped object's friction parameters. This is a common situation given that a robot may for instance grasp novel objects and tools relevant for a task. Furthermore, it may be difficult in practice to accurately measure some of the friction parameters given their dependence on e.g. contact geometry and pressure distribution.

This motivates the main contribution of our work, which is performing pivoting with a closed loop adaptive controller that accounts for imprecise estimates of the torsional friction parameters. The control scheme uses visual tracking of the object and force measurements from tactile sensors at the fingertips. Comparing to our previous work on closed loop pivoting [24] we do not rely on assumptions such as saturation of the control input and achieve enhanced tracking control performance as a result of the following improvements:

- Improved torsional friction modeling using results from previous studies on soft finger mechanics.
- Incorporation of tactile sensing for control of the gripping force.
- Online adaptation of the torsional friction coefficient. This allows us to successfully pivot the object given errors in the initial estimate of this coefficient.

This paper is organized as follows: Section 2 contains the related work, Section 3 contains the contact and dynamics model of the system, in Section 4 we formulate the adaptive control law and Section 5 shows our experimental results. Finally, we present our conclusions and planned future work in Section 6.

2 Related Work

In-hand manipulation, i.e., repositioning an object in a robot's hand, has been a long standing research topic in robotics where several aspects of modeling, motion planning and control have been addressed. Early studies by Tournassoud et. al. showed how regrasping can be accomplished by repeatedly picking and placing an object on a surface from different grasping positions [20]. This procedure can however be time consuming and the number of possible regrasps is limited by the number of stable poses in which the object can be placed on the surface. Researchers thus quickly realized the need for more advanced dexterous manipulation skills. One proposed solution was to control the motion of the fingers of a robot hand to achieve a desired repositioning of a grasped object via e.g. rolling, sliding and finger gaiting [9, 22].

On the other hand, other studies promoted the idea of leveraging the robot's environment to facilitate in-hand manipulation. Brock et. al. were among the first to propose the idea of augmenting a robot's dexterity through controlled slip of a grasped object due to externally applied forces [2]. Dafle et. al. defined the concept of *extrinsic dexterity* and showed how a robot manipulator with a rather simple gripper can still perform meaningful in-hand manipulation by using a diverse set of primitive actions which take advantage of resources external to the robot such as gravity and contact with the environment [5]. This idea of leveraging the robot's environment has also been used e.g. in the context of grasping [7].

These works have highlighted the importance of contact and friction modeling as central components to dexterous manipulation. Goyal developed the concept of limit surfaces which describe both the bounds on the wrenches that can be applied on a grasped object slippage occurs and the sliding motion of the object once slippage takes place [8]. Howe et. al. further developed these ideas and proposed computationally tractable approximations of limit surfaces in the context of manipulation planning and control [11].

Friction modeling has also been studied for the design of friction identification and compensation schemes in mechanical systems [6, 15]. However, the control techniques developed in these studies cannot be directly applied to our work since they consider friction as an additive disturbance, while in our case friction represents a control input. In this sense, our controller for pivoting holds some resemblance to antilock braking systems (ABS) in vehicles, however, the objective of these works is to maximize the traction force between the tire and the road [23].

Tactile sensing has also played an instrumental role in robotic manipulation, motivated in part by the essential role that it plays in even the most basic pick-and-place manipulation tasks carried out by humans [12]. Many studies have addressed the problem of slippage detection through tactile sensing, however, the main focus has been on grasp control for slippage prevention rather than controlled slip [14, 21]. Some works have also proposed online estimation of friction parameters [21], but have focused on friction forces rather than torsional friction as in our case.

Some more recent works have studied mechanical modeling and design as well as motion planning aspects of in-hand manipulation with extrinsic dexterity. Dafle et. al. studied the mechanics of prehensile pushing, analyzing the effect of pushers with different contact geometries on the slippage of a grasped object [3]. Dafle et. al. also designed fingertips which allow a robot to easily transition between a fixed grasp on an object and a pinch grasp in which the object can freely rotate [4].

Shi et. al. proposed a motion planning framework that determines the required manipulator accelerations that achieve a desired sliding motion of an object relative to the robot's hand [18]. This work addresses a scenario similar to ours, namely an object held by a two-finger pinch grasp, and has the advantage of reconfiguring 3 degrees of freedom of the object's pose. Although the simulations in the study validate the proposed approach, the experiments do not match the expected performance which the authors attribute in part to lack of feedback control and tactile sensing.

Also closely related to our work is the open-loop pivoting framework proposed by Holladay et. al. [10]. In this work the robot first plans a pinch grasp on an object resting on a surface and subsequently lifts it following a precomputed motion plan. The object can only be rotated between a discrete set of stable poses given that the pivoting is done open loop without online tracking of the object's pose and without control of the gripping force.

In contrast to these recent works [10, 18] which employ open-loop motion planning strategies we focus on using adaptive feedback control with online vision tracking and tactile sensing for controlling the gripping force.

3 Modeling

In this section we specify the friction and dynamics models that describe the pivoting action. Let us denote with θ the angular position of the object relative to the gripper as shown in Fig. 2. The objective of pivoting is to rotate a grasped object from an initial angular position θ_0 to a desired orientation θ_d. We control the rotational motion of the object by varying the torsional friction τ_f generated by the fingertips, which we control with the gripping force. We assume that the gripper has one degree of freedom with two soft hemispherical fingertips and that the object rotates around a fixed axis of rotation connecting the fingertips.

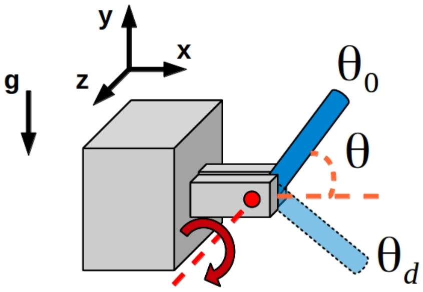

Figure 2: Modeling of the pivoting task. The gravity vector is denoted by $\mathbf{g}$, θ is the relative orientation between the object and the gripper and θ_0, θ_d are the initial and desired angular positions respectively.

We model the torsional friction interaction in pivoting based on previous studies on mechanical modeling of soft fingers. These models allow us to establish a relationship between the torsional friction at the fingertips and their applied gripping force, which we will then use in the control design. Furthermore, we assume that the gripper is in a fixed position, such that the motion of the object is solely determined by the gravitational torque on its center and the torsional friction.

3.1 Soft finger contact model

Robotic fingertip contact models have been traditionally classified in three categories according to their friction properties as hard-finger contacts without friction, hard-finger contacts with friction and soft finger contacts [1, 17]. The soft finger contact model assumes that the finger can exert friction forces tangential to the contact surface as well as torsional friction around the direction normal to the contact surface. Furthermore, there is a nonlinear relationship between the maximum force and torque that can be exerted on an object held in a soft finger grasp until slippage of the object occurs [8, 11, 14]. This boundary is known as a limit surface and can be approximated by an ellipsoid [18]

$$\mathbf{f}^\top \mathbf{A} \mathbf{f} = 1 \tag{1}$$

where $\mathbf{f} = [f_x, f_y, \tau_z]$ represents the friction wrench applied at the contact with (f_x, f_y) being the tangential friction force components and τ_z the torsional friction around the normal. Assuming isotropic friction the matrix $\mathbf{A} \in \mathbb{R}^{3x3}$ becomes a diagonal matrix whose elements are the maximum friction force and moment

$$\mathbf{A} = \mathrm{diag}(f_{t,max}^{-2}, f_{t,max}^{-2}, \tau_{z,max}^{-2}) \tag{2}$$

where the maximum tangential force $f_{t,max}$ can be modeled as Coulomb friction

$$f_{t,max} = \mu f_n \tag{3}$$

where μ is the friction coefficient and f_n the force applied in the normal direction of the contact. On the other hand, the maximum torsional friction $\tau_{z,max}$ before a grasped object rotates exhibits a more complex behavior that depends on the geometry of the contact area and the pressure distribution. We assume that the grasped object has a locally smooth surface at the contact locations, such that the contact patches are circular. The maximum torsional friction thus assumes a Coulomb-like model [11, 25]

$$\tau_{z,max} = a\beta\mu f_n \tag{4}$$

where a is the radius of the contact surface and the constant β depends on the local pressure distribution. This parameter may be for example $\beta = 0.589$ in the case of a hertzian pressure distribution or $\beta = 0.667$ in the case of a uniform distribution [11].

When the external wrenches applied on an object are contained within the ellipsoid limit surface (i.e. $\mathbf{f}_{ext}^\top \mathbf{A} \mathbf{f}_{ext} \leq 1$), the object remains static. Once the object starts sliding, the limit surface model assumes that the friction wrenches remain on the limit surface and that the sliding velocity is perpendicular to the ellipsoid. In our case we assume that the object is grasped sufficiently far from its center of mass so that the gravitational torque is large compared to the object's weight. Hence, the translational motion of the object is negligible with respect to its rotational motion and the torsional sliding friction τ_f is approximately equal to $\tau_{z,max}$ from Eq. (4)

$$\tau_f = a\beta\mu f_n \tag{5}$$

It is important to note that the limit surface model ignores potential velocity-dependent sliding friction phenomena such as the Stribeck effect and viscous friction. Despite this limitation, similar to the approach taken in previous works [18] we will assume in our controller design that the model described by Eq. (5) captures the most representative components of the torsional sliding friction during the pivoting task, namely the dependence on the applied gripping force.

In order to complete our model we also require a deformation model that relates the normal force f_n and contact radius a. Xydas et. al. have shown that hemispherical fingertips follow a power-law deformation model [25]

$$a = cf_n^{\gamma} \tag{6}$$

where c is a constant and the exponent γ has a value between 0 and 1/3 depending on the fingertip material. Substituting (6) in (5) we obtain the following torsional friction model

$$\tau_f = \mu_{tors} f_n^{1+\gamma} \tag{7}$$

where we denote $\mu_{tors} = c\beta\mu$ as the torsional friction coefficient.

3.2 Pivoting dynamics

Given our assumption that the gripper is in a static position, the rotational dynamics of the object during slippage is determined by the gravitational torque and the torsional friction of the fingers. The rotational dynamics of the object around the **z** axis shown in Fig. 2 is given by

$$I\ddot{\theta} = \tau_g + \tau_{f_1} + \tau_{f_2} \tag{8}$$

where I is the moment of inertia of the object around the axis of rotation at the fingertips, $\ddot{\theta}$ the angular acceleration of the object, τ_g the gravitational torque exerted on the object's center of mass and τ_{f_i} with $i \in [1, 2]$ the torsional friction generated at the contacts between the grasped object and each of the fingertips.

We assume that the grasp is symmetric such that the normal forces f_{n_i} exerted by each finger on the object are equal and that both fingertips have the same deformation and friction parameters such that $\tau_{f_1} = \tau_{f_2}$. If gravity is aligned with the **y** axis as shown in Fig. 2, i.e. $\mathbf{g} = g\mathbf{y}$, and by using the torsional friction model (7) we then obtain the following nonlinear rotational dynamics

$$I\ddot{\theta} = -mgl_{cm}\cos\theta + 2\mu_{tors} f_n^{1+\gamma} \tag{9}$$

where m is the object's mass, g gravity and l_{cm} the distance between the axis of rotation and the object's center of mass.

4 Control Design

Our control design is guided by the following observations and assumptions

1. The inertial parameters (I, m, l_{cm}) of the object are known but we allow some uncertainty in the torsional friction coefficient μ_{tors}. The inertial parameters can be obtained by using e.g. wrist-mounted force-torque sensors prior to the pivoting task [13]. The torsional friction coefficient μ_{tors} is however more difficult to measure in practice given its dependence on contact geometry and pressure distribution. This justifies the use of an adaptive controller with adaptation on μ_{tors}.

2. The visual model of the object is known and the angular position θ of the object is tracked by a vision system.

3. The normal forces f_n exerted by the fingers are measured via tactile sensors.

4. The gripper is oriented such that the gravitational torque can rotate object towards the desired reference, i.e. $\mathrm{sgn}(\tau_g) = \mathrm{sgn}(\theta_d - \theta_0)$.

5. The exponent γ from the soft finger deformation model (6) is known. This parameter depends on the fingertip material and can be estimated offline by using either (6) or (7).

6. The angular position θ of the object must not overshoot past the reference angle θ_d since we perform passive pivoting. The manipulator would otherwise have to rotate the gripper to perform passive pivoting again, or we would need to generate angular momentum on the object by accelerating the manipulator.

7. The object is initially at rest and in a secure grasp.

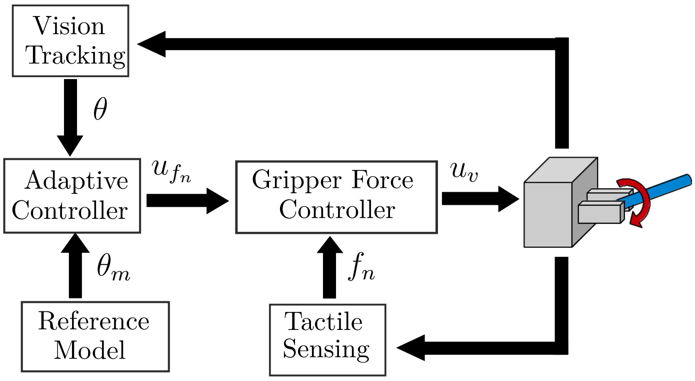

Figure 3: Overview of our proposed control scheme for pivoting.

Following assumptions 2) and 3) we decompose our controller in two subcontrollers as shown in the diagram in Fig. 3. First, an adaptive controller takes as input the angular position θ measured by the vision system and the desired angular position θ_m given by the reference model and computes a reference normal force u_{f_n} to control the trajectory of the object. This reference force u_{f_n} is then used together with tactile measurements of the normal force f_n by a PI controller to adjust the velocity of the fingers, minimizing the error between the measured and reference normal force.

4.1 Adaptive controller

We choose model reference adaptive control given that we aim to perform the pivoting task given errors in the torsional friction coefficient μ_{tors}, which represents a parametric uncertainty in the nonlinear model (9).

Adaptive control performs tracking control by driving the system's state $\mathbf{x}(t) = [\theta(t), \dot{\theta}(t)]^\top$ along a state trajectory $\mathbf{x}_m(t) = [\theta_m(t), \dot{\theta}_m(t)]^\top$ defined by a reference model. This reference model is designed by the user and describes the ideal response that the system should follow, satisfying the control requirements and constraints of the task. In our case the angular position response should not overshoot, thus, we design the reference model as a critically damped second order system with unit DC gain with the following transfer function

$$H_m(p) = \frac{\theta_m}{\theta_{in}} = \frac{\lambda_0^2}{(p + \lambda_0)^2} \tag{10}$$

where the reference input θ_{in} follows a trapezoidal velocity profile.

To formulate our controller, we rewrite the model from Eq. (8) considering the normal force as a control input u_{f_n}

$$h\ddot{\theta} + b\tau_g = u_{f_n}^{1+\gamma} \tag{11}$$

where $h = 0.5I\mu_{tors}^{-1}$ and $b = 0.5\mu_{tors}^{-1}$. We then define the following tracking control error s

$$s = \dot{\tilde{\theta}} + \lambda\tilde{\theta} \tag{12}$$

where $\tilde{\theta} = \theta - \theta_m$ and $\dot{\tilde{\theta}} = \dot{\theta} - \dot{\theta}_m$ are the angular position and velocity errors respectively and λ is a constant.

We can then formulate the following standard adaptive control law [19]

$$u_{f_n}^{1+\gamma} = \hat{h}\ddot{\theta}_r - k_s s + \hat{b}\tau_g \tag{13}$$

The control law is composed of a velocity error and feedforward acceleration term $\hat{h}\ddot{\theta}_r$, a tracking error term $k_s s$, and a nonlinear gravity compensation term $\hat{b}\tau_g$. The reference angular acceleration $\ddot{\theta}_r$ is given by $\ddot{\theta}_r = \ddot{\theta}_m - \lambda\dot{\tilde{\theta}}$, k_s is a positive tracking control gain and $\hat{h}, \hat{b}$ are adaptive estimates of h and b given by

$$\dot{\hat{h}} = -\alpha_h s\ddot{\theta}_r \tag{14a}$$

$$\dot{\hat{b}} = -\alpha_b s\tau_g \tag{14b}$$

where α_h, α_b are positive adaptation gains. It is important to note that the online estimates (14a), (14b) are not guaranteed to converge to the correct values unless persistent excitation conditions are met. We do not consider this a major limitation since the scope of our work is to perform the pivoting task and not accurate estimation of the friction parameters. The control scheme does however guarantee convergence of the tracking error s which implies that the object pivots to the desired orientation.

4.2 Gripper force controller

We regulate the normal force f_n by opening and closing the fingers with a PI controller

$$u_v = k_p \tilde{f}_n + k_i \int_0^t \tilde{f}_n dt \tag{15}$$

where u_v is the velocity set point commanded to the gripper, k_p, k_i are the controller gains and $\tilde{f}_n = f_n - u_{f_n}$ is the error between the measured normal force f_n and the normal force set point u_{f_n} from the adaptive control law of Eq. (13). The controller is tuned such that $f_n \to u_{f_n}$.

5 Experimental Evaluation

We evaluated our proposed adaptive controller on a robot platform equipped with a 1 DOF 2-finger parallel gripper with Optoforce[1] tactile sensors and an RGBD camera as shown in Fig. 4. We track the object's pose throughout the experiments using *Simtrack*, a model-based vision tracking system that generates realtime pose estimates at 30 Hz [16]. The control loop operates also at 30 Hz.

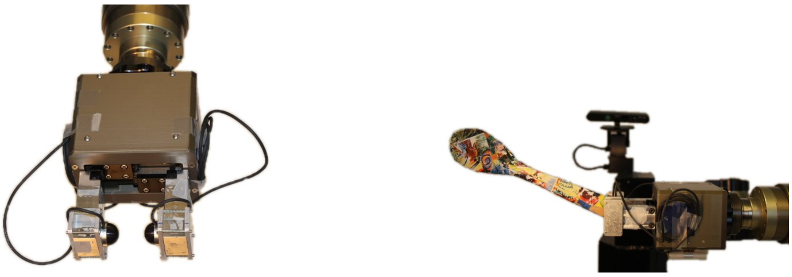

(a) (b)

Figure 4: Robot platform with parallel gripper and Optoforce tactile sensors at the fingertips used in our experimental evaluation.

The Optoforce tactile sensors provide 3-axis force measurements at 100 Hz, and we chose them for these experiments given their low cost, robustness and suitability for force control. The sensors operate based on an optical principle providing high resolution force measurements of 0.03N with noise levels of approximately 0.01N, which are not commonly available from other types of tactile sensors.

In our experiments we grasp an object whose inertial and frictional parameters are given in Table 1. Furthermore, Table 2 shows the controller gains and parameters used in the adaptive control law (13) and the PI gripper force controller (15). We kept the control gains fixed throughout the experiments.

---

[1] www.optoforce.com

$I [\mathrm{kg} * \mathrm{cm}^2]$	10.64
m [g]	48.5
l_{cm} [cm]	12.22
μ	0.47
μ_{tors}	0.643x10^{-3}

Table 1: Inertial and frictional parameters of the grasped object.

k_s	23.0
λ	10.0
γ	0.1849
k_p	5.0x10^{-4}
k_i	2.0x10^{-5}

Table 2: Controller gains and parameters used throughout the experiments.

We obtained the torsional friction coefficient μ_{tors} and the power-law exponent γ using Eq. (5) through measurements of the torsional friction τ_f provided by the force/torque sensor in our manipulator's wrist and tactile measurements of the normal force f_n. However, the hardware limitations of our system made it difficult to accurately estimate these parameters: the torsional friction measurements from the force/torque sensor had a low signal to noise ratio and were also affected by gravity compensation errors, which generated significant errors in the estimated μ_{tors}. We tuned this parameter by running the controller with different values of the friction coefficient as will be explained further on.

To obtain the control gains we first tuned the gripper force controller gains (k_p, k_i) following standard practice for PI controller tuning. We then tuned the tracking control gain k_s by first deactivating the estimators, i.e. setting $\alpha_h = \alpha_b = 0$ in Eq. (14) and using the ground truth values of the object's inertial and friction parameters in the controller. An excessive tracking gain k_s caused the object to stop repeatedly along the trajectory given that it would enter the stiction regime. On the other hand, a low k_s tended to generate large overshoots in the angular position θ of the object with respect to the reference trajectory. We chose $\lambda = 10.0$ for the tracking control error (12) in order to give a higher relative weight to position tracking errors rather than velocity tracking errors given the higher quality of pose estimates provided by our vision tracker with respect to the angular velocity estimates. We designed the reference trajectory slow enough to avoid motion blur that would deteriorate the vision tracker's performance, yet fast enough to avoid stiction effects.

We evaluated our controller both under errors in the initial estimate of the torsional friction coefficient μ_{tors} and when modifying the frictional properties of the material in contact with the fingertips. We thus performed the following set of experiments:

- **Effect of initial estimate of μ_{tors} without adaptation**. We deactivate the adaptive estimators from Eq. (14), essentially transforming our controller in a feedback linearizing controller. We then show the controller's behavior assuming different values of the torsional friction coefficient μ_{tors} in the control law (13).
- **Effect of initial estimate of μ_{tors} with adaptation**. We repeat the previous set of experiments and show how adaptation is critical to accomplish the pivoting task despite errors in the initial estimate of μ_{tors}.
- **Change of object frictional properties**. We further examine the adaptive controller's performance by using the same test object as in the previous experiments but changing the material at the point of contact with the fingertips, modifying thus the friction coefficient. We show that although there is an evident reduction in tracking control performance, the object still pivots to the desired position.

5.1 Effect of initial estimate of μ_{tors} without adaptation

In this set of experiments we deactivated the estimators by setting $\alpha_h = \alpha_b = 0.0$ in the adaptation law (14) and executed the controller with 3 different values of the torsional friction coefficient μ_{tors} in the control law (13). The reference trajectory $\theta_m(t)$ from the reference model and the angular position $\theta(t)$ of the object relative to the gripper for each case are shown in Fig. 5.

As mentioned previously, this experiment allowed us to adjust the approximate torsional friction coefficient we obtained using the wrist-mounted force-torque sensor. In our experimental trials the controller achieved the best tracking performance with $\mu_{tors} = 0.643\text{x}10^{-3}$. Furthermore, the object stopped prematurely before reaching the goal angular position when the coefficient was below this optimal value, for example with $\mu_{tors} = 0.3\text{x}10^{-3}$ as shown in Fig. 5. This happens because a lower μ_{tors} magnifies the nonlinear gravity compensation term $b\tau_g$ in the control law (13), causing the controller to exert excessive gripping force. Analogously, an overestimated torsional friction coefficient, such as $\mu_{tors} = 1.0\text{x}10^{-3}$, reduces the gravity compensation term and causes the object to slip past the desired angular position. This experiment clearly illustrates how errors in μ_{tors} affect the control performance and justifies the use of adaptive control in our approach.

Fig. 6 shows the normal force input u_{f_n} of the adaptive controller, as well as the normal force measured by the tactile sensor f_n when $\mu_{tors} = 0.643\text{x}10^{-3}$. The figure shows that there is a force control error, which can be explained in part by the tracking errors in the gripper's internal velocity controller as evidenced in Fig. 7 which shows differences between the commanded gripper velocity u_v and the gripper's velocity v measured by encoder feedback. This occurs in practice because

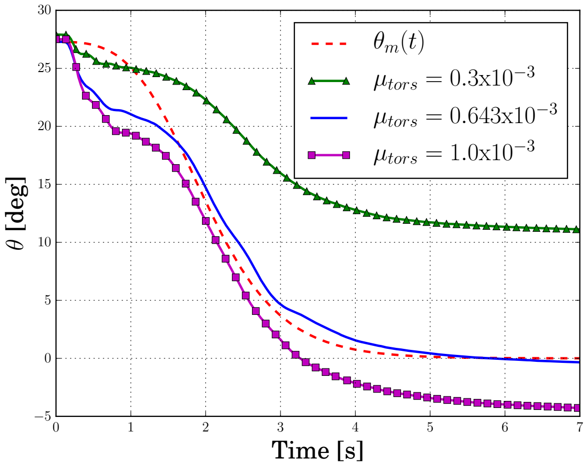

Figure 5: Reference angular position θ_m and angular position θ of the object under different values of μ_{tors} in the control law without adaptation.

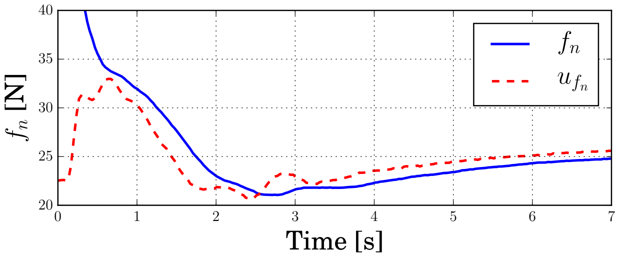

Figure 6: Gripping force control input u_{f_n} and measured normal force f_n with $\mu_{tors} = 0.643\text{x}10^{-3}$.

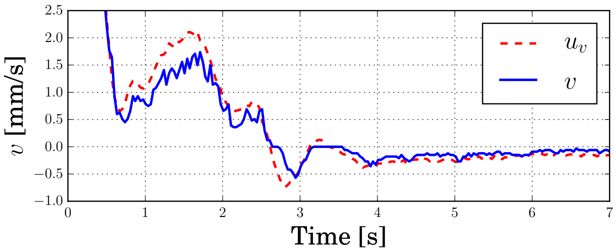

Figure 7: Gripper velocity set point u_v and gripper velocity v with $\mu_{tors} = 0.643\text{x}10^{-3}$.

the internal controller's tracking performance degrades at low velocities. We could reduce part of the force control errors by using a more aggressive PI force controller, but in practice this caused the object to enter the stiction regime and lag behind the reference trajectory.

5.2 Effect of initial estimate of μ_{tors} with adaptation

We tuned the adaptation gains from (14a) and (14b) to $\alpha_h = 1.5$ and $\alpha_b = 7.5\text{x}10^3$ respectively and repeated the previous set of experiments to analyze the controller's performance when using the proposed update laws. Fig. 8 shows the object's angular position with different initial estimates of μ_{tors}, while keeping the controller and adaptation gains fixed.

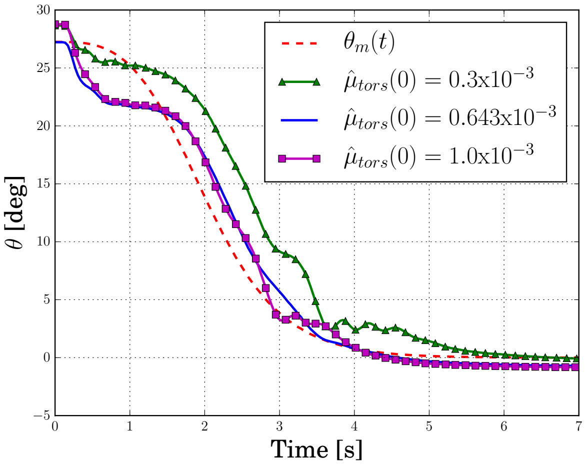

Figure 8: Reference angular position θ_m and angular position θ of the object under different initial estimates of μ_{tors} when using the adaptive estimators.

We observe that the adaptive controller achieves the best performance when starting with the correct torsional friction coefficient estimate $\hat{\mu}_{tors}(0) = 0.643\text{x}10^{-3}$. Furthermore, in contrast to the previous set of experiments, the controller manages to converge to the desired angular position θ_d with both an underestimated ($\hat{\mu}_{tors}(0) = 0.3\text{x}10^{-3}$) and an overestimated ($\hat{\mu}_{tors}(0) = 1.0\text{x}10^{-3}$) coefficient. In all cases the steady state error was less than 1 degree.

Fig. 9 and 10 show the control inputs to the system when $\hat{\mu}_{tors}(0) = 0.3\text{x}10^{-3}$. Once again, there are force control errors. As previously mentioned, the adaptive estimates are not guaranteed to converge to the true values, and Fig. 11 confirms this. This figure shows the torsional friction coefficient estimate $\hat{\mu}_{tors} = 0.5\hat{b}^{-1}$ which does not reach the ground truth value.

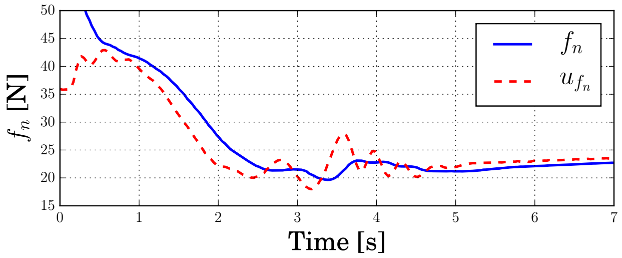

Figure 9: Gripping force control input u_{f_n} and measured normal force f_n when using adaptation and $\hat{\mu}_{tors}(0) = 0.3\text{x}10^{-3}$.

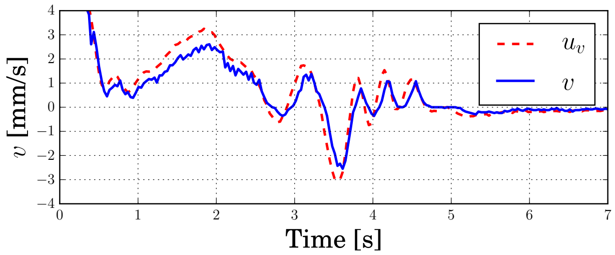

Figure 10: Gripper velocity set point u_v and gripper velocity v when using adaptation and $\hat{\mu}_{tors}(0) = 0.3\text{x}10^{-3}$.

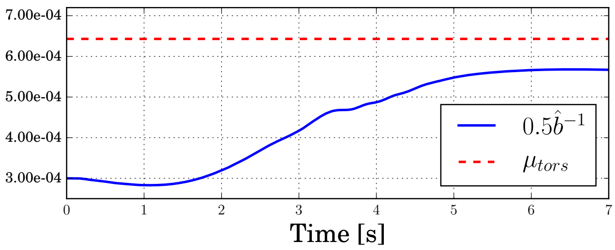

Figure 11: Adaptive estimate of the torsional friction coefficient $\hat{\mu}_{tors} = 0.5\hat{b}^{-1}$.

5.3 Change of object frictional properties

In this last set of experiments we substituted the manipulated object's material ($\mu = 0.47$) with a lower friction material $\mu = 0.37$ and a material with higher friction coefficient $\mu = 1.08$. Once again, we kept the controller and adaptation gains fixed. The experimental results are shown in Fig. 12 and Fig. 13. Although the adaptive controller shows inferior tracking performance when compared to the previous experiments, it still converges to the desired object orientation within acceptable steady state errors of 1.64 and 0.5 degrees respectively.

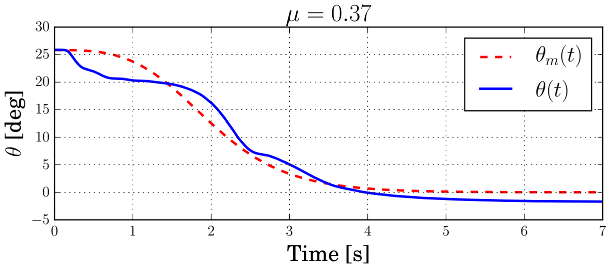

Figure 12: Angular position θ of the object when using a new material with $\mu = 0.37$.

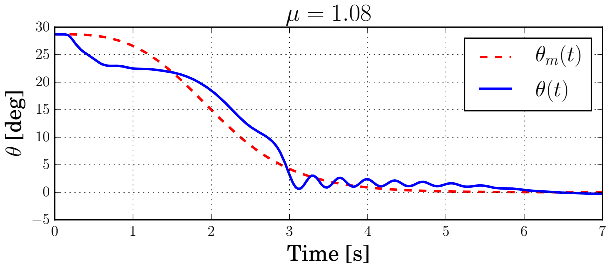

Figure 13: Angular position θ of the object when using a new material with $\mu = 1.08$.

6 Conclusions and Future Work

We have presented an adaptive control approach for pivoting with extrinsic dexterity by means of gravity and controlled slip. Given that wrongly estimated friction coefficients are a common source of error for in-hand manipulation, we designed an adaptive controller that accounts for errors in the torsional friction coefficient. In our controller we use visual tracking of the object's angular position and force measurements from high resolution and low noise tactile sensors. Our experimental results show how an incorrect torsional friction coefficient can have a negative impact in the performance of a feedback linearizing controller for pivoting, yet the proposed adaptation law compensates for this parametric error and manages to pivot the object successfully. Our approach complements recent works on in-hand manipulation with extrinsic dexterity since we make use of closed loop feedback control and tactile sensing.

One of the limitations of our work is that we perform passive pivoting by keeping the gripper static, which limits the range of possible regrasps unless we first rotate the gripper to reconfigure its alignment with gravity. We can extend the approach by accelerating the manipulator, reformulating the proposed adaptive controller to cope with disturbances generated by the inertial forces. We can also extend our approach to include prehensile pushing against external contacts, which opens the possibility to generate also translational displacements of the grasped object in the robot's hand.

References

[1] A. Bicchi and V. Kumar. Robotic grasping and contact: a review. In *IEEE International Conference on Robotics and Automation*, volume 1, pages 348 –353 vol.1, 2000.

[2] D.L. Brock. Enhancing the dexterity of a robot hand using controlled slip. In *IEEE International Conference on Robotics and Automation*, pages 249–251 vol.1, Apr 1988.

[3] N. Chavan-Dafle and A. Rodriguez. Prehensile pushing: In-hand manipulation with push-primitives. In *IEEE/RSJ International Conference on Intelligent Robots and System*, pages 6215–6222, Sept 2015.

[4] N. Dafle, M.T. Mason, H. Staab, G. Rossano, and A. Rodriguez. A two-phase gripper to reorient and grasp. In *International Conference on Automation Science and Engineering*, 2015.

[5] N.C. Dafle, A. Rodriguez, R. Paolini, Bowei Tang, S.S. Srinivasa, M. Erdmann, M.T. Mason, I. Lundberg, H. Staab, and T. Fuhlbrigge. Extrinsic dexterity: In-hand manipulation with external forces. In *IEEE International Conference on Robotics and Automation*, pages 1578–1585, May 2014.

[6] C.C. De Wit, H. Olsson, K.J. Astrom, and P. Lischinsky. A new model for control of systems with friction. *IEEE Transactions on Automatic Control*, 40(3):419–425, Mar 1995.

[7] Clemens Eppner, Raphael Deimel, Jose Alvarez-Ruiz, Marianne Maertens, and Oliver Brock. Exploitation of environmental constraints in human and robotic grasping. *The International Journal of Robotics Research*, 34(7):1021–1038, June 2015.

[8] Suresh Goyal. *Planar sliding of a rigid body with dry friction: limit surfaces and dynamics of motion.* PhD thesis, Cornell University, 1989.

[9] L. Han and J.C. Trinkle. Dextrous manipulation by rolling and finger gaiting. In *IEEE International Conference on Robotics and Automation*, volume 1, pages 730–735 vol.1, May 1998.

[10] A. Holladay, R. Paolini, and M.T. Mason. A general framework for open-loop pivoting. In *IEEE International Conference on Robotics and Automation*, pages 3675–3681, May 2015.

[11] Robert D Howe and Mark R Cutkosky. Practical force-motion models for sliding manipulation. *The International Journal of Robotics Research*, 15(6):557–572, 1996.

[12] Roland S Johansson and J Randall Flanagan. Coding and use of tactile signals from the fingertips in object manipulation tasks. *Nature Reviews Neuroscience*, 10(5): 345–359, 2009.

[13] D. Kubus, T. Kroger, and F.M. Wahl. On-line rigid object recognition and pose estimation based on inertial parameters. In *IEEE/RSJ International Conference on Intelligent Robots and Systems*, pages 1402–1408, Oct 2007.

[14] C. Melchiorri. Slip detection and control using tactile and force sensors. *IEEE/ASME Transactions on Mechatronics*, 5(3):235 –243, sep 2000.

[15] Henrik Olsson, Karl J Åström, C Canudas De Wit, Magnus Gäfvert, and Pablo Lischinsky. Friction models and friction compensation. *European journal of control*, 4(3):176–195, 1998.

[16] Karl Pauwels and Danica Kragic. Simtrack: A simulation-based framework for scalable real-time object pose detection and tracking. In *IEEE/RSJ International Conference on Intelligent Robots and Systems*, 2015.

[17] J.K. Salisbury. *Kinematics and Force Analysis of Articulated Hands*. PhD thesis, Stanford University, 1982.

[18] Jian Shi, J.Z. Woodruff, and K.M. Lynch. Dynamic in-hand sliding manipulation. In *IEEE/RSJ International Conference on Intelligent Robots and Systems*, pages 870–877, Sept 2015.

[19] J.J.E. Slotine and W. Li. *Applied Nonlinear Control*. Prentice Hall, 1991. ISBN 9780130408907.

[20] P. Tournassoud, T. Lozano-Perez, and E. Mazer. Regrasping. In *IEEE International Conference on Robotics and Automation*, volume 4, pages 1924–1928, Mar 1987.

[21] M.R. Tremblay and M.R. Cutkosky. Estimating friction using incipient slip sensing during a manipulation task. In *IEEE International Conference on Robotics and Automation*, pages 429–434 vol.1, May 1993.

[22] J.C. Trinkle and J.J. Hunter. A framework for planning dexterous manipulation. In *IEEE International Conference on Robotics and Automation*, pages 1245–1251 vol.2, Apr 1991.

[23] C. Ünsal and P. Kachroo. Sliding mode measurement feedback control for antilock braking systems. *IEEE Transactions on Control Systems Technology*, 7(2):271–281, Mar 1999.

[24] F.E. Vina B., Y. Karayiannidis, K. Pauwels, C. Smith, and D. Kragic. In-hand manipulation using gravity and controlled slip. In *IEEE/RSJ International Conference on Intelligent Robots and Systems*, pages 5636–5641, Sept 2015.

[25] Nicholas Xydas and Imin Kao. Modeling of contact mechanics and friction limit surfaces for soft fingers in robotics, with experimental results. *The International Journal of Robotics Research*, 18(9):941–950, 1999.